Statistical Analysis of Deterministic Textures in Steel Sheet Production

A thesis submitted for the Degree of Doctor of Philosophy

Alessandro Porrino

Department of Design & Systems Engineering,
Brunel University

March 2004

Abstract

Textured surfaces are universally adopted in the steel sheet production industry, and manufacturers are continuously improving the quality of the finished products through intense research in the surface characterisation field.

Deterministic Surfaces are textured with specifically designed rolls in order to present a certain degree of regularity, which allows better control over the functional behaviour of the metal sheets.

The regularity of the texture impressed on the steel sheets also allows unconventional approaches to surface characterisation and to the assessment of the texture's structure. Statistical analysis is the most effective way to target the isolation of the deterministic part of the surface, which represents the desired product, from the stochastic part, called 'noise' and associated with the inaccuracies of production and measurement.

This work addresses the problem of characterisation of deterministic textures through statistical analysis, proposing innovative filtering techniques aimed at the realisation of an On-line Process Control System.

Firstly the techniques proposed are theoretically formulated and studied, addressing in particular the physical meaning of the geometrical parameters extracted through statistical analysis of highly correlated portions of the textures. A method for isolating the deterministic textures present on a surface, called the Statistical Surface Filter, is presented and discussed in detail, and tested on existing laboratory samples.

Secondly the filter is applied to preliminary measurements acquired by an innovative on-line measurement system currently under development, and evidence is shown that the technique is effective in separating the information regarding the regular patterns from the stochastic noise. The possible applications to on-line Statistical Process Control are discussed.

Thirdly, the Statistical Surface Filter is tested on a set of measurements representing texturing rolls and textured sheets with different characteristics; statistical analysis of the surface parameters extracted from the filtered surfaces show that the technique allows the assessment of the different contributions of the various stages of the texturing process to the final product.

Finally, a software package is implemented for the practical application of the filtering techniques and the parameters extraction; the algorithms that perform the statistical filtering are described and discussed, concluding with the operations of optimisation and fine-tuning for production-line implementation.

Acknowledgements

An acknowledgment is certainly due to OCAS for the support given to the Department of Design and Systems Engineering of Brunel University during the Statistical Filter Project, in particular to Prof. Michel Vermeulen who has followed the project throughout its duration with interest and professionalism.

Many other people deserve mention for sharing with me the advice and the wisdom that is needed by the student, and many others should be mentioned because they have given me support and the friendship.

Only a few, as it has to be, are mentioned here. The order is rigorously alphabetical, with the exception of the first positions, which belong to my family.

Rosanna Stefano and Daniele, Agathe, Alan, Brian, Clive, Enza, Fabio, Franco, Linda, Lyn, Mike, Monica, Patrick, Raffaele, Renato, Roberto, Tanja, Valeria, Zafiris.

...Thank you!

Table of Contents

Table of Figures

1. Introduction

"The most exciting phrase to hear in science, the one that heralds new discoveries, is not 'Eureka!' ('I found it!') but rather 'hmm....that's funny...'"

- Isaac Asimov.

1.1 The AUTOSURF Project

The continuous expansion and globalisation of the Automotive Industry are making the market more and more competitive; industrial and academic researchers are exploring all aspects of car production in order to improve and optimise every aspect of the production process.

Metal panel surfaces represent an important branch of Automotive Industry research, leading to an increasing emphasis on the three-dimensional nature of surfaces and the relationship to pressing and painting performance.

The European Union has recently sponsored two major projects in the area of three-dimensional surface metrology:

- **'SurfStand'** [SurfStand website] was concerned with the definition and exploration of surface standards and where Huddersfield University was a major contributor.
- **'Autosurf'** [Autosurf website] was concerned with investigating new parameters with respect to automotive sheet metal production and painting.

Figure 1-1 - Autosurf Consortium

AUTOSURF (BE-97-4140) was a research project carried out with the financial support of the European Community, under the framework of BRITE-EURAM III Programme; the partners logos are depicted in Figure 1-1. The

project started on 1st March 1998, ended in March 2001 and was co-ordinated by Brunel University.

"The purpose of the project is to specify, objectively, autobody steel sheet material surface topography to optimise the perceived conflicting requirements for pressing, assembly and painting performances in order to significantly improve quality whilst reducing cost and waste" [Autosurf website].

One of the main objectives of the project was concerned with the definition of stable 3D parameters for future standardisation. A large number of surfaces produced by different techniques and instruments have been measured with different software, so that the statistical analysis of the measurements gave an important contribution to surface topography knowledge.

The outcomes of the AUTOSURF project were considered to be a most reliable source of information, and therefore will be often referred to throughout this work.

The AUTOSURF project generated also some spin-off activities that became independent projects, of which in particular:

- The Gram-Schmidt filter, subsequently renamed 'Semi-Deterministic Surface Statistical Filter'.

- The SCOUT project: SCOUT is the name of the software that supported most of the AUTOSURF research work. Born as a rudimentary collection of 'Matlab' procedures, it grew steadily to become an integrated package comprising approximately 200 pages of source code, later equipped with a graphical interface and circulated to the research community employing the Open-Source Philosophy [Sacerdotti et al. 2002].

The first mentioned is the project here described, whilst the second one constitutes its mathematical reference and software support.

1.2 The collaboration between OCAS and Brunel University on Semi-Deterministic Surface Filtering.

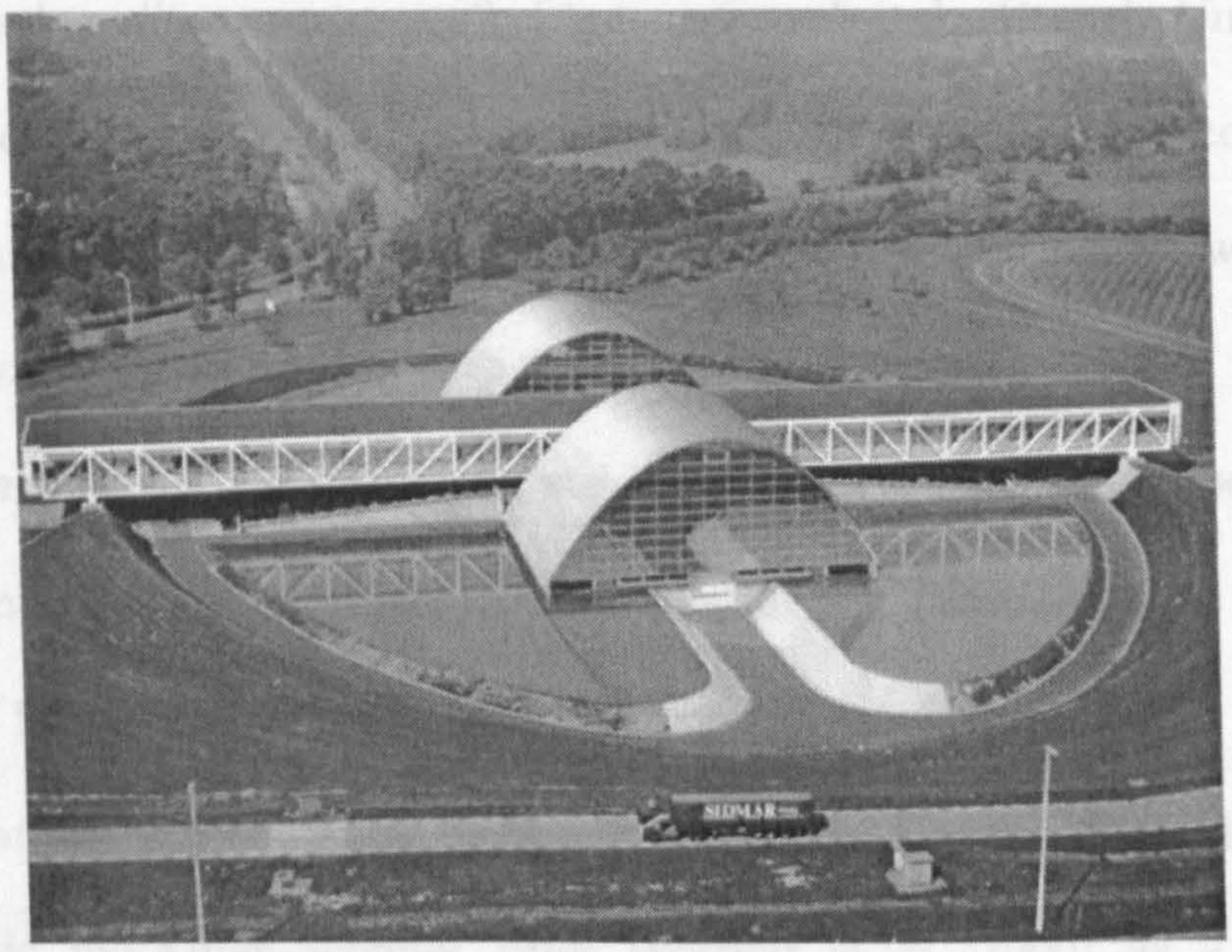

Figure 1-2 - OCAS

OCAS (OnderzoeksCentrum voor Aanwending van Staal), located near SIDMAR in Ghent, is the R&D centre of the SIDMAR Group, the flat products sector of the ARBED Group. Shareholders are SIDMAR (Belgium), STAHLwerke BREMEN (Germany), ACERALIA (Spain), ALZ (Belgium) and Laminoir de Dudelange (Luxembourg). OCAS's application research activities focus on forming (deep drawing, hydroforming, …), on the latest joining techniques (laser welding, adhesive bonding and tailor welded blanks, …) and on traditional and innovative surface technology (metallic, ceramic and organic coatings, …) [OCAS website].

OCAS has been active partner of the Autosurf consortium, where the collaboration with Brunel University on surface topography started: OCAS played an important role in task 1.6 of the Autosurf project, whose aim was "*to formulate specific novel 3D surface topography characterisation parameters as appropriate to enable objective measurement of pseudo-stochastic, semi-*

deterministic and deterministic surface topographies. These will be directly related to specific surface-effects, including frictional characteristics, fluid retention and galling resistance" [Autosurf website]. Brunel University, coordinator of the project, was also strongly involved in task 1.6 and concerned mainly with the parameters formulation, while OCAS contribution was more oriented towards the correlation with the surface performances.

It is clear that, in order to obtain stable meaningful parameters, the surface measurements had to be firstly filtered/conditioned (Section 2.4), therefore OCAS and Brunel University started collaborating on filtering issues from the beginning of the project. When, in May 2000, Brunel University developed and made public the Gram-Schmidt filter [Porrino et al. 2000] as a tool for parameters extraction and noise reduction on semi-deterministic surfaces, OCAS recognised the opportunity to develop the filter as an independent project regarding features extractions for statistical process control purposes. In November 2001, after the conclusion of the Autosurf Project, the **Semi-Deterministic Surface Statistical Filter** Project was officially started (from now on will be referred to simply as "Statistical Filter" or "GS Filter" for historical reasons related to the Gram-Schmidt first implementation).

1.3 The collaboration with CRM

CRM (Centre for Research in Metallurgy) is the joint research centre for the European iron and steel major groups and the non-ferrous metals industry of Benelux. The CRM Active Member Companies are large international steel groups involved in a common research programme: ARBED S.A. Group

ARCELOR, CORUS GROUP plc, USINOR S.A. Group ARCELOR and every one of their subsidiary companies in the iron and steel industry [CRM website].

Comparing this and the previous section we notice that CRM and OCAS have common shareholders/Active Members; this leads to collaboration on different projects regarding metallurgy in general.

While Brunel University and OCAS were developing the Statistical Filter, OCAS and CRM were collaborating on developing on-line roughness measurement of hot rolled strips [Moreas at al. 2002].

OCAS soon realised that the two projects could be beneficial to each other:

- instead of analysing standard off-line laboratory measurements, the Statistical Filter could be applied to on-line acquired measurements
- instead on analysing and post-processing the measurements with standard techniques, the on-line measurements could be filtered with the innovative feature-oriented Statistical Filter for immediate parameters extraction

Ultimately a working **On-line Statistical Process Control System** could be developed and implemented on the production line.

1.4 Research Objectives and Structure

The research work carried out during the past three years is related to the Statistical Filter and Autosurf Projects. The main objective can be stated as:

to improve the quality of semi-deterministic textured steel sheets through an innovative statistical filtering technique applicable to on-line process control.

The issues addressed are each associated with a chapter as follows:

- Chapter 2 - State-of-the-Art. Various sources related to the research topic, mainly scientific publications, are reviewed and commented on, in order to illustrate the current status of the research on the subject.
- Chapter 3 - Research Methodology. A methodology for the achievement of the objectives stated above is formulated.

- Chapter 4 - The "Statistical Filter". The filtering technique that is at the base of the research is here analysed, and its potentiality and limitations exposed.
- Chapter 5 - Adaptation of the Statistical Filter for Statistical Process Control. The Statistical filter is here adapted to the on-line measurements techniques that will enable on-line process control.
- Chapter 6 - Parameters extraction. Once the filter and its potentiality and limitations have been thoroughly analysed using both off-line and on-line measurements, the filter is here tested for practical implementation. Statistical analysis of the filter's application on a significant number of samples is presented.
- Chapter 7 - Software Implementation. The software that performs the filtering and parameters extraction is here analysed, targeting in particular the issues of time consumption, accuracy and feasibility.
- Chapter 8 - Optimisation for production-line implementation. After the various theoretical aspects of the research have been considered, the practical implementation in industrial environment requires a final stage of adaptation/fine tuning.
- Chapter 9 - Conclusions. A synthesis of the results achieved is provided.

2. State-of-the-Art

The first step of this research has been the acquisition of the necessary knowledge of the subject, and its mathematical and logistical aspects. An research on the available literature found more than 80 papers and scientific publications, books and software references, as well as scientific and industrial web sites.

An exhaustive survey on mathematical modelling of surface topography in autobody manufacture has been published by Sacerdotti [Sacerdotti et al 2000(d)] during the Autosurf project, of which Sacerdotti was coordinator.

The main source of information has been the signal processing research field including academic and industrial publications.

This chapter is intended to illustrate the present condition of research in the industrial surface texturing industry, and is organised as follows:

- Sections 2.1 and 2.2 contain a brief description of the automotive industry environment and of the most common off-line surface measurement instruments.
- In Section 2.3 the most common and advanced surface filtering techniques are analysed and discussed.
- Section 2.4 describes the various surface parameters developed by the research community during several years, and analyses the current state of their standardisation process.
- Section 2.5 describes the Gram-Schmidt based statistical filter. An exhaustive analysis is dedicated to this technique, which constitutes the mathematical structure and base of this project.
- Section 2.6 contains a final discussion on the present state of research on surface filtering and steel sheet production control.

2.1 Steel sheets used in the automotive industry

It is known that pressed sheet metal surfaces need to retain lubricant during the forming process and deliver consistent frictional behaviour [Thomas 1982]. To achieve this, the current practice is to texture the roll surfaces of sheet metal rolling presses to impart particular attributes to the rolled sheet surface [Scheers et al. 1996], such as enclosed valleys, defined peak spacing and roughness heights [Staeves et al. 1998, Stout at al. 2001]. Thus, the texture of the rolls will determine the sheet topography. At present there are at least four consolidated techniques for texturing the rolls: Shot Blasting (SB), Electrical Discharge Texturing (EDT), Laser Texturing (LT) and Electron Beam Texturing (EBT). The most common of these are EBT and EDT, and the majority of research publications are concerned with defining these surfaces by areal parameters which it is hoped will eventually be used for process control. Areal parameters are calculated on a surface measurement, as opposed to linear parameters, which are calculated on profiles.

At present, the industrial standard for surface quality control relies on off-line measurement of a statistically meaningful number of samples. An on-line measurement and analysis system is required to be very fast and robust, due to the speed of the steel sheet movement and to the hard working environment during rolling.

The next two sections provide a description of the steel sheet production process and of the available texturing methods for a better understanding of process control requirements and limitations.

2.1.1 Sheet Metal Processing

Once the steel has been produced as liquid steel from pig iron, it is converted into slabs that are ready to be processed.

The slabs from the continuous casting machine are rolled to a flat steel strip, which meets all customers' requirements. The transformation can be performed either by hot rolling or by hot and cold rolling.

- The hot rolling mill consists of a slab stockyard, where the slabs arriving from the continuous caster cool down, are checked for faults, and if necessary are then scarfed with oxygen-natural gas torches, and the hot strip mill, where the slabs are reheated in one of the walking beam furnaces. They are then rolled to form a strip with a thickness range from 1.25 to 12.7 mm. After leaving the finishing mill the steel strip is cooled and coiled. The hot rolled coils are then transported either to the cold rolling mills, or to the finishing section of the hot rolling mill where the hot rolled coils are packed as finished product.
- In the cold rolling mills, the hot rolled strip is transformed into a finished product: cold rolled sheet with a thickness range from 0.3 to 3.0 mm. This process is performed in different stages. First the steel is pickled with acid and subsequently cold rolled in a tandem mill to the thickness required by the customer. The cold rolled coil is subsequently annealed either by batch annealing or continuous annealing. Afterwards the annealed coil is skinpassed. If required, the cold rolled coils are cut into sheets in the finishing section. The finished material, either coils or cut sheets, is packed and shipped to the customer [OCAS website].

This research is concerned with the cold rolling stage of production, in particular with the tandem mill and skinpass sections. The rolls used in these two stages can be textured in order to obtain a certain controlled roughness on the sheet, which confers important functional characteristics to the final product.

The main purpose of surface topography characterisation is the quality control of the texture impressed on the rolls, and the texture transferred from the rolls to the sheets.

The following section illustrates the most common techniques for texturing the rolls.

2.1.2 Texturing techniques

Although the Statistical Filter has been applied only to EBT surfaces, it is beneficial to analyse also the other available texturing techniques in order to understand the evolution of surface texturing, the market requirements and the production difficulties.

- **Shot Blast Texturing (SBT)**

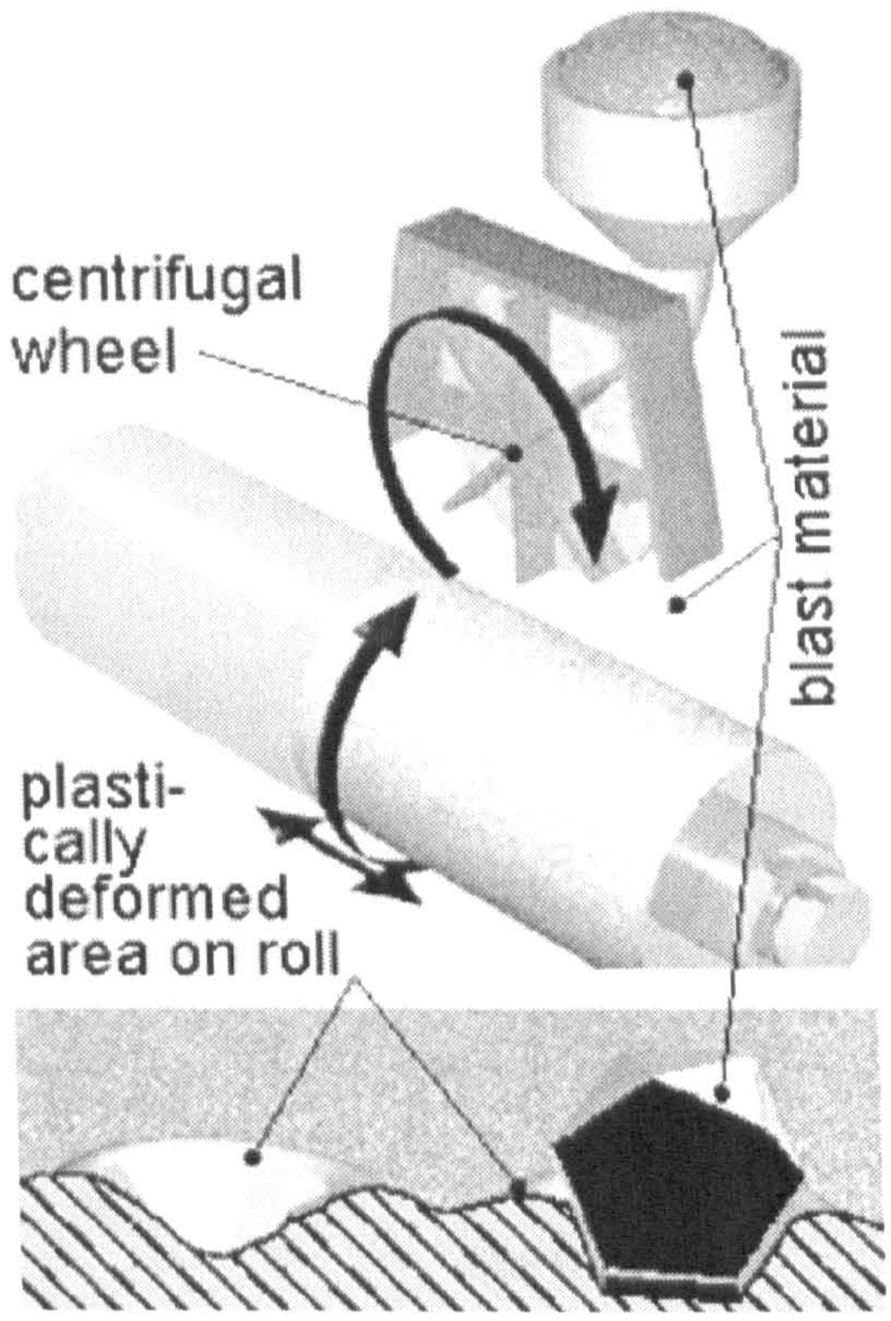

Figure 2-1 - SBT production process [Darmstadt website]

The shot blasting technique was introduced about 50 years ago. However, increased emphasis, mainly in the automotive industry, on maintaining stable forming conditions and on attaining a superior paint finish, has made the demands on the sheet's surface more stringent. Hence the variations of the surface topography have to be kept in the narrow range as specified by the customer. The surface produced by shot blasting is completely random, i.e. no regular patterns are present in the surface. One problem with shot blasting is controlling the process accurately enough due to the randomness of the process. Another problem with shot blasting

is the limited usable hardness of the rolls due to the shot particles limited ability to yield plastic deformation on a roll surface which is too hard. The Shot Blast Texturing method gives a stochastic texture with a very low reproducibility; on the other hand it is the fastest and the cheapest method for texturing rolls. A centrifugal wheel throws sharp-edged blast material on the roll [Horowitz, 1982; Ritterbach 1997] causing a high concentration of small random deformations of its surface. The final roughness of the roll can be controlled by altering the various variables defining the process: the speed of the centrifugal wheel, the blast material used, the period of treatment and so on. The working principle of the process is shown in Figure 2-1 [Darmstadt website].

- **Electrical Discharge Texturing (EDT).**

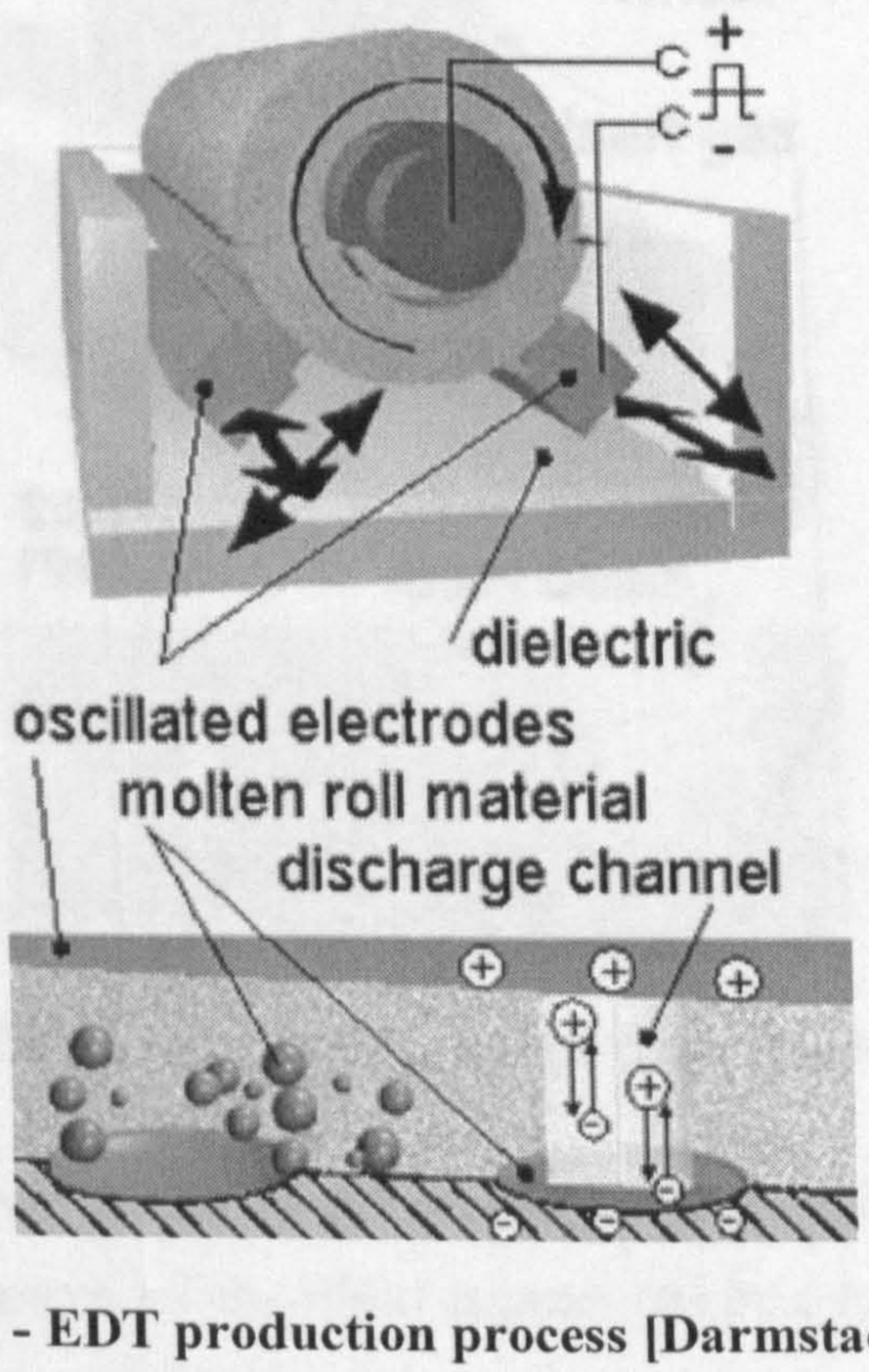

Figure 2-2 - EDT production process [Darmstadt website]

The roll rotates in a chamber filled with a dielectric while electrodes are moved radially and oscillated in an axial direction [Heberer, 1987; El-Menshawy, 1991; Aspinwall, 1992]. The electrodes release a regular discharge pulse causing a current to flow to the roll through the dielectric. A small area of

the roll surface vapourises, and a gas bubble forms in the dielectric. After each pulse the bubbles explode, ejecting the material around the bubble's site, where a valley is left. The roughness can be varied regardless of roll hardness via such parameters as voltage, control cycles and electrode distance; the repeatability is largely improved compared with SBT, but the surface presents no regularity (it is then a *stochastic surface*) because the site where the electrical discharge will occur cannot be controlled. The working principle of this technique is represented in Figure 2-2 [Darmstadt website].

- **Laser Texturing (LT).**

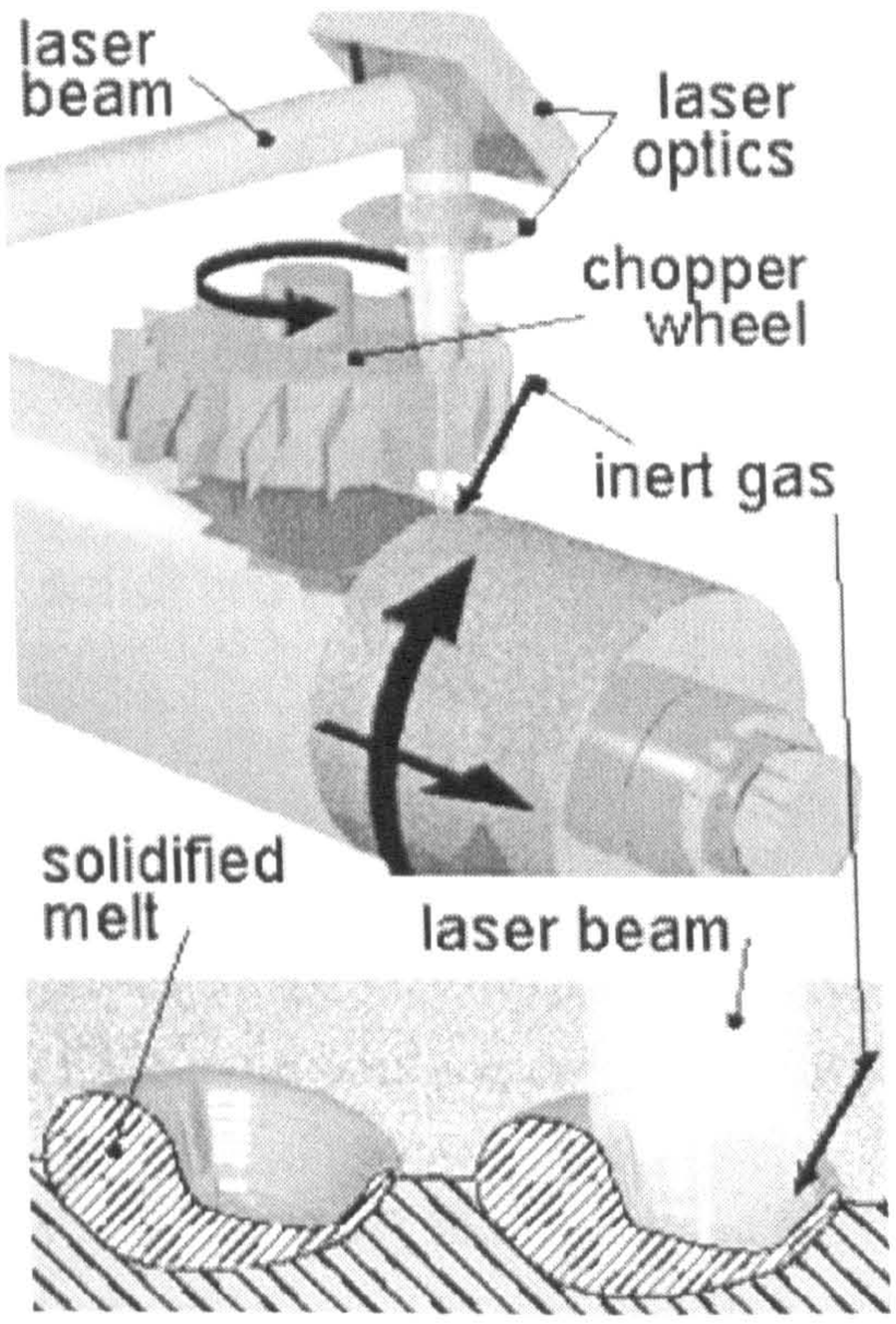

Figure 2-3 - LT production process [Darmstadt website]

As in EDT, a small portion of the surface is vapourised in order to roughen the surface, but in case of LT the effect is produced by a laser beam focused on the roll [Crahay et al., 1985]. The laser beam is continuous but it reaches the surface in pulses due to a chopper wheel that interrupts the beam. The molten metal either builds up in a bulge around the rim of the crater or is accumulated on one side of the crater where it solidifies. The production process is represented graphically in Figure 2-3 [Darmstadt website]. The rotational and

axial movements imposed on the roll provide the desired distribution of features. Roughness can be varied via laser power, axial motion, roll and chopper wheel speed as well as the inert gas. The position of each beam pulse can be controlled, therefore the texture is not stochastic as for SBT and EDT, but deterministic.

2.1.3 Electron Beam Texturing (EBT)

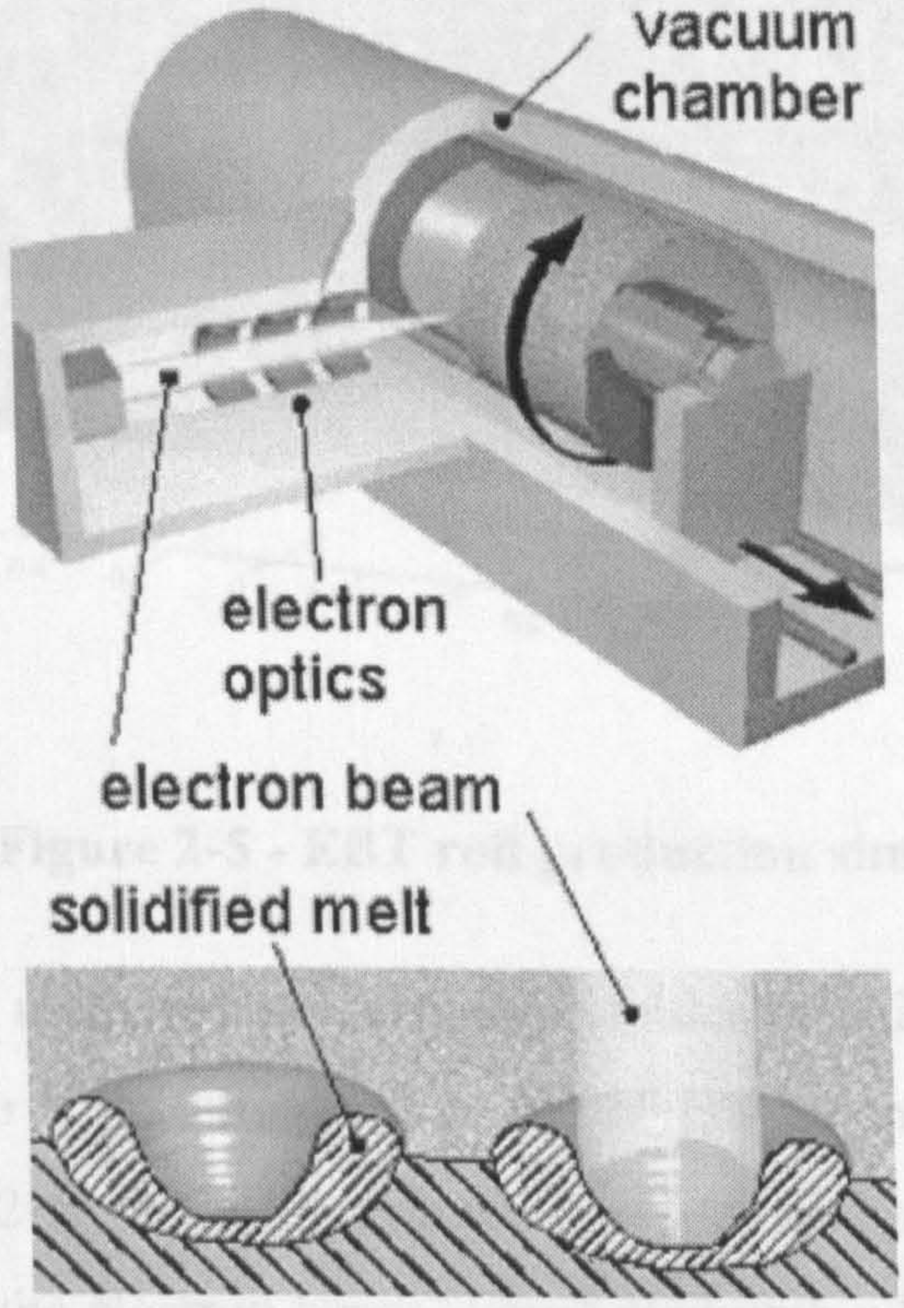

Figure 2-4 - EBT production process [Darmstadt website]

The roll material is melted locally, like in LT and EDT texturing, but using a pulsating electron beam; the process is depicted in Figure 2-4 [Darmstadt website]. The roll is rotated and axially moved in a vacuum chamber, while the beam is shot at its surface with an appropriate frequency [Sibetex Seminars, 1992-1996]. The beam vapourises the metal leaving a hole (crater), and part of the vapourised metal deposits around it in the shape of a ring. It is possible to synchronise the rotation of the roll with the shooting frequency so as to have the craters spaced uniformly in all directions. As in laser texturing, the craters can be made to overlap to such an extent that the regular structure is no longer noticeable. These surfaces are sometimes referred to as *pseudo-stochastic*.

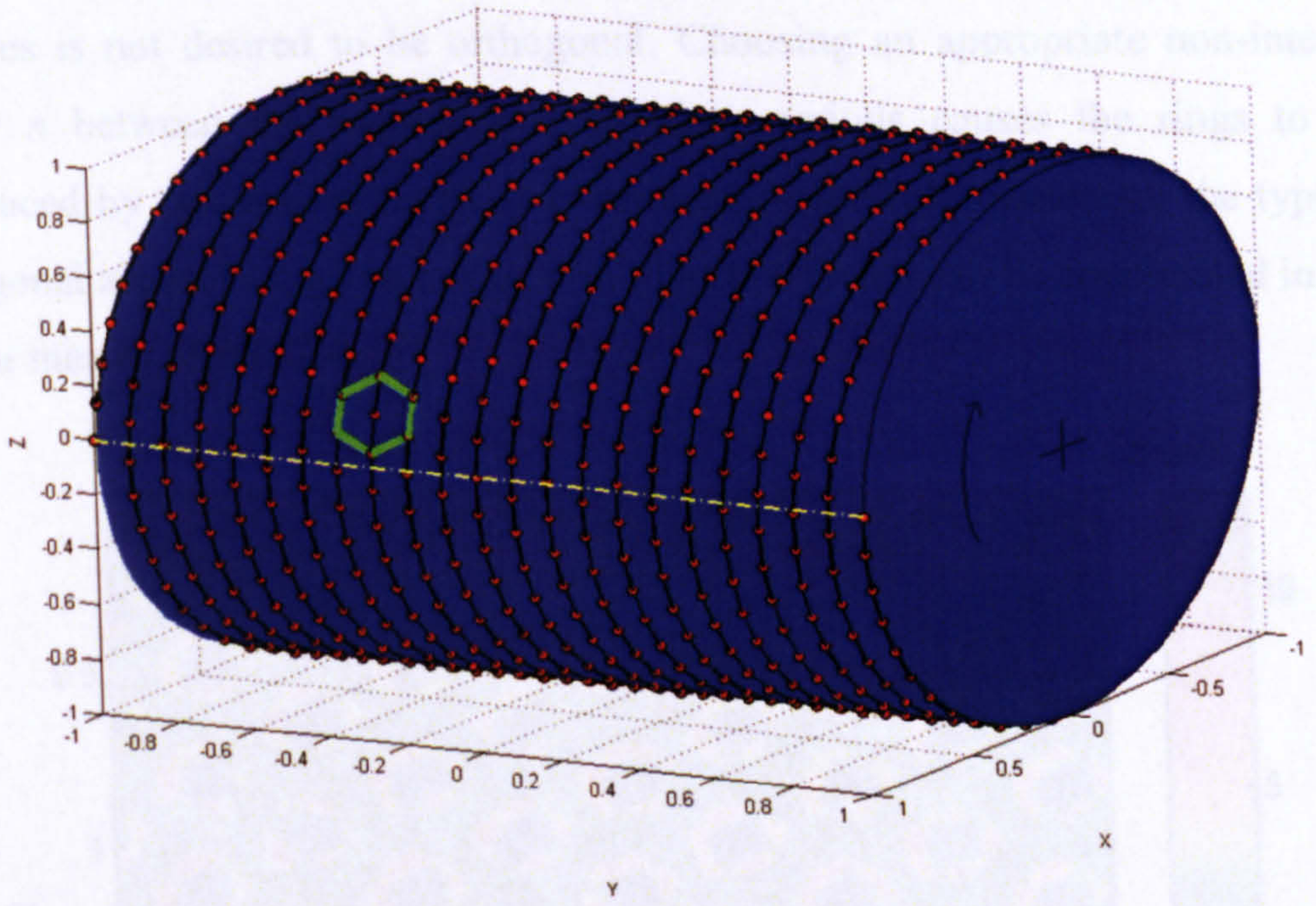

Figure 2-5 - EBT roll production simulated

The roll can be modelled as a regular cylinder of unitary height and radius, with axis along the Y direction and centre of gravity in the origin of axes, as depicted in Figure 2-5. The rolling direction is assumed anticlockwise respect to the XZ plane, and the electron beam is modelled with a horizontal line (parallel to X) moving on the Z=0 plane (the trace of the electron beam is depicted in the figure as a yellow dashed line).

The rotation of the roll combined with the axial movement draws on the roll a spiral whose equation can be expressed in parametric form:

$$X(t)=\cos(2\pi*f*t)$$

$$Y(t)=v*t \qquad \text{[equation 2-1]}$$

$$Z(t)=\sin(2\pi*f*t)$$

Where f is the frequency of rotation of the roll and v is the speed of the beam's axial translation. To synchronise the 'shooting' frequency of the beam f_b with the rotation frequency f it is sufficient to make sure that their periods ($1/f$) are proportional to an integer n: $1/f_b=n*1/f$. In this way the beam will shoot n times per each complete turn of the roll and always restart from the same position.

EBT are not produced with this kind of synchronisation because the grid of features is not desired to be orthogonal. Choosing an appropriate non-integer factor n between the rotation and shooting periods causes the rings to be misplaced by a constant factor at every turn of the roll, conferring the typical hexagonal aspect (see green hexagon in Figure 2-5) that can be appreciated in the colour map of Figure 2-6.

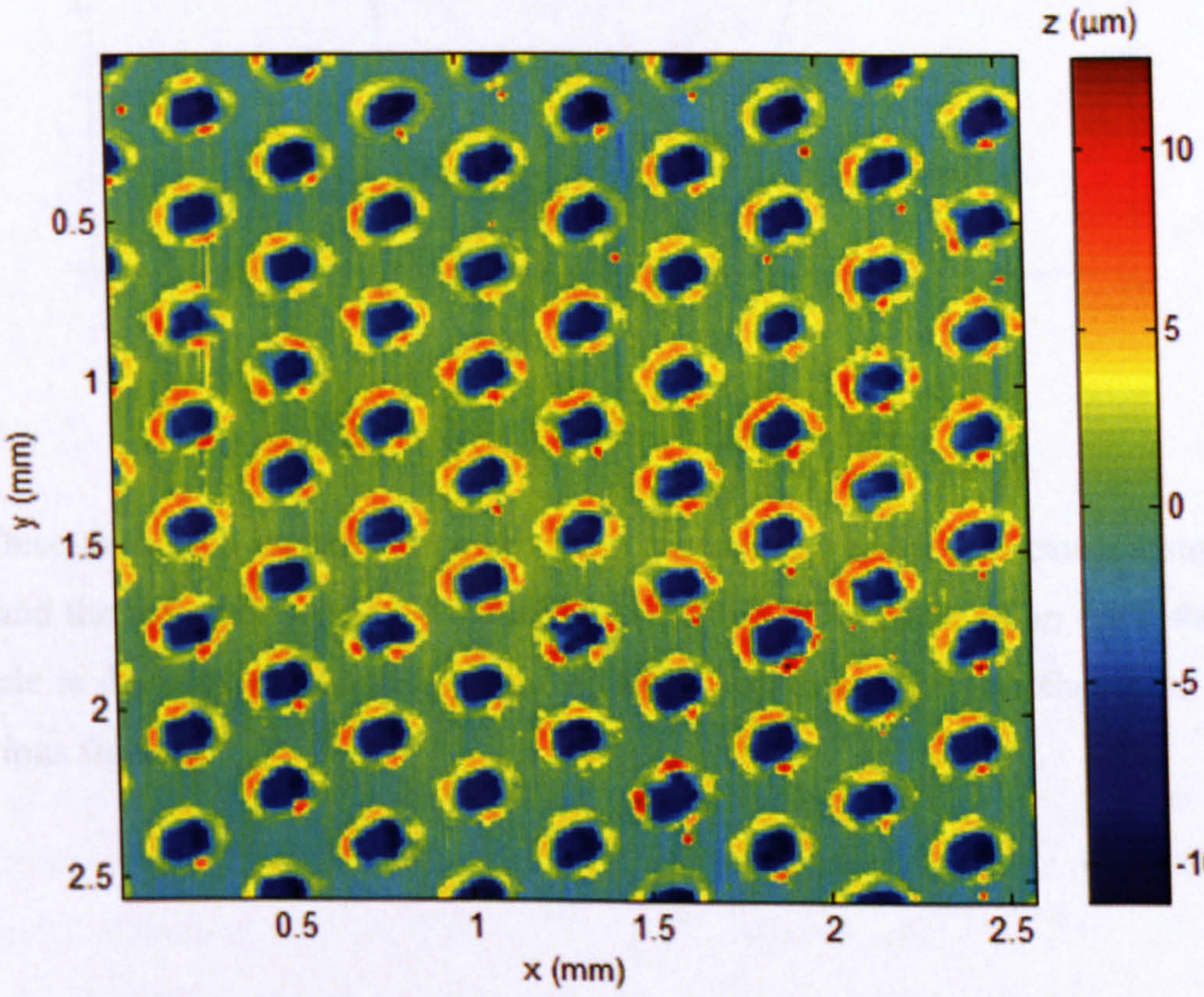

Figure 2-6 - Colour map of a typical EBT roll

The shape of the ring is well represented in section, as in Figure 2-7 which shows a profile extracted from the measurements of Figure 2-6.

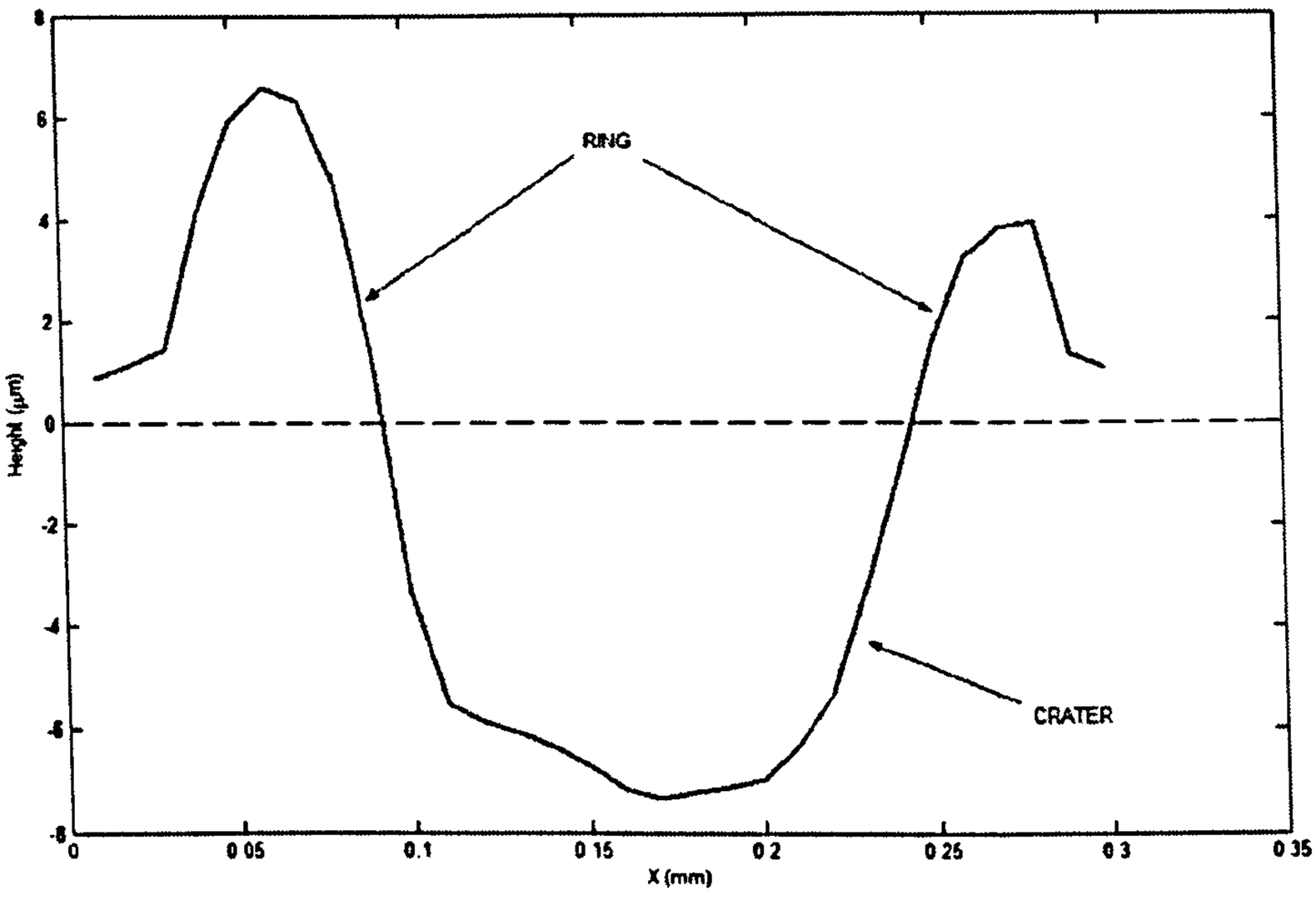

Figure 2-7 - Profile of ring on roll.

Once the roll is impressed on the sheet surface the crater will cause a small hill and the ring will produce a circular depression. The shape of an EBT sheet sample is depicted in Figure 2-8 (the texturing roll is not the one shown in the previous figures).

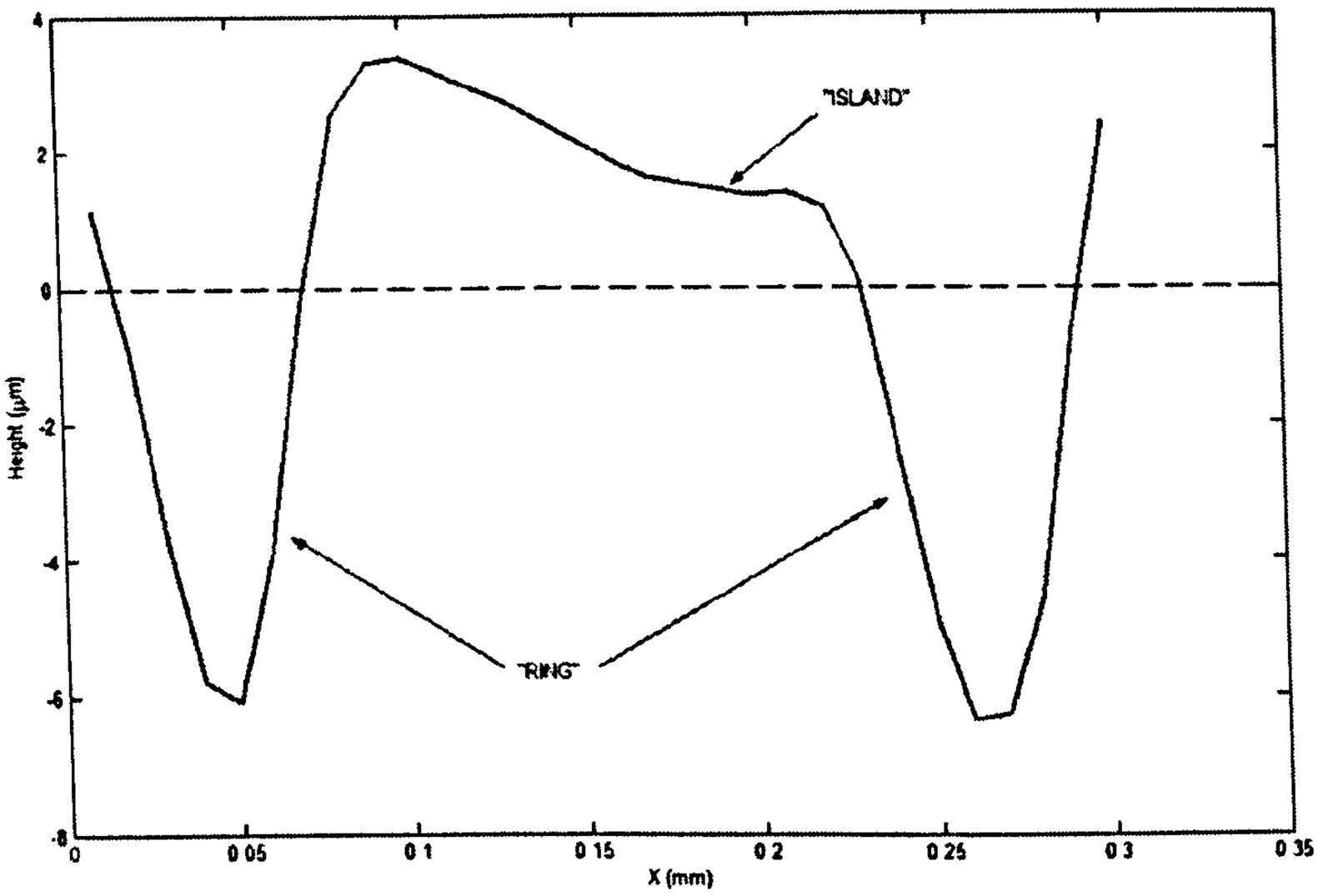

Figure 2-8 - Profile of ring on sheet.

2.1.4 Double patterned surfaces

Traditional steel production involves only one texture to be imposed on the sheet, in the skinpass section. In order to obtain an apparently random texture, still maintaining control over the roughness, in recent years double patterning has been introduced into production. The rolls at the tandem and skinpass mills are both roughened with an EBT texture with different parameters (orientation, rings radii and distances). This allows strict control and repeatability of the production process, introducing a higher degree of 'randomness' to the surface texture. Double patterned surfaces are analysed and discussed in section 4.

2.2 Surface Measurement technologies

Stylus instruments [Sherrington et al. 1988 (a)] are currently the "standard" for surface characterisation of surface topography on steel sheet surfaces. The measuring method is based on direct contact between the sensor (stylus) and the measured surface [Damir 1973]. Today, many stylus equipments provide for 3D measurements by simply measuring multiple parallel 2D profiles, forming a grid

of data points i.e. a raster scan to represent the surface topography. The main advantage of the stylus instrument is that the technique is well known and applicable on most kind of surfaces. Some disadvantages are that it can deform surface asperities elastically or even plastically [Pawlus et al., 2004] which can influence the measured result [McCool 1984] and, due to the slow traversing speed, the measuring times will be long, especially for 3D measurements.

Optical instruments [Sherrington et al. 1988 (b)] can be divided into two groups of measuring principles: focus detection and interferometry. An advantage of optical instruments is that they are measuring in a non-contact mode and hence do not affect the surface at all. The focus detection instruments work in a similar manner to stylus instruments except that, instead of a stylus, the measurement is performed by a light beam (usually a laser beam), which is focused onto the measurement surface as a spot of about 1μm in diameter. The measuring speed is often considerably greater than that of stylus instruments and is dependant on the control system, which keeps the light beam in focus at the surface. Since this method completely relies on how accurate the focus can be detected on top of the surface it is sensitive to high slopes in the surface topography. The critical angle of surface inclination is often between 10-15 degrees. For steel sheet surfaces the maximum slope is between 5-10 degrees hence, steel sheet surfaces are suitable for measurement with focus detection systems [Sacerdotti 2000]. Of instruments based on interferometry the Vertical Scanning Interferometry (VSI) instruments are the most used. The measurement principle is based on white-light which is directed, by a beam splitter, to the surface and to a reference mirror and when the two light beams are recombined, interferometric fringes occur. The fringes are detected by a CCD-camera. By moving the optical system vertically the fringes pattern changes dependant on the surface topography of the sample. By data processing, the fringe pattern monitored by the CCD camera is transformed to surface topography data. VSI instruments produce results quickly; only seconds are needed to perform a measurement. Depending on the optical set up measurement areas from a few

microns square up to around 55 mm square can be measured. The VSI technique generates a 3D measurement but, by data processing in computer software, profile analysis is possible. The main advantage of VSI instruments is the short measurement time. For flat surfaces such as steel sheet surfaces the limited vertical measurement range of around 0.5 mm is no problem since this more than covers the range likely to be encountered. A disadvantage, which is common to optical instruments, is the sensitivity to contamination by oil and dust which may yield distorted results [Breitmeier 2004] [Bergstrom et al. 2004].

2.2.1 Stylus instruments

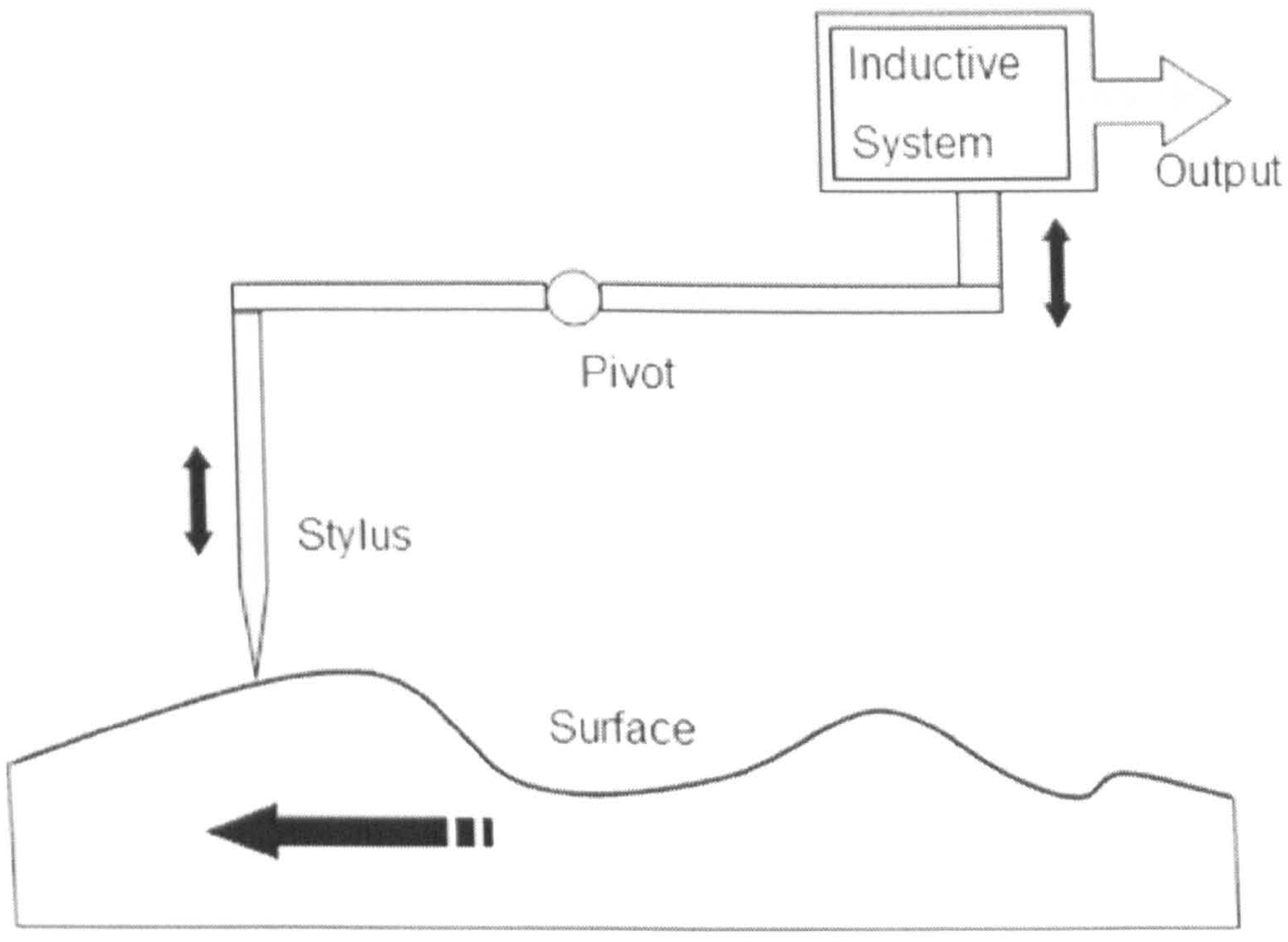

Figure 2-9 – Stylus System

Stylus instruments [Whitehouse 1994] are the standard measuring devices for surface characterization, and they are based on the contact of a sensor (stylus) with the surface. Figure 2-9 shows the working principle of stylus instruments.

Although contact instruments can measure only "lines" across the surface, 3D measurements are performed by simply repeating the linear measurements along a set of parallel lines, thus creating a matrix of points.

The technique is very time-consuming, especially in the case of 3D measurements, where several 2D measurements have to be taken in sequence.

Optical instruments, which include interferometric types [Whitehouse 1994] discussed in the next paragraph, have the main advantage of being non-contact devices, which means that they cannot affect the surface topography [Whitehouse 1975, Thomas 1978, Sherrington et al. 1986].

They are generally faster than stylus instruments, and can perform a surface measurement in a few minutes.

2.2.2 Focus detection optical instruments

The concept of focus detection implies that the surface heights are measured by maintaining the focus of an illuminated light spot on the sample surface. In order to maintain the focused spot on the measured surface the focusing lens (or the surface itself) has to be moved vertically, and this determines the surface heights. Since the diameter of the spot is very small (typically in the order of 1μm), three dimensional measurements can be performed via a raster scan of the spot of light over the surface. The working principle of this instrument is shown in Figure 2-10 [Scheers 1998]: a small lens directs a focused laser beam to the surface, and the reflected beam is fed to a photodiode focus detector [Hamilton et al. 1982, Mignot 1983]. The movement of the focusing lens is recorded as the height variation of the surface.

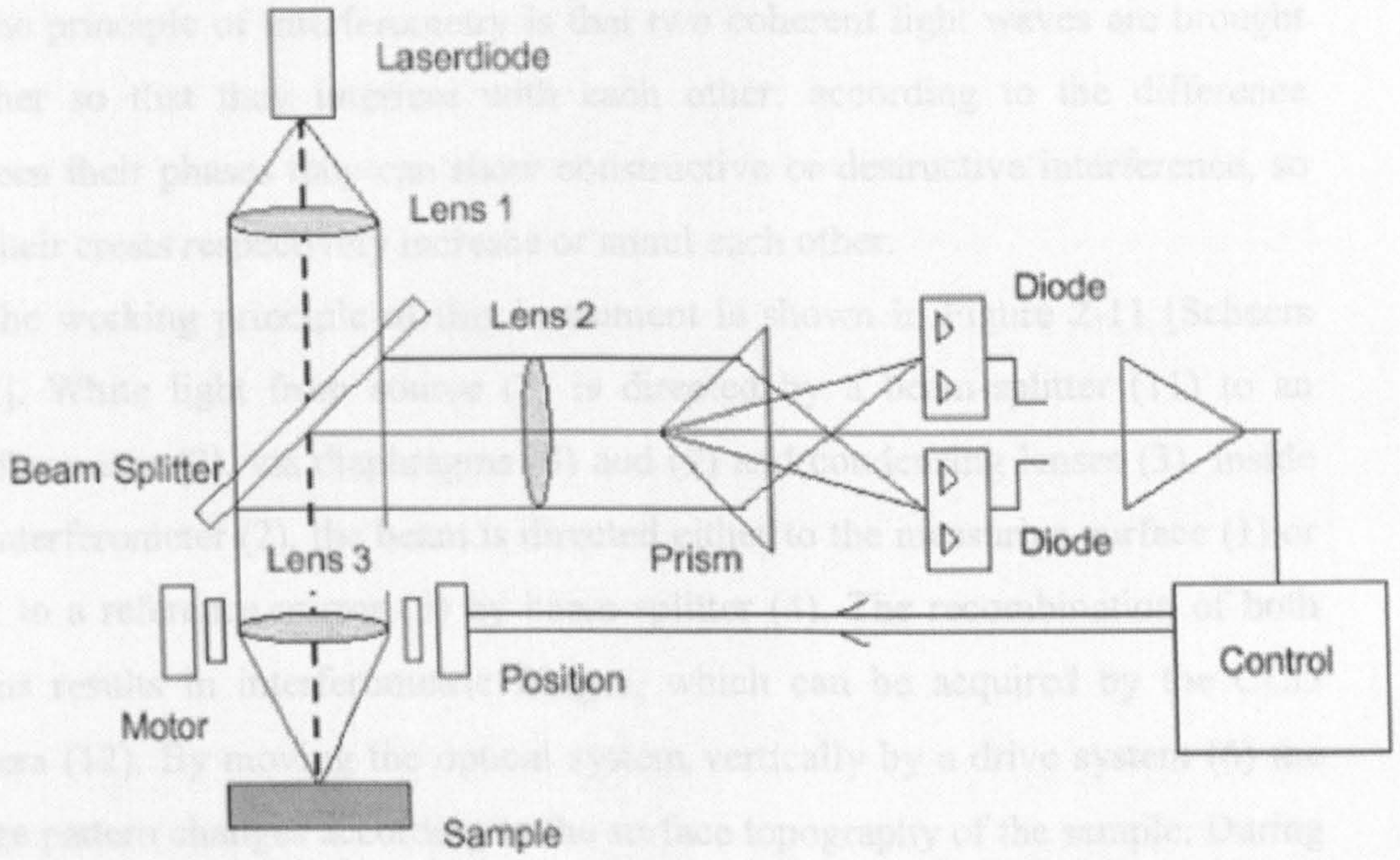

Figure 2-10 – Focus Detection Optical Instrument

2.2.3 Interferometry

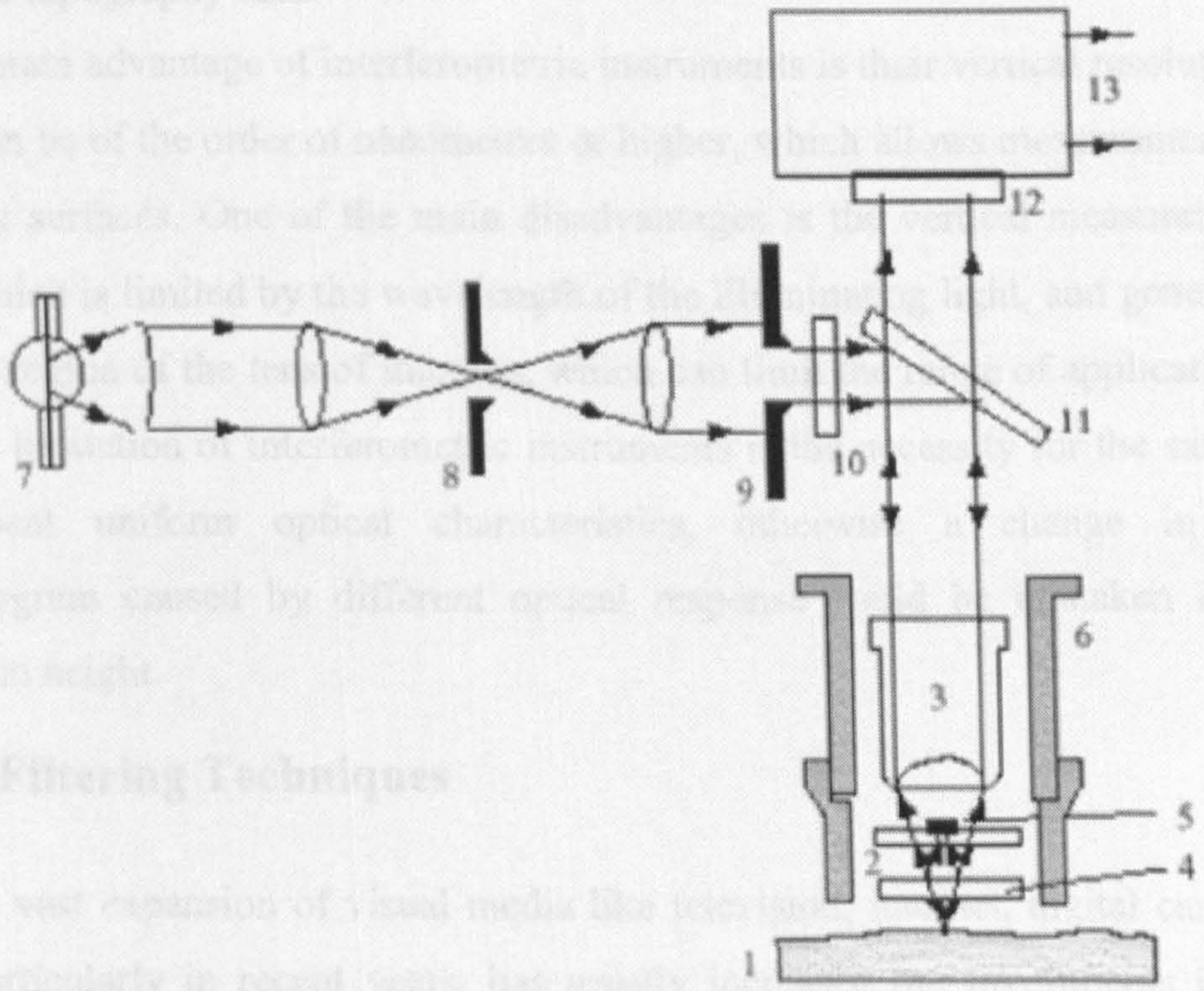

Figure 2-11 - Interferometry

The principle of interferometry is that two coherent light waves are brought together so that they interfere with each other; according to the difference between their phases they can show constructive or destructive interference, so that their crests respectively increase or annul each other.

The working principle of this instrument is shown in Figure 2-11 [Scheers 1998]. White light from source (7) is directed by a beam-splitter (11) to an interferometer (2), via diaphragms (8) and (9) and condensing lenses (3). Inside the interferometer (2), the beam is directed either to the measuring surface (1) or back to a reference mirror (5) by beam-splitter (4). The recombination of both beams results in interferometric fringes, which can be acquired by the CCD camera (12). By moving the optical system vertically by a drive system (6) the fringe pattern changes according to the surface topography of the sample. During this movement the interference signal of each CCD-pixel is monitored by a system of parallel processors, searching for maximum interference, meaning in-focus position of the corresponding sub-area of the surface [Hariharan 1985]. By data processing, the fringe pattern monitored by the CCD camera is transformed to surface topography data.

The main advantage of interferometric instruments is their vertical resolution, which can be of the order of nanometres or higher, which allows measurement of very fine surfaces. One of the main disadvantages is the vertical measurement range which is limited by the wavelength of the illuminating light, and generally is in the region of the tens of microns, which can limit the range of applications. Another limitation of interferometric instruments is the necessity for the sample to present uniform optical characteristics, otherwise a change in the interferogram caused by different optical response could be mistaken for a change in height.

2.3 Filtering Techniques

The vast expansion of visual media like television, internet, digital cameras etc., particularly in recent years, has greatly increased the investments in the image processing research field: state-of-the-art user-friendly software is

available in great quantity, and the quality of the algorithms used is guaranteed by years of research and standardisation.

Surface filtering research benefits from its strong relationship with image processing, due to the common bi-dimensional representation of data. Surfaces are defined as $\eta(x_k,y_l)$, while images are commonly represented as $f(m,n)$ [Matlab website (a)].

The following figures will help visualise these concepts.

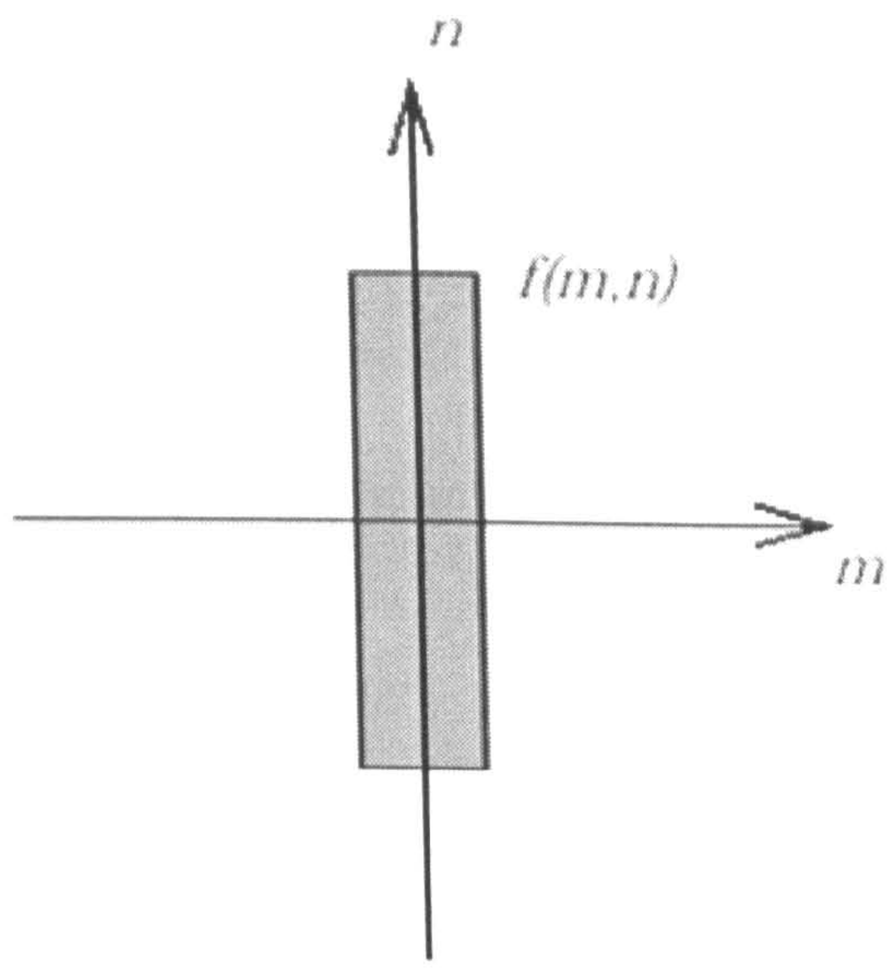

Figure 2-12 – Example image as *f(m,n)*

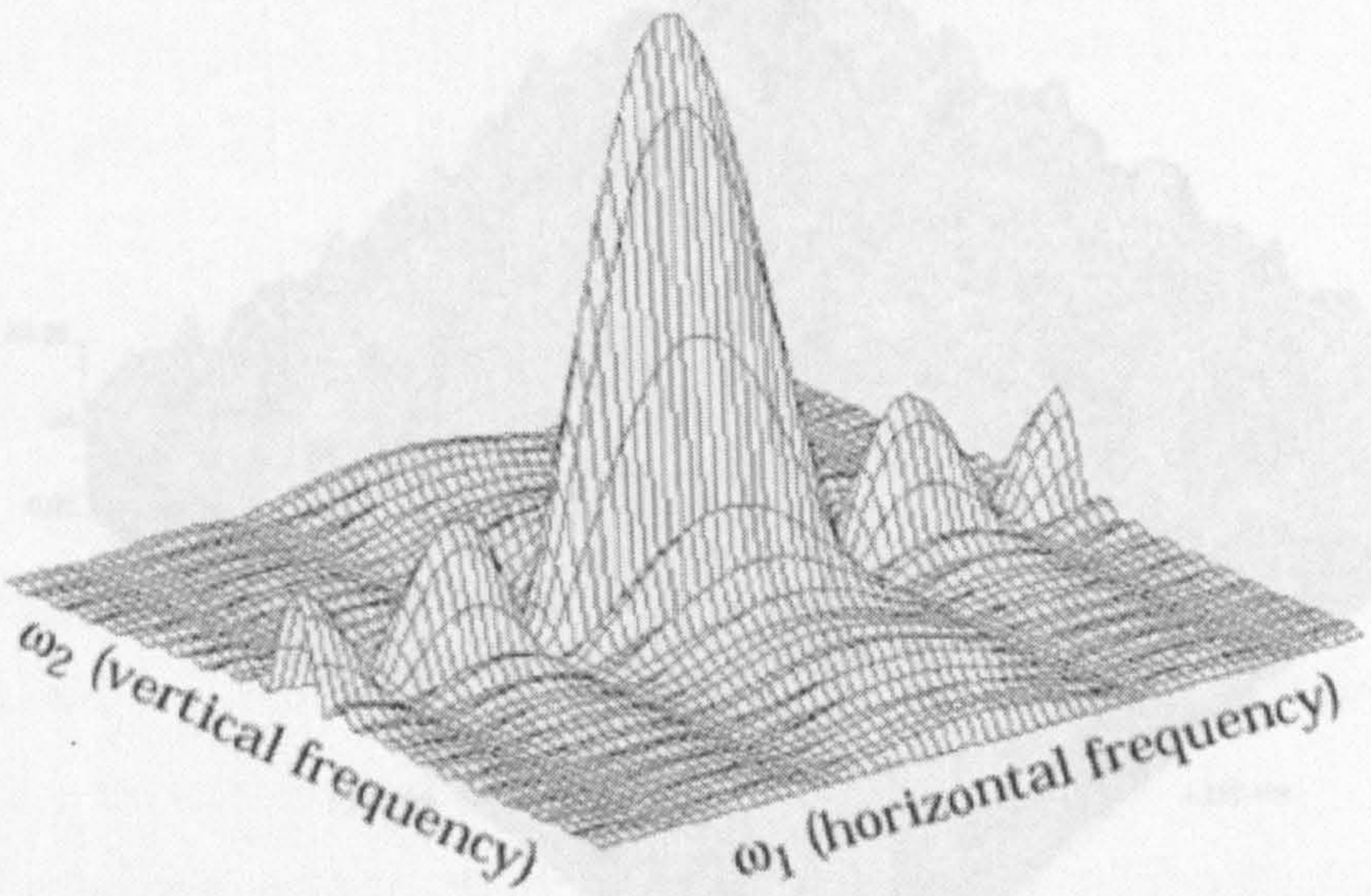

Figure 2-13 – Fourier transform of *f(m,n)*

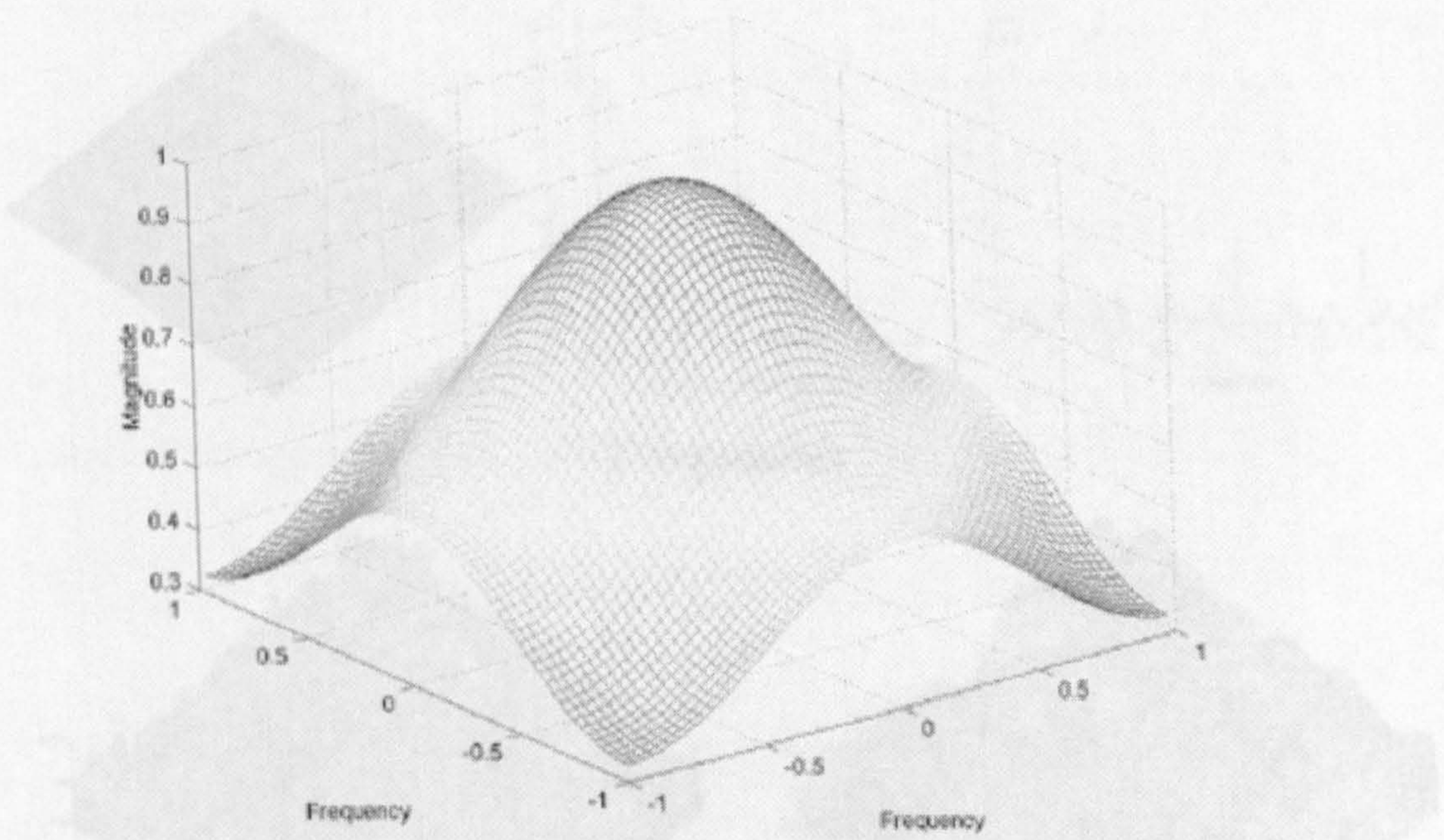

Figure 2-14 – Frequency response of an example Gaussian filter.

Figure 2-12 and Figure 2-13 show the Fourier transform of a basic image while Figure 2-14 shows a Gaussian filter, as in the Image Processing Toolbox Reference of Matlab [Matlab website (b)].

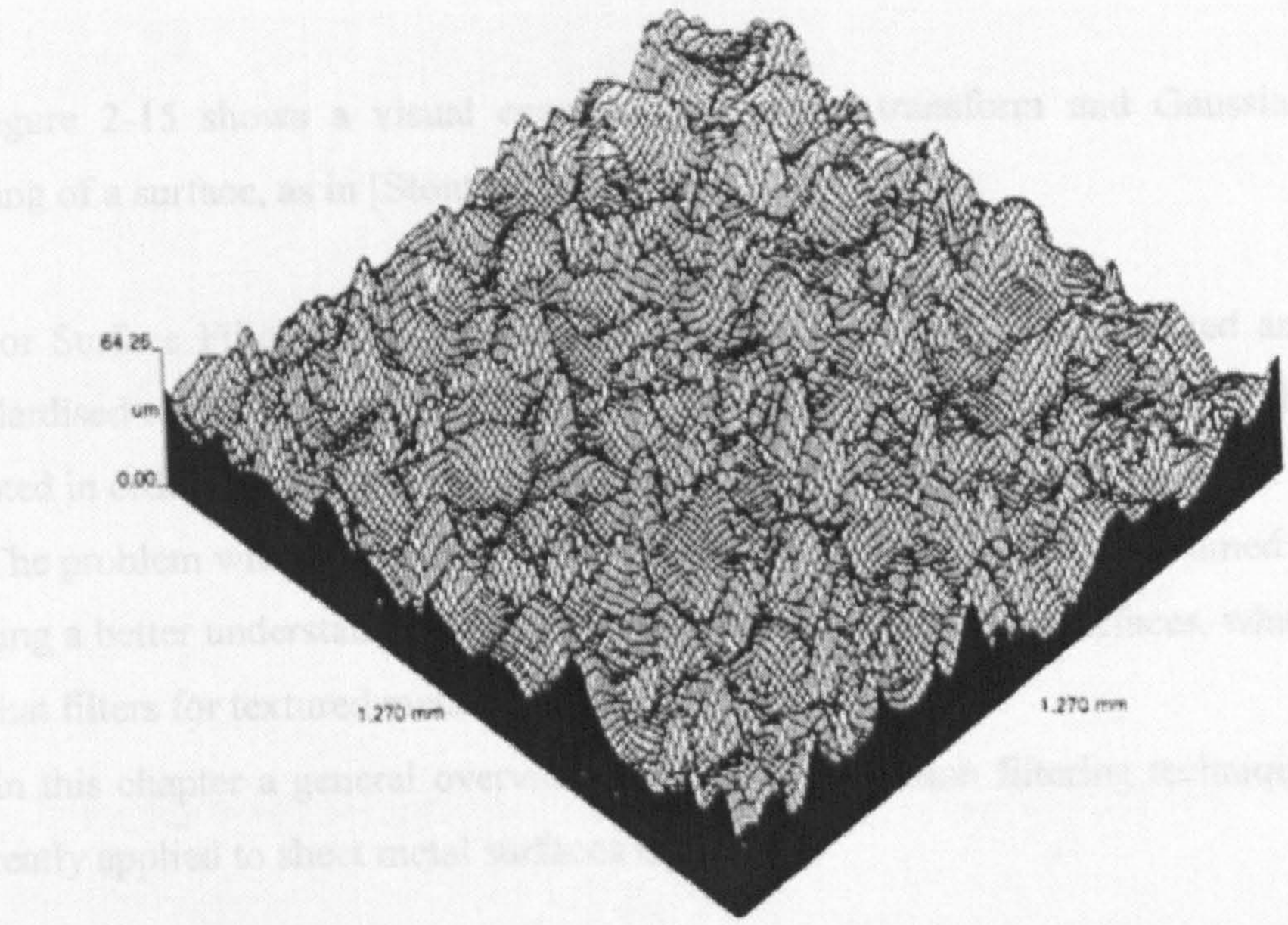

Surface (Space Domain)

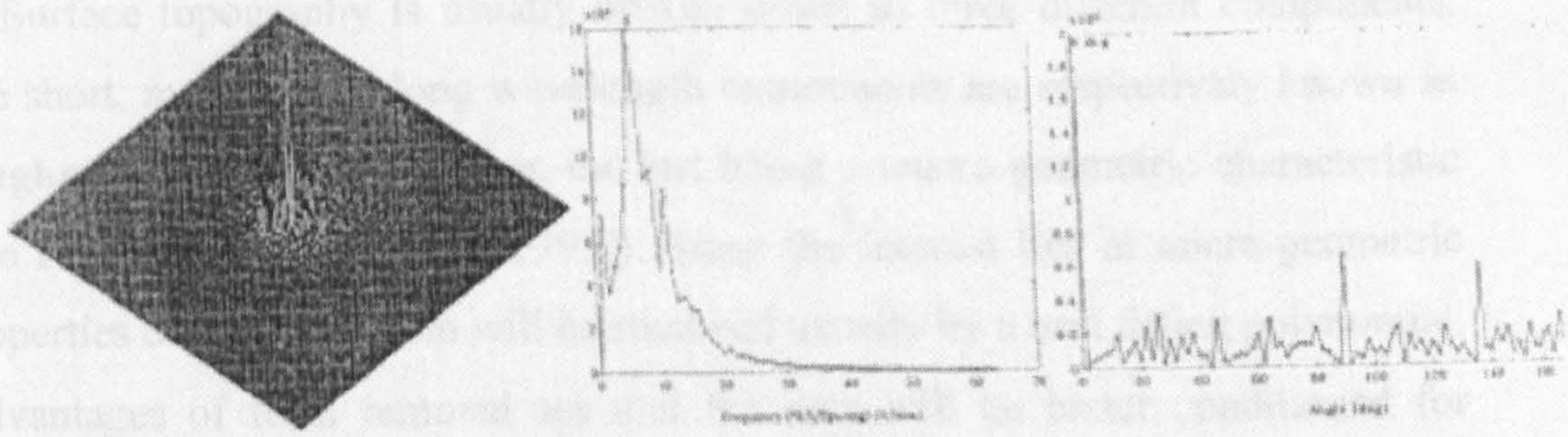

Frequencies

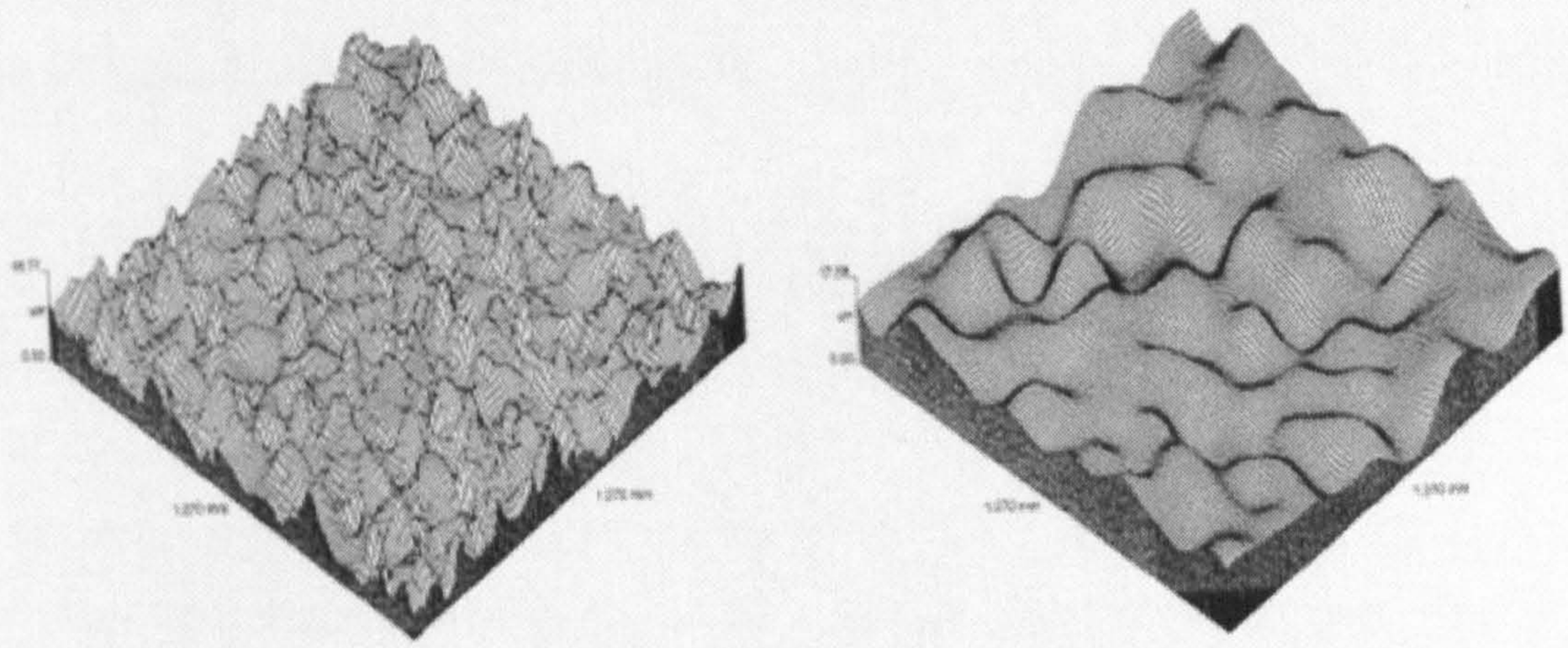

Roughness and Waviness (Gaussian Filtering)

Figure 2-15 – Gaussian filtering [Stout et al 1993]

Figure 2-15 shows a visual example of Fourier transform and Gaussian filtering of a surface, as in [Stout et al 1993].

For Surface Filtering for industrial applications, the use of established and standardised techniques is not always satisfactory, and new techniques had to be adopted in order to meet the needs of industrial production and quality control.

The problem with signal/image processing filters is that they are not aimed at gaining a better understanding of the functional behaviour of the surfaces, which is what filters for textured metal surfaces are desired to do.

In this chapter a general overview of the most common filtering techniques currently applied to sheet metal surfaces is given.

2.3.1 Frequency filtering

Surface topography is usually broken down to three different components. The short, medium and long wavelength components are respectively known as **roughness, waviness** and **form**, the last being a macro-geometric characteristic (see Figure 2-16 [Stout et al 1993]). Since the interest lies in micro-geometric properties of surfaces, form will be removed usually by a best fitting polynomial. Advantages of form removal are that the data will be better conditioned for computer calculations, i.e. smaller numbers need to be processed [Rosen 1998].

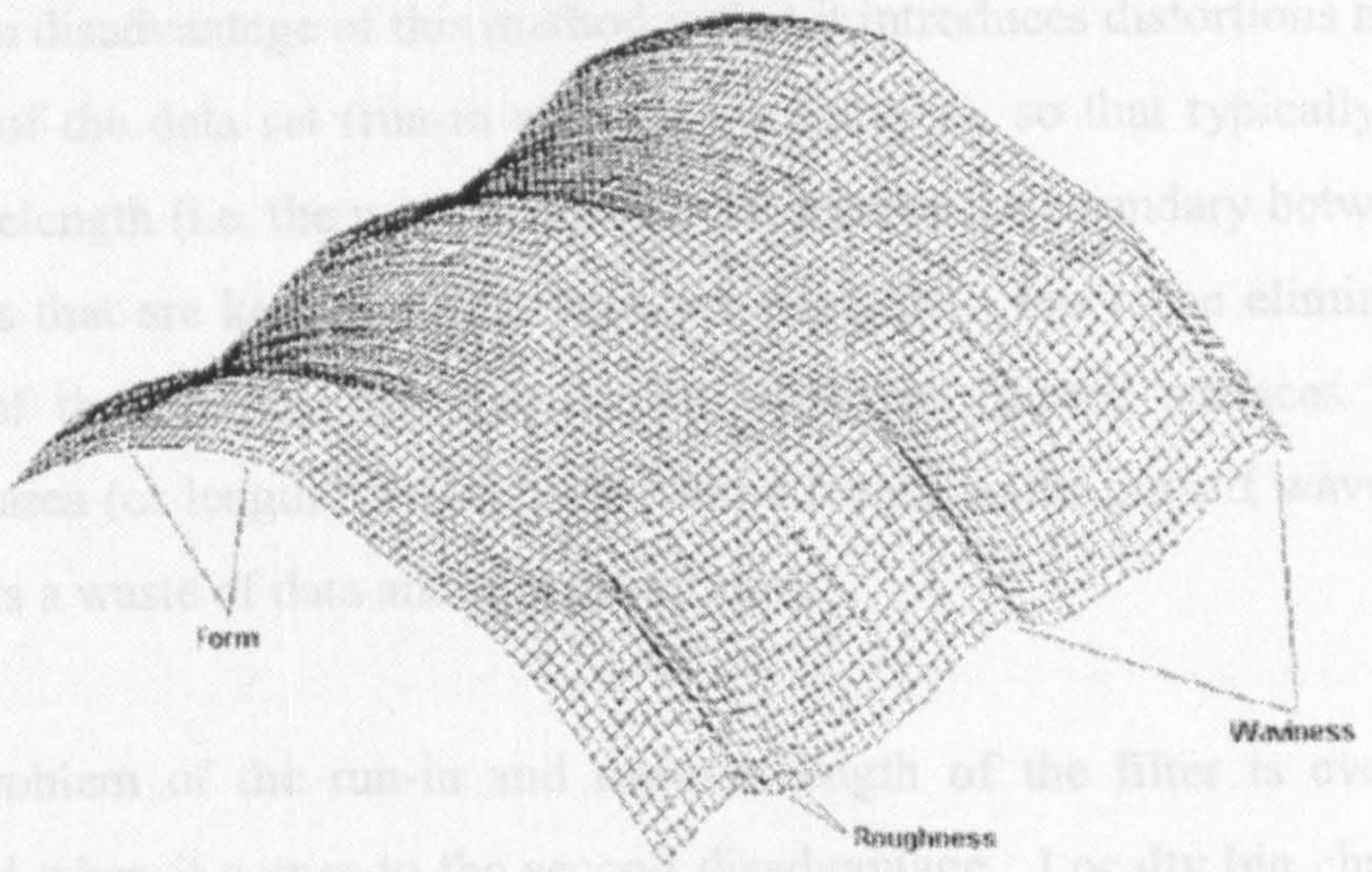

Figure 2-16 - Roughness, Waviness and Form [Stout et al 1993]

The process of separating roughness and waviness is called filtering and the most common type is by power spectral analysis (see Figure 2-15) [Stout et al 1993], switching from the time (actually space in this case) domain to the frequency domain through the Fourier transform. Waviness is generally an undesired characteristic that can often be related to production faults, while roughness is impressed on surfaces in order to obtain a certain functional behaviour, and thus needs to be controlled and measured. The problem of separating roughness and waviness lies mainly in the definition of the wavelength that separates them: there is no clear definition of the boundary between "medium" and "short" wavelengths.

2.3.2 Gaussian Filtering

Gaussian filters have for a long time been used as the standard filter for separation of wavelength bands out of the topography measurements. Today the digital Gaussian filter is standardised in 2D (ISO 11562: 1996, DIN 4777) and commonly used as well for 3D. Advantages of this filter are that it is simple to understand and implement and does not introduce incorrect phase data, i.e. wavelengths close to the cut-off wavelength will never be amplified with negative numbers (turning peaks to valleys) [Stout et al. 2000].

The main disadvantage of this method is that it introduces distortions near the boundaries of the data set (run-in and run-out lengths), so that typically half a cut-off wavelength (i.e. the wavelength that represents the boundary between the wavelengths that are kept and those that are discarded) has to be eliminated at each end of the sample, this means that Gaussian filtered surfaces will be reduced in area (or length for 2D) by the same length as the cut-off wavelength, causing thus a waste of data and measuring time.

This problem of the run-in and run-out length of the filter is even more pronounced when it comes to the second disadvantage. Locally big changes of the amplitude are also called outliers and, even if they are of small wavelength, they can have an influence on the filtered data [Rousseeuw et al. 1987, Huifen et al. 2002]. This is especially evident for a smooth surface like a fine EBT sheet with its unavoidable sharp and deep craters. The low-pass fraction of the filtered image will be distorted around the locations of the craters by induced artificial waviness, sometimes to an unacceptable extent. To overcome this the valley suppression filter was introduced (DIN 4776 and later ISO 13565-1:1996), where local valleys where removed before the filtering and "glued" back after the filtering action, in order to minimise the influence of local deep valleys. This approach solves the problem for many engineering surfaces, but still problems occur for steel sheet surfaces of the EBT type.

Another approach to the problem of outliers is the Robust Gaussian Filter, based on the maximum likelihood estimation in time-series modelling [Kay et al. 1994] [Coifman et al. 1994]. The filter has a regression approach where a re-weighting function is introduced to compensate for the variation in the quality of the data. Data assumed to have high level of precision are assigned a high weighting factor, while data with low level of precision have a low weighting factor. The filter will be regressed according to a given tolerance, so that the best mean value surface can be found.

The Gaussian filter is not very sharp in its transfer characteristics, and this means that wavelengths in a quite wide band around the cut-off wavelength will still be present in the filtered data, however, reduced in amplitude. The ideal filter has a sharp characteristic which means that the wavelength band transmitted above or below the cut-off wavelength (low-pass or high-pass filtering) is zero.

Matlab software offers a wide range of functions to perform 3D data filtering and manipulation, including many advanced and recently developed filters [Matlab website (a)].

2.3.3 Wavelet filters

The main disadvantage in Fourier analysis applied to surface characterisation is the fact that it provides only frequency-based information, so that no information about location is given. Wavelet analysis represents an attempt to overcome this problem, transforming space domains into scale-based domains, which not only represents the frequency events, but also shows their location [Swelden 1994(a)].

Wavelet filters are based on the concepts of wavelet transform, just as Fourier filters originate from the theory of Fourier transform; where Fourier analysis decomposes a signal into harmonics, wavelet analysis uses translated and dilated (or compressed) versions of a function ?, called the mother wavelet [Lee et al. 1998].

Many types of wavelets have been proposed and applied in signal processing, each presenting different advantages for various applications; in general their main disadvantage is the complexity of their algorithms, which often makes their use too time-consuming for practical applications.

In particular for surface analysis a cubic lifting wavelet [Jiang et al. 1998] filter was introduced in order to apply the advantages of the wavelet approach to surface filtering. This filter is built using a lifting scheme [Swelden 1994(b)], which has the great advantage of having a very simple and fast algorithm.

The application of wavelets to the isolation of features has given satisfactory results over a variety of applications, but unfortunately the problem of identifying and isolating EBT rings on rolls and sheets is not suitable for wavelet analysis: firstly, the shape of the features varies too much from one surface to the other to allow the choice of one mother wavelet that suits them all. Secondly, the introduction of multiple patterns complicates greatly the problem, introducing an increasing level of randomness in the surface. Thirdly, the computational complexity of wavelets is incompatible with the time limits imposed by the on-line process control environment.

2.3.4 Other frequency filters

All the common 2D frequency filters can be applied to surfaces just obtaining a three-dimensional version of their frequency response, an operation easily implemented in Matlab.

Figure 2-17 shows a normal EBT surface, and in Figure 2-18 and Figure 2-19 its Fourier Transform is depicted. It can be noticed the concentration of the signal in the lowest frequencies area, and the regular pattern of peaks clearly visible in the 'colourmap' representation.

In Figure 2-20 the frequency response of a low-pass filter is shown on the left, and its 3D version can be seen on the right (the filter shown is called "equiripple" because of the regularity of the amplitude of the oscillations inside and outside the pass-band). By simply multiplying the Fourier Transform of the given surface by the filter's frequency response, it is possible to obtain the filtered surface in the frequency domain.

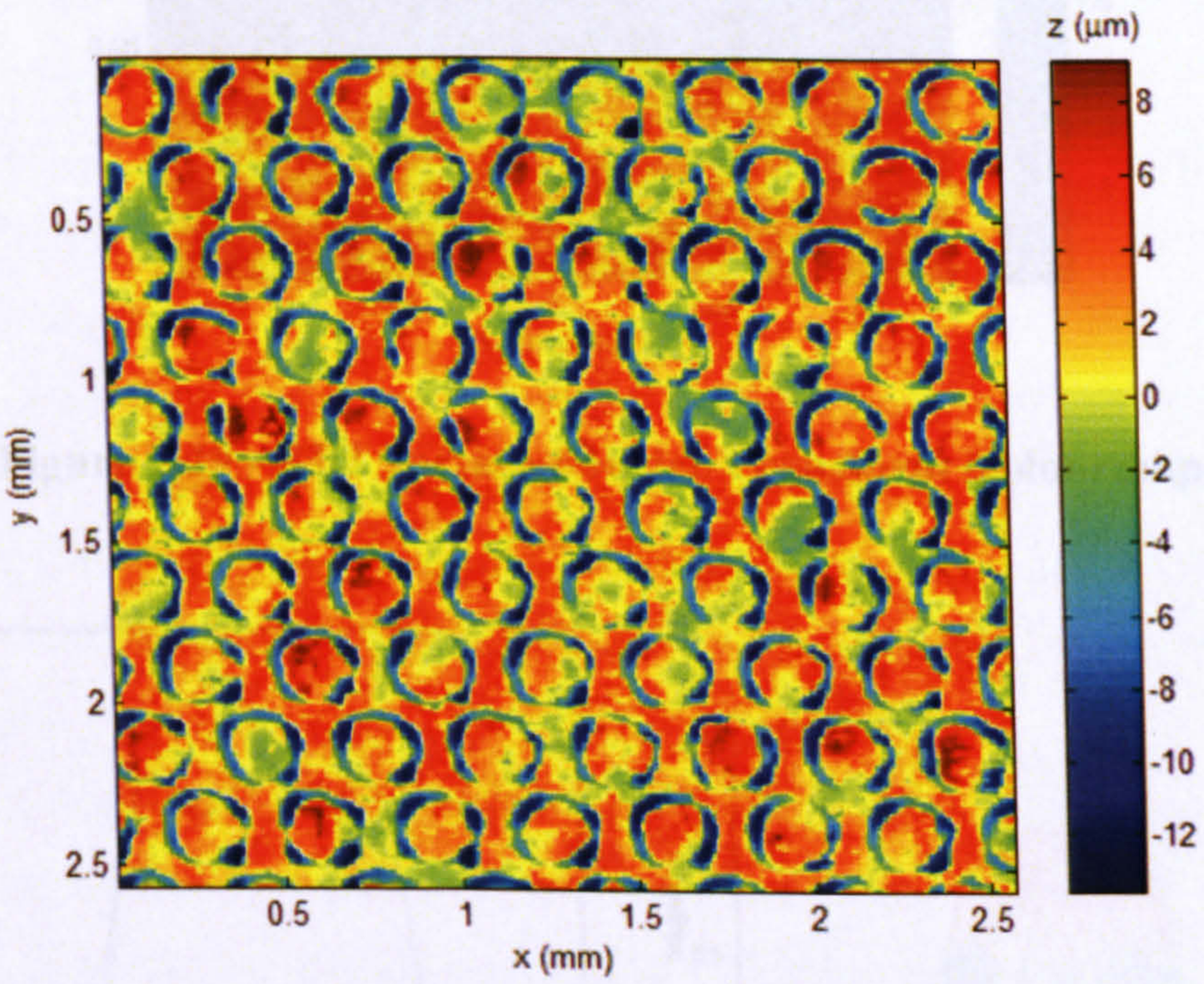

Figure 2-17 – EBT Surface

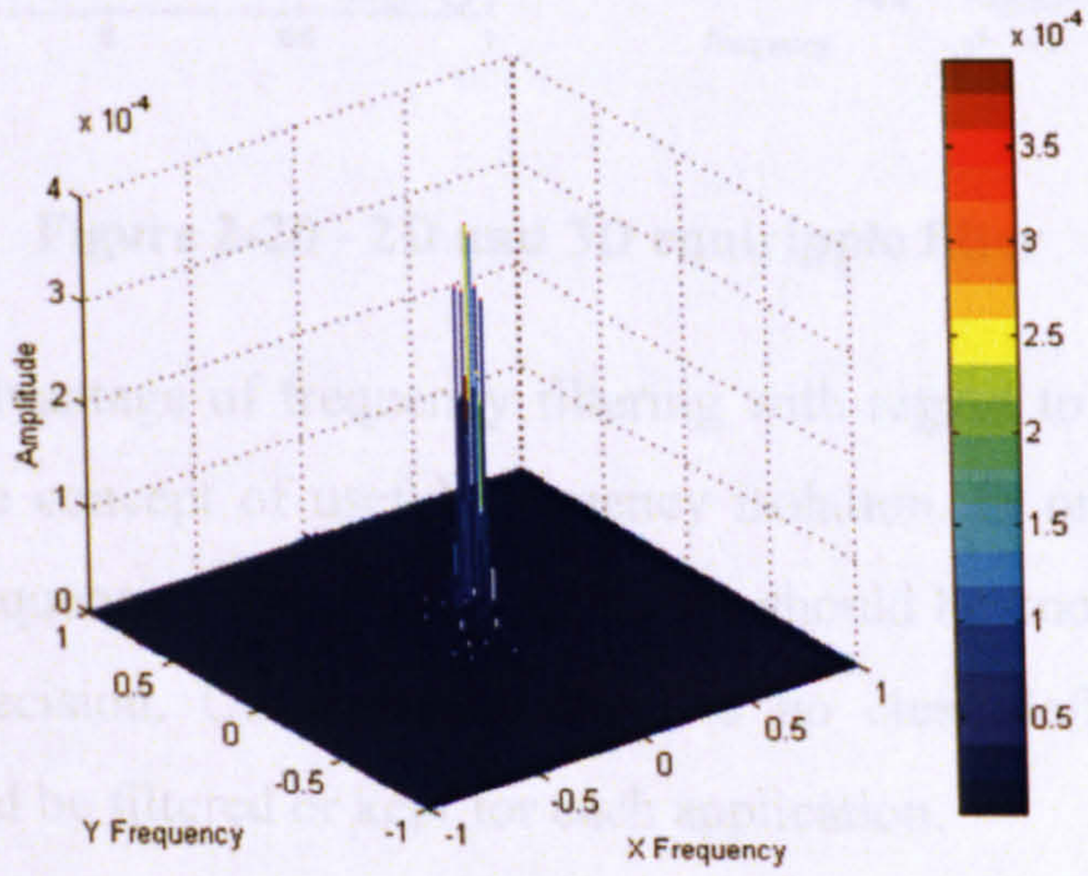

Figure 2-18 – EBT surface Fourier Transform (isometric view)

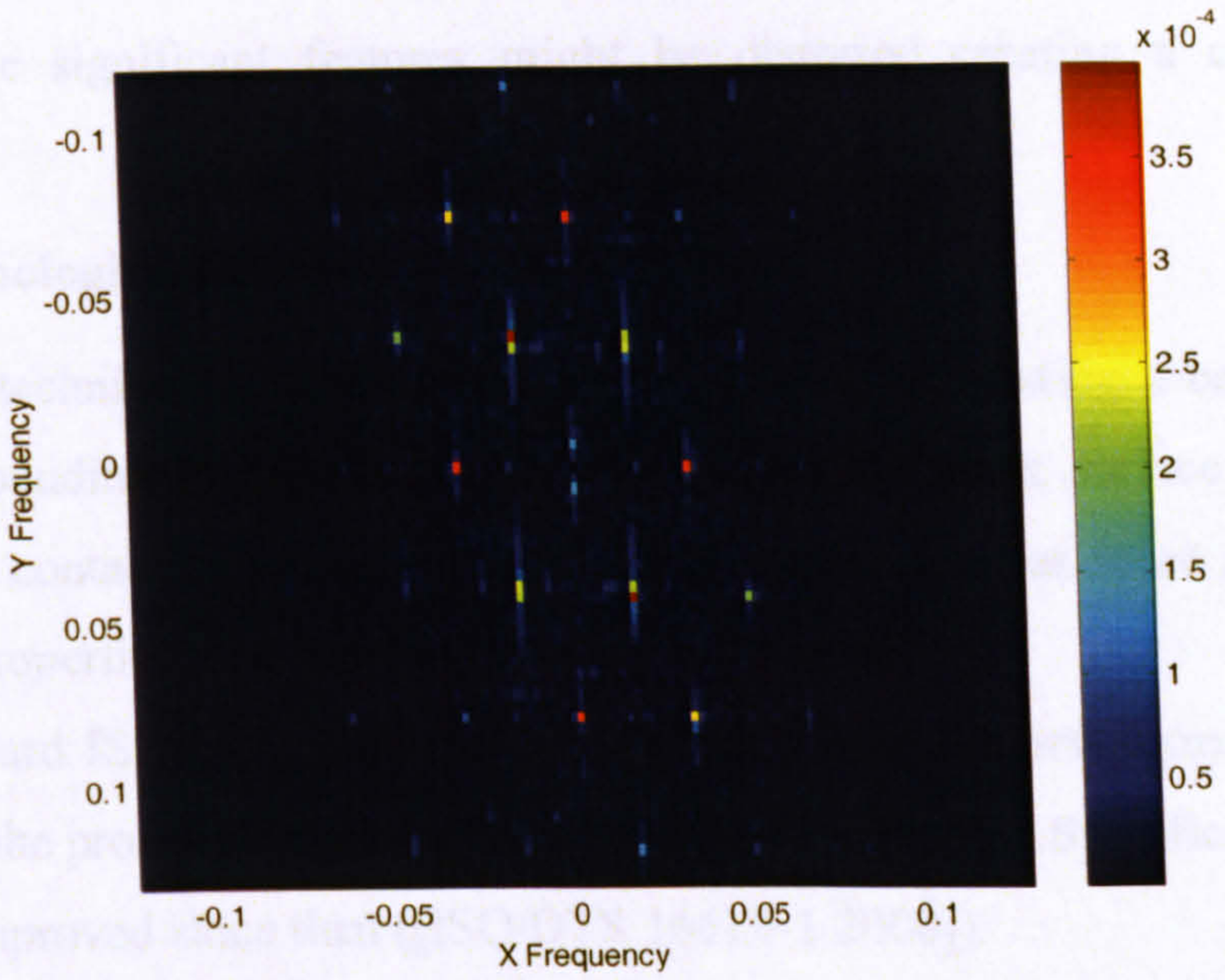

Figure 2-19 - EBT surface Fourier Transform (colourmap)

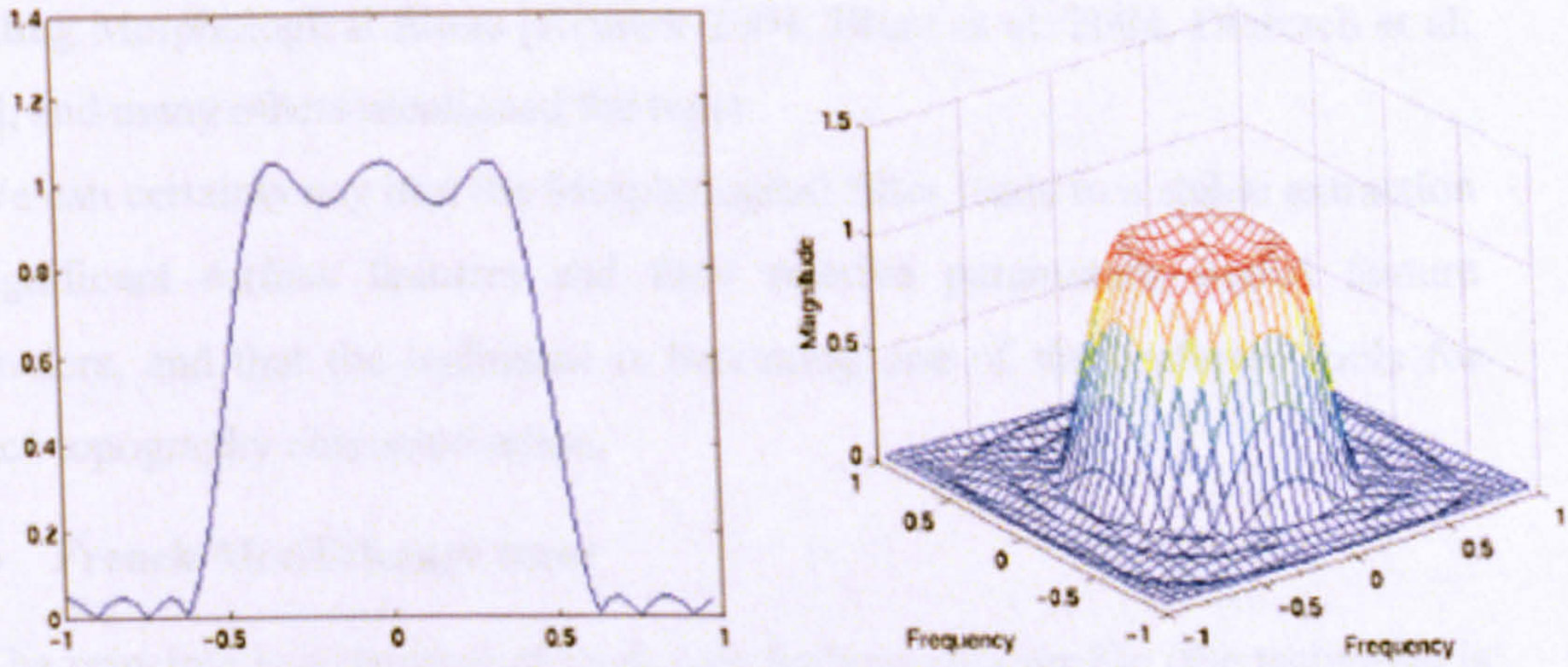

Figure 2-20 - 2D and 3D equiripple filter

The main disadvantage of frequency filtering with regard to the purpose of this research is the concept of useful frequency isolation. In order to obtain a useful filter the frequencies that are of importance should be known a priori and with a certain precision. Unfortunately there is no clear definition of what wavelengths should be filtered or kept for each application.

Moreover, frequency filters assume that a surface can be decomposed into similar sinusoids with different wavelengths; unfortunately, real surfaces contain

multi-scalar features that do not necessarily present periodic frequencies, therefore some significant features might be distorted creating a confusing output.

2.3.5 Morphological filters

This new technique constructs a reference line by simulating a ball with a radius corresponding to the die radius rolling over the sheet surface. Since it simulates the contact between two surfaces, it is perceived as more related to tribological properties than standard filtering techniques.

The standard ISO 3472 published in 1993 contains the first formal official definition of the profile method for GPS (Geometrical Product Specification) and it has been improved since then ([ISO/DTS 16610-1 2000]).

At the present the technique is widely adopted and accepted by the research community, but is also still a matter for further research. At the Chemnitz International Colloquium of Surfaces ICS2004 at least 3 papers were presented regarding Morphological filters [Krystek 2004, Blunt et al. 2004, Dietzsch et al. 2004], and many others mentioned the topic.

We can certainly say that the Morphological filter leads to a stable extraction of significant surface features and their relative parameters, called feature parameters, and that the technique is becoming one of the preferred tools for surface topography characterization.

2.3.6 French Motif/change trees

The principle is a removal of irrelevant features of a profile (the technique is applied to bi-dimensional data) using simple algorithmic rules [Scott 2000, Takahashi et al 1995]. The technique has been used since the early nineteen-eighties, particularly in the French Automotive industry, and it has been improved, studied and developed since.

The potential of the technique is widely recognised, and modern ways of interpreting French Motifs or new ways to implement them are still being evaluated. Scott in particular [ISO Standard 12085, Scott 1997] has carried out research work in order to adapt French Motifs to 3D analysis, leading to the

definition of the 3D Areal Motif Technique: this technique is highly functionally oriented and makes the advantages of traditional motifs available for surface characterisation.

2.3.7 Discussion

Filtering technology in surface metrology has been reviewed, with particular emphasis to the functional characteristics of each technique.

Each filtering method presents advantages and disadvantages, and different applications call for different filters. Morphological filters and 3D Areal Motifs are the most functionally oriented methods, and the only ones aimed to describe the significant morphological features of areal measurements; none of the existing techniques is specifically designed for the isolation of the periodic features of deterministic textured surfaces, which is the main purpose of this work.

For the Statistical Filter Project surfaces have been pre-filtered using a first order polynomial removal (elimination of the regression plane); higher order polynomial removal or Gaussian filters have been used in some cases (see section 5) to obtain smoother autocorrelation functions, necessary for the technique (see section 2.5).

2.4 Surface Parameters

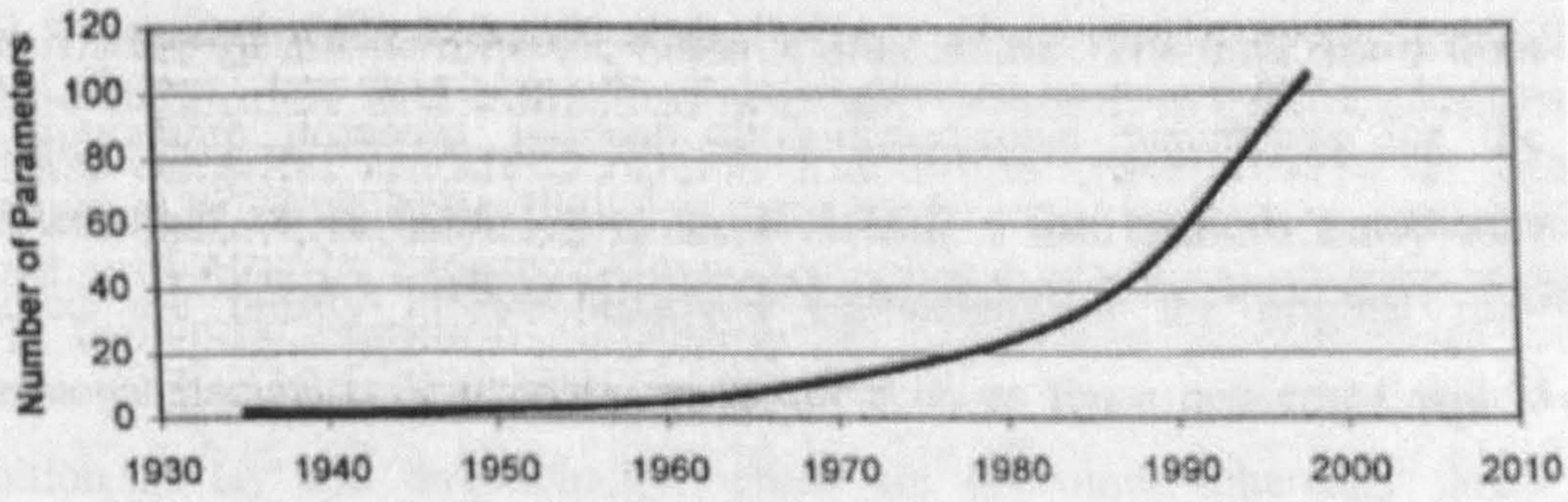

Figure 2-21 - The "Parameter Rash"

In 1982 it was suggested [Whitehouse 1982] that the number of parameters for surface finish measurements was becoming too large: this phenomenon was

referred to as "The parameter rash". It can be noticed in Figure 2-21 [Hedziora et al. 2004] that since 1982 the rash did not slow down at all: it seems to have accelerated instead.

Publications and discussions of all sorts have targeted the problem, but no solutions have been adopted yet, likely because the research community is still confused and divided on the topic [Leach et al. 2002].

On the one hand, different textures call for different parameters, and so do different production processes, and especially different applications of the sheets; these and other factors have been increasing throughout the years (more textures proposed, new production processes adopted, innovative filtering techniques, etc.), hence the rash.

On the other hand, researchers, suppliers and customers have the problem of choosing between a hundred and more parameters. Especially they need to agree on the parameters to adopt for the determination of the quality related tolerances.

The solution of the problem is not near, and is not in the scope of this work: the parameters calculated and studied in Section 6 are the ones OCAS has indicated for EBT production quality control. Their variability and validity has been studied, but with no means of industrial standardisation, at least at the present time.

The first attempt to provide a three-dimensional set of parameters came as a result of a European Union funded research programme. The final report from this programme proposed fourteen three-dimensional parameters for the characterisation of surfaces [Stout et al 1993]. The fourteen parameters proposed are mostly three-dimensional equivalents of the original two-dimensional parameters but some are novel such as those concerned with a definition of lay and directionality, which are of course inherently three-dimensional in nature. All 14 parameters were given the designation 'S' to represent surface. The 'Birmingham Fourteen' (termed the "B'ham 14") parameter set as they have become known have since been used by many

workers, particularly since these parameters have now been incorporated into standard surface finish measuring equipment and instruments.

Name	Description / Functional Characteristics
Sq	**Root Mean Square Deviation of the Surface.** This is a dispersion parameter defined as the root mean square value of the surface departures within the sampling area. Statistically it is the standard deviation of the height distribution.
Sz	**Ten Point Height of the Surface.** This is an extreme parameter defined as the average value of the absolute heights of the five highest peaks and the depths of the five deepest pits or valleys (eight neighbours method) within the sampling area.
Ssk	**Skewness of Topography Height Distribution.** This is the measure of asymmetry of surface deviations about the mean plane. This parameter can effectively be used to describe the shape of the topography height distribution. For a Gaussian surface which has a Symmetrical shape for the surface height distribution, the skewness is zero. For an asymmetric distribution of surface heights, the skewness may be negative if the distribution has a longer tail at the lower side of the mean plane. It will be positive if the distribution has a longer tail at the upper side of the mean plane. This parameter can give some indication of the existence of "spiky" features.
Sku	**Kurtosis of Topography Height Distribution.** This is a measure of the peakedness or sharpness of the surface height distribution and characterises the spread of the height distribution. A Gaussian surface has a kurtosis value of 3. A centrally distributed surface has a kurtosis value larger than 3 whereas the kurtosis of a well spread distribution is smaller than 3. By a combination of the skewness and the kurtosis, it may be possible to identify surfaces which have a relatively flat top and deep valleys.
Sds	**Density of Summits of the Surface.** This is the number of summits of a unit sampling area (eight neighbours method)
Str	**Texture Aspect Ratio of the Surface** This is a parameter used to identify texture strength i.e. uniformity of texture aspect. It is defined from the auto-correlation function. Str can be defined as its ratio of the fastest to slowest decay to correlation length, 0.2, of the AACF function. In principle, the texture aspect ratio has a value between 0 and 1. Larger values, say Str>0.5, of the ratio indicates uniform texture in all directions i.e. no defined lay, Smaller values, say Str<0.3, indicates an increasingly strong directional structure or lay. Since the size of the sampling area is finite, it is possible that the slowest decay of the AACFs of some anisotropic surfaces never reaches 0.2 within the sampling area. In this case the longest distance of the AACF along the slowest decay direction can be used instead.
Sal	**The Fastest Decay Auto-correlation Length.** This is a parameter in length dimension used to describe the auto-correlation character of the AACF. It is defined as the horizontal distance of the AACF which has the fastest decay to 0.2. In other words the Sal is the shortest autocorrelation length that the AACF decays to 0.2 in any possible direction. For an anisotropic surface Sal is in a direction perpendicular to the surface lay. A large value of Sal denotes that the surface is dominated by low frequency (or long wavelength) components. While a small value of the Sal denotes the opposite situation.
Std	**Texture Direction of the Surface.** This is the parameter used to determine the most pronounced direction of the surface texture with respect to the y axis within the frequency domain, i.e. it gives the lay direction of the surface.
SΔq	**Root mean square value of surface slope within the sampling area**

Ssc **Arithmetic Mean Summit Curvature of the Surface.**
This is defined as the average of the principal curvatures of the summits within the sampling area. The sum of the curvatures of a surface at a point along any two orthogonal directions is equal to the sum of the principal curvatures.

Sdr **Developed Interfacial Area Ratio.**
This is the ratio of the increment of the interfacial area of a surface over the sampling area. The developed interfacial area ratio reflects the hybrid property of surfaces. A large value of the parameter indicates the significance of either the amplitude or the spacing or both.

Sm **Material Volume of the Surface.**
The material volume is defined as the material portion enclosed in the 10% bearing area and normalised to unity. The material volume and the material volume ratio are not only geometrical descriptors of the surface, but also have significant functional implications. The material volume may reflect wear and the running-in properties. On the other hand, for a "flat-topped" surface, such as a honed surface, the material volume ratio may increase quickly, whereas for a spiked surface, such as a bored surface, the function shows a slow increase with the truncation level. Thus functionally, the material volume reflects the resistance against wear and friction. Surfaces with a rapid increase in the material volume ratio show good running-in properties whereas those with a slow increase of the functions indicates that the top part of the material is easily worn.

Sc **Core Void Volume of the Surface.**
A core void volume is enclosed from10% to 80% of surface bearing area and normalised to the unit sampling area.

Sv **Valley Void Volume of the Surface.**
The valley void volume of the unit sampling area is defined as a void volume at the valley zone from 80% to 100% surface bearing area. The void volume is proposed here to provide a direct inspection of lubrication and fluid retention of surfaces. It represents the fluid retention ability of a highly worn surface. For a flat topped surface, such as a honed surface, the core void volume may decrease quickly with the truncation level, whereas for a spiked surface, such as a bored surface, the function shows a slow decrease. Thus functionally, the void volumes reflect the fluid retention property.

The Belgian Steel Industry Research Association tested the Birmingham 14 parameters with automotive panel pressing performance and also proposed further parameters specifically for defining EBT surfaces [Vermeulen et al 1995].

A German research group from the University of Erlangen-Nuremberg suggested parameters (acl, aop, aclm exemplified in Figure 2-22) which define fluid retention properties [Pfestorf et al 1998].

The research conducted within the Autosurf Consortium led to the formulation of a few innovative parameters that could be considered stable with respect to the maximum number of factors, such as software, measurement system, filtering, etc. [Autosurf website], [Sacerdotti et al. 2000(c)].

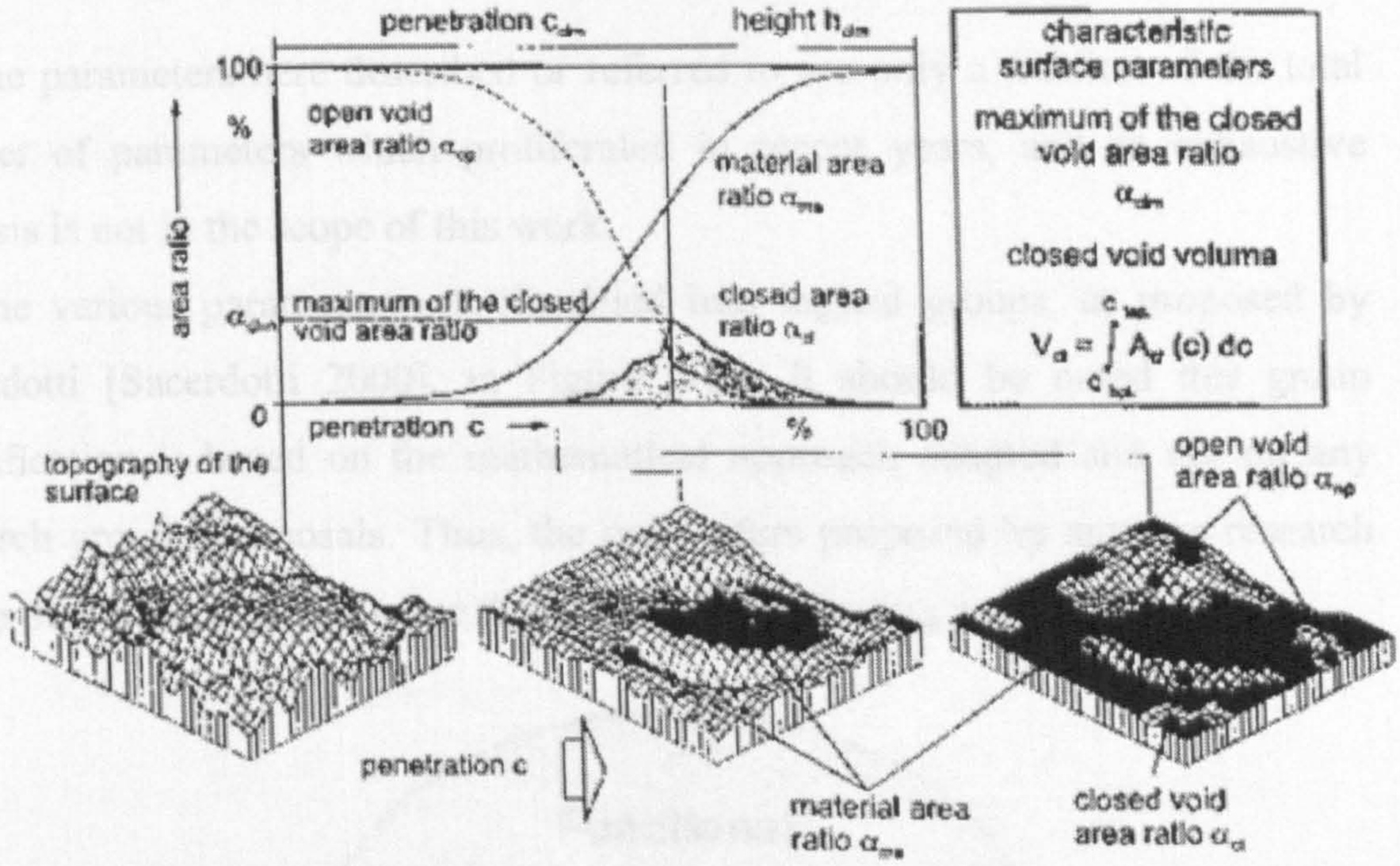

Figure 2-22 - Void Volume Parameters

An exhaustive analysis of the existing parameters and their relation with functional performances has been carried out by Sacerdotti [Sacerdotti 2000] at Brunel University, again as part of the Autosurf Project; with respect to the scope of the Statistical Filter Project, the conclusions can be summarised in two main points:

- Most of the parameters resulted highly unstable with respect to the sampling area or the frequency range of the surfaces [Sacerdotti et al. 2000(e),(b),(f)]
- Some areal parameters are correlated with functional performances of the surfaces, but due to the wide range of functional requirements, it is impossible to find a functional characterisation method that covers them all.

2.4.1 Discussion

The parameters here described or referred to are only a fraction of the total number of parameters which proliferated in recent years, and an exhaustive analysis is not in the scope of this work.

The various parameters are classified into logical groups, as proposed by Sacerdotti [Sacerdotti 2000], in Figure 2-23. It should be noted this group classification is based on the mathematical approach adopted and not on any research group's proposals. Thus, the parameters proposed by any one-research group may be included in more than one of the following groups.

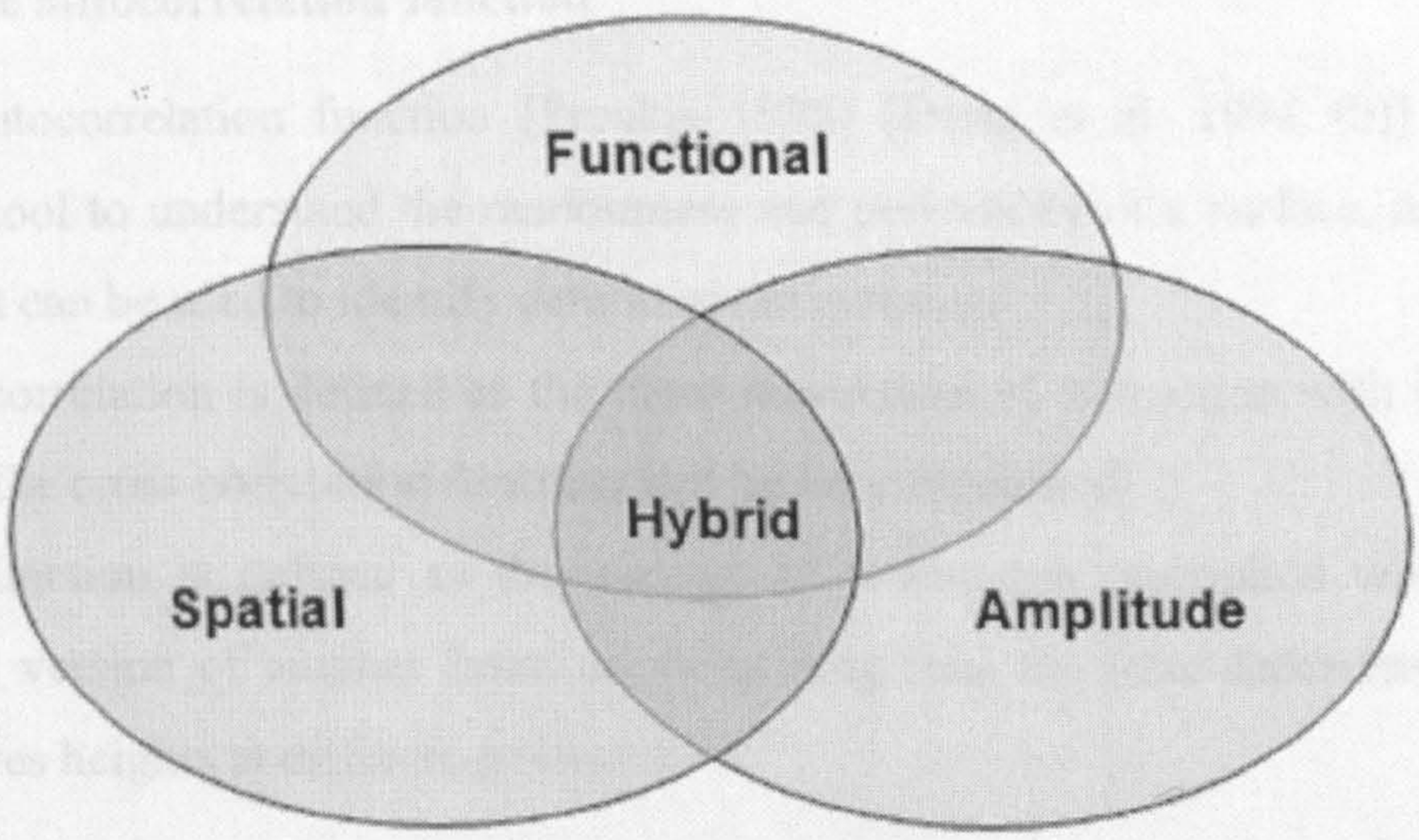

Figure 2-23 - Parameters classification

The approach to the characterisation of surfaces in 3D appears to be different between academia and industry. Industrialists want a few simple parameters, preferably expressed in physical units which can be used for convenient process control. On the other hand, academics tend to take a more complex view and derive parameters that are not always easy to use practically. These two views are essentially opposing and sometimes in conflict!

In conclusion, the choice of the surface parameters to adopt in each application is still left to the researchers/industries involved, and there is no clear standardised code of practice for their use. This leads to confusion, on the one

hand, and to an 'anarchic' freedom in the use of the existing parameters or in the creation of new ones on the other hand.

2.5 EBT Statistical Filter

This filter was made public on May 2000 by the publication of the paper "Application of Gram-Schmidt Decomposition for Filtering of Electron-Beam-Textured Surfaces" [Porrino et al., 2000]. An accurate description of the filter and its outcomes is given in this chapter, starting with the introduction of the autocorrelation function, the mathematical core of the filter.

2.5.1 The autocorrelation function

The autocorrelation function [Proakis 1995] [Dong et al. 1994 (b)] is a powerful tool to understand the randomness and periodicity of a surface, and in this case it can be used to identify deterministic patterns.

Auto-correlation is defined as the cross-correlation of a function with itself, therefore the cross-correlation function will be here illustrated.

The function is defined as the average of a function multiplied with the translated version of another function, describing thus the inter-dependence of the surfaces heights at different positions.

Definition 2-1: Let $\eta(x_k,y_l)$, with $k=0,..,M-1$, $l=0,..,N-1$ represent a distribution of surface heights, being $x_k=x_0+k\Delta_x$ and $y_l=y_0+l\Delta_y$, where (x_0,y_0) is the left bottom corner of the surface domain.

The surface representation defined above will be referred to as $\eta(x_k,y_l)$ for the remaining of this project. The autocorrelation function will be referred to as $R(\tau_i, \tau_j)$ where $\tau_i=i\Delta_x$ and $\tau_j=j\Delta_y$.

Then the cross-correlation function (XCF) for two surfaces η_1 and η_2 is defined as [Dong et al., 1994 (b)]:

$$R(i\Delta_x, j\Delta_y) = E[\eta_1(x,y)\eta_2(x+i\Delta_x, y+j\Delta_y)] =$$

$$= \frac{1}{(M-|i|)(N-|j|)} \sum_{k=k_1}^{k_2} \sum_{l=l_1}^{l_2} \eta_1(x_k, y_l)\eta_2(x_{k+i}, y_{l+j}) \qquad \text{[Equation 2-2]}$$

where

$i \in [-(M-1), M-1]$, $j \in [-(N-1), N-1]$

$k_1 = max(0,-i)$, $k_2 = min(M-1, M-1-i)$

$l_1 = max(0,-j)$, $l_2 = min(N-1, N-1-j)$

It can be noticed that the XCF is a function of the displacement in the x and y direction, being therefore bi-dimensional like the surfaces it was generated from.

The ACF is simply an XCF applied to two identical surfaces, which is the cross-correlation of a function with itself.

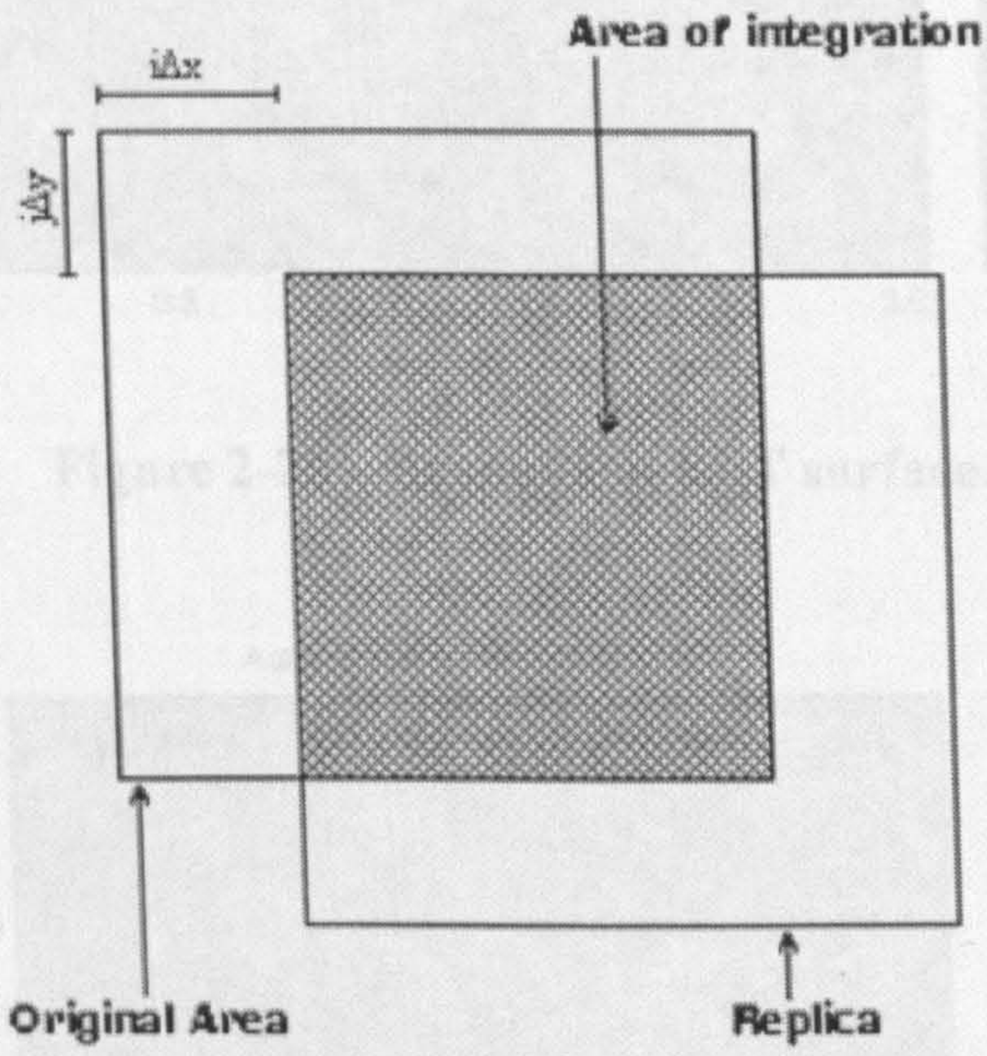

Figure 2-24 – ACF working principle

Figure 2-24 shows a visual example of how the Autocorrelation function of a surface is built, according to [Equation 2.1]: at each step of the double sum the surface $\eta(x_k,y_l)$ ('Original Area' in the figure) is multiplied with $\eta(x_{k+i},y_{l+j})$ ('Replica' in the figure), which is a translated copy of itself. At each step of the

sum the indices change and the replica is virtually 'moved' over the original area, and at each step a value is assigned to $R(i\Delta_x,j\Delta_x)$. The autocorrelation obtained has linear dimensions nearly double that of the given surface: a domain defined by *[0,..,M-1],[0,..,N-1]* is transformed by the ACF into *[-(M-1),M-1],[-(N-1),N-1]*.

It is important to notice that the ACF spacing remain the same as the surface generating it.

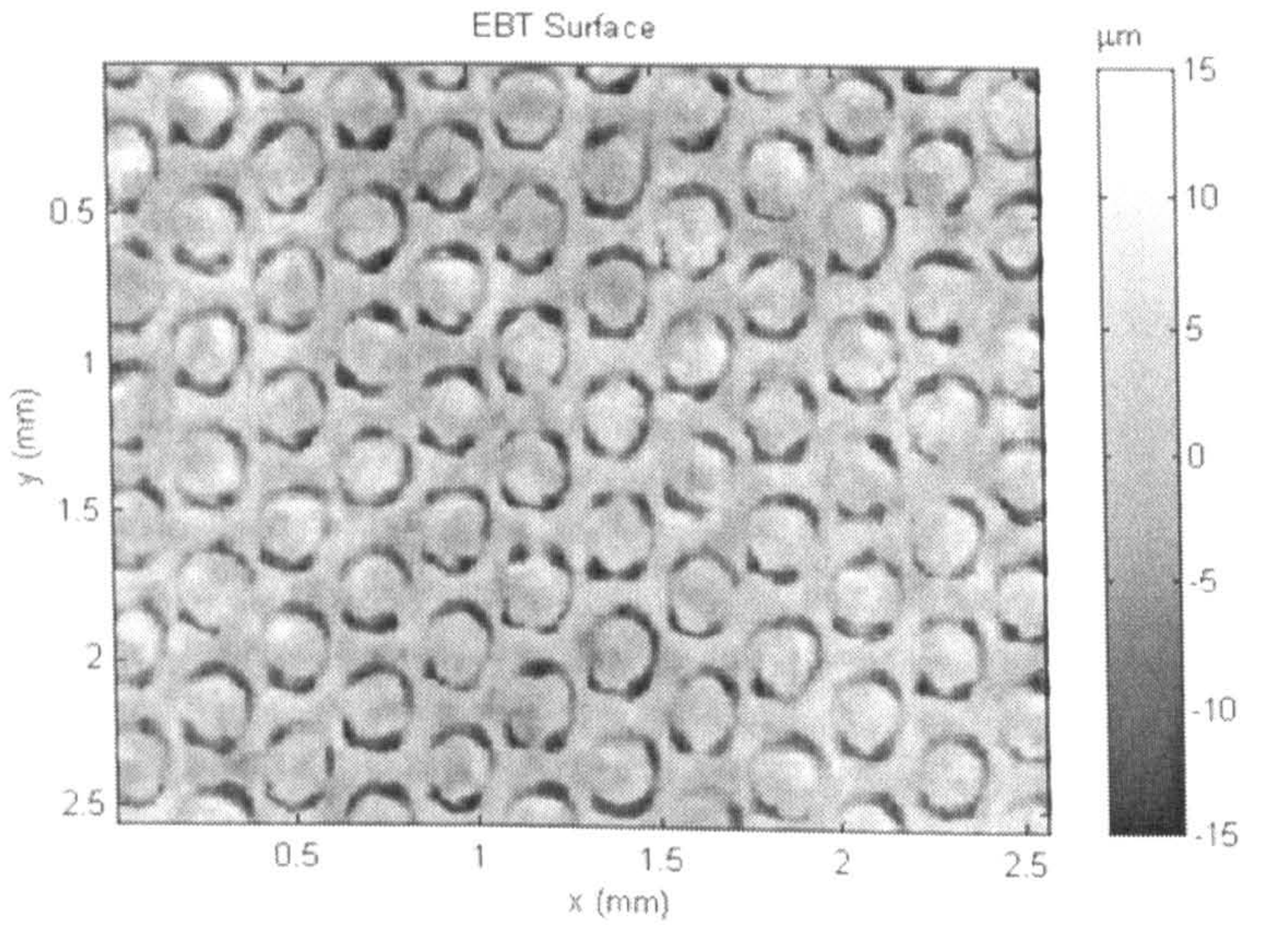

Figure 2-25 - Example of EBT surface.

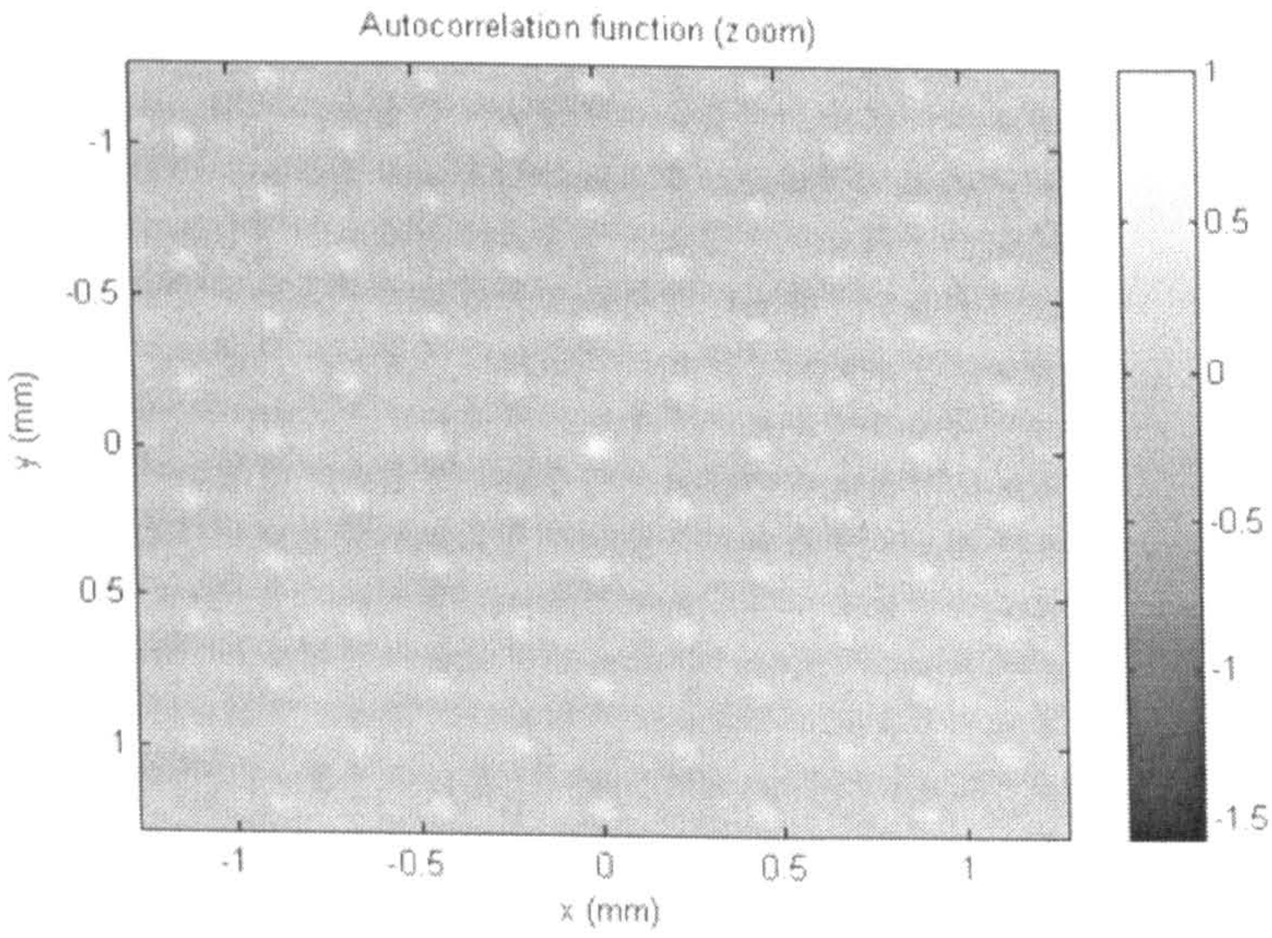

Figure 2-26 - Autocorrelation function (zoomed).

In Figure 2-25 and Figure 2-26 an EBT surface and its auto-correlation map are shown. Notice that the complete autocorrelation map is defined in the range [-2.55,2.55]mm in both dimensions; figure 2-26 shows just a zoom of the central part of it ([-1.275,1.275]mm), of the same size of the EBT surface. The remaining part of the ACF is not considered for reasons that are clarified in the next section.

It can be observed that the auto-correlation has a periodic pattern, and the highest peaks of the function are located on the vertices of hexagons. Every peak is an indication of high correlation between the surface and its translated replica. This pattern suggests the feasibility of isolating the single hexagons and manipulating them statistically to extrapolate the noise and the deterministic pattern from the surface data.

2.5.2 The Gram-Schmidt based surface decomposition

The main pattern can be isolated 'cutting' a number (W) of circular portions (*clusters*) of the EBT surfaces. The choice of circular clusters is due to the fact that they are algorithmically easier to implement than hexagonal ones.

The cluster radius (ρ) can be determined on the auto-correlation map, averaging the distances from the central peak $(0,0)$ to the nearest six (6) peaks, this being the portion least affected by edge effects [Proakis 1995].

The autocorrelation map is cut in the range $x \in [-(M-1)/2,(M-1)/2]$, $y \in [-(N-1)/2,(N-1)/2]$ so that its domain becomes exactly overlapping to the domain of the surface to be analysed. Then a number (W) of circles are cut in the surface, with centres (x_s,y_s) corresponding to the peaks of the autocorrelation map.

$$C_s = \left\{ x_i, y_j \mid \sqrt{(x_i - x_s)^2 + (y_j - y_s)^2} \le \rho \right\} \qquad \text{[Equation 2-3]}$$
$$s = 1..W$$

The base cluster C_0 is determined by averaging the heights of the W clusters previously obtained. This will be hypothesised as the best representation of the surface. Figure 2-27 shows the appearance of cluster C_0 for the surface of Figure 2-25.

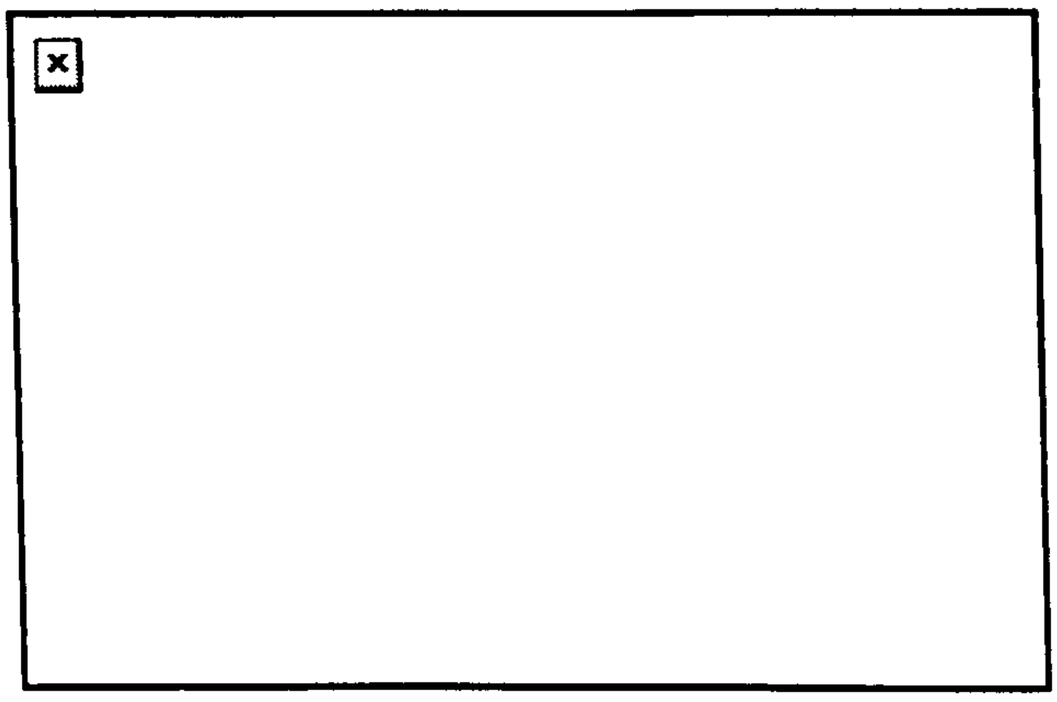

Figure 2-27 - Base cluster C_0.

A qualitative confirmation of the goodness of the approximation is obtained if the shape is smooth and well defined. According to the Gram-Schmidt [Proakis 1995] decomposition, a series of orthonormal clusters O_s, $s=0..W-1$ will be generated according to the formula below:

$$O_0' = C_0; O_0 = \frac{O_0'}{\|O_0'\|}$$

$$O_r' = C_r - \sum_{i=0}^{r-1} \langle C_r, O_i \rangle \cdot O_i; O_r = \frac{O_r'}{\|O_r'\|} \qquad \text{[Equation 2-4]}$$

$$r = 1..(W-1)$$

Inner product and norm definition is extended from vectorial calculus:

$$\langle C_r, C_s \rangle \equiv \sum_{x_k, y_l \in C_r} C_r(x_k, y_l) \cdot C_s(x_k, y_l)$$

[Equation 2-5]

$$\|C\| \equiv \sqrt{\langle C, C \rangle}$$

With this procedure, any of the original clusters C_s can be exactly described as the weighted sum of the orthonormal clusters $\{O_0,..,O_{W-1}\}$, which therefore form a *complete* basis:

$$C_s = \sum_{r=0}^{W-1} a_{s,r} O_r$$ [Equation 2-6]

where $a_{s,r} = \langle C_s, O_r \rangle$ and $s=1,..,W$.

Due to the completeness of the basis, it can be shown that the following relation holds [Proakis 1995] between the squared norm and the coefficients of the expansion:

$$\|C_s\|^2 = \sum_{k=0}^{W-1} a_{sk}^2$$ [Equation 2-7]

It is to be noted that if a^2_{sk} is very small, it can be omitted with no substantial alteration of the norm of C_s, and therefore of C_s itself. Approximate versions of the entire surface can thus be obtained by considering only the most relevant terms in the decomposition of each cluster C_s:

$$C_s \approx \sum_{r \in S_s} a_{sr} O_r$$ [Equation 2-8]

where $S_s = \{ r / a_{sr}^2 \geq threshold \}$

(the threshold may be chosen according to the required precision).

Figure 2-28 shows that, in our example, for each cluster C_s only two coefficients are meaningful (a_{s0} and a_{ss}) while all the others can be considered negligible; the ratio between a^2_{ss} and a^2_{s0} varies in the range 0.3 – 0.7. Therefore, it can be argued that O_0 is the most important term, and that the other terms O_s are needed to represent the noise deviation of C_s from O_0 (in fact O_s is needed to represent C_s only). As a consequence, a 'noiseless' representation of the original surface can be obtained using just the first component in the expansion, for each of the clusters C_s with $s=1,..,W$.

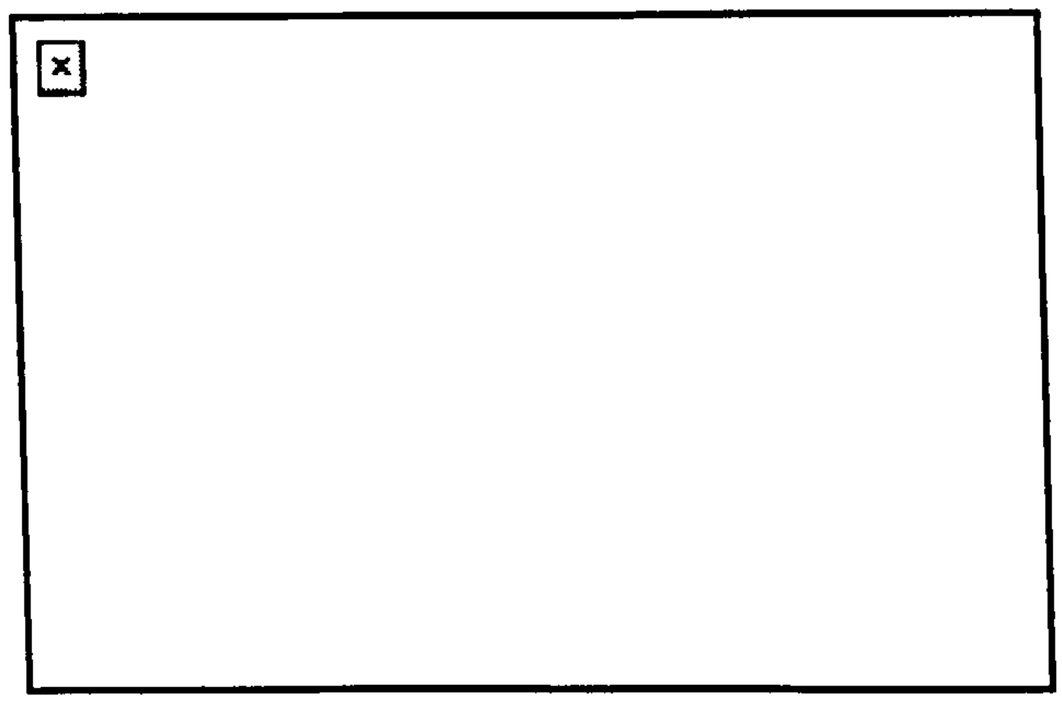

Figure 2-28 - Representation of the coefficient Matrix

The Gram-Schmidt standard procedure starts with $O_1' = C_1$, and goes on until O_w', defining W orthogonal clusters, as before. However it has been shown that the introduction of C_0 allows representation of each of the original clusters with one component only of the expansion.

A question arises about the surface reconstruction in the region where superposition occurs between two or more adjacent circular clusters. As far as the reconstruction is perfect (as the complete Gram-Schmidt decomposition assures), any of the two or more expansions of the surface can be used for the superposition regions. If, on the contrary, only the most significant term(s) of the decomposition are considered, a strategy must be envisaged to define the approximate values of the surface in these regions, and the edge effect may occur. Our choice was to approximate $C_s \approx C_0$, for any s and to replicate it: if the edge effect occurs, then a periodic pattern should appear on the autocorrelation function of the difference between the original and the reconstructed surfaces.

2.5.3 Results overview

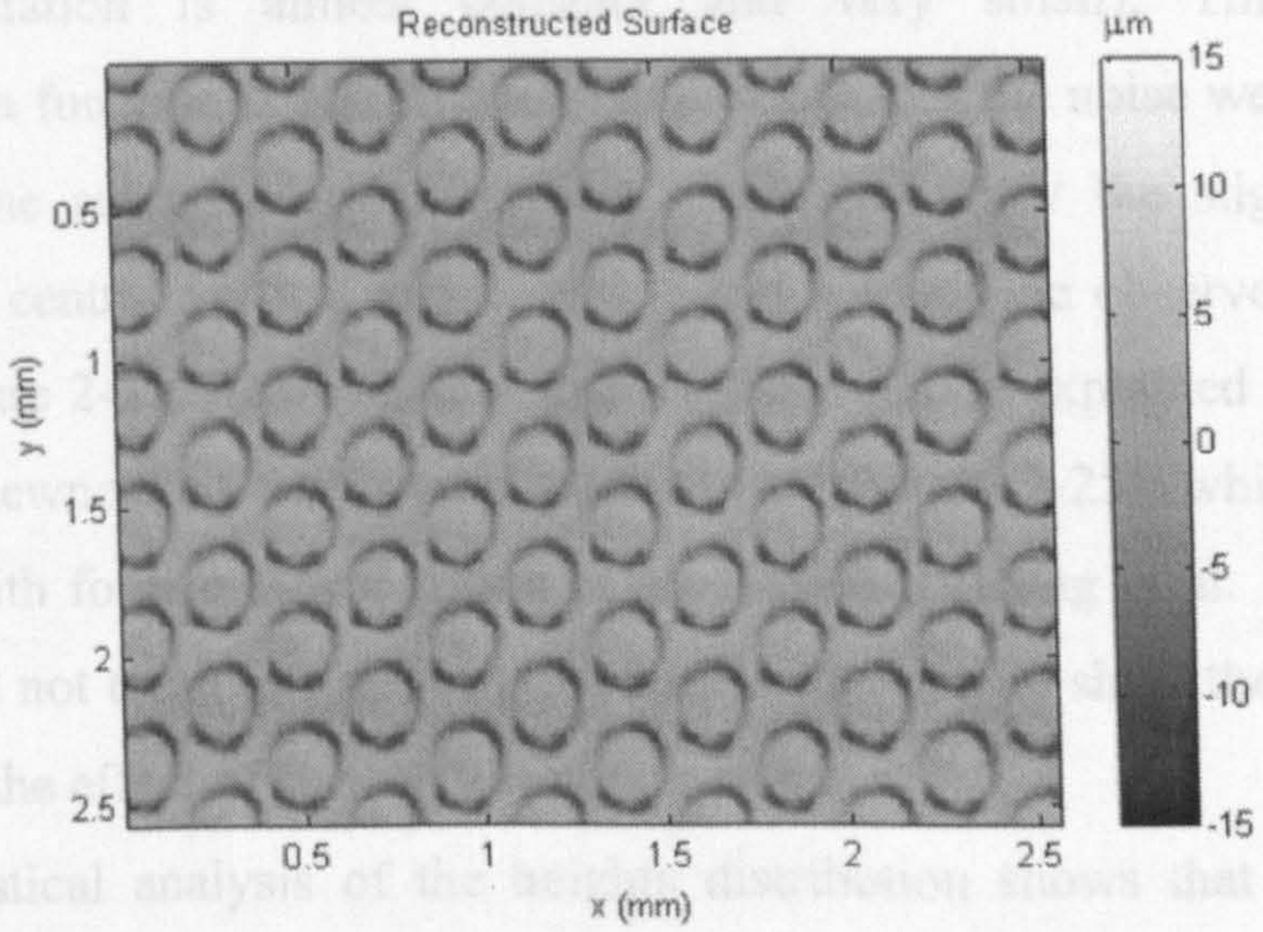

Figure 2-29 - Reconstructed surface.

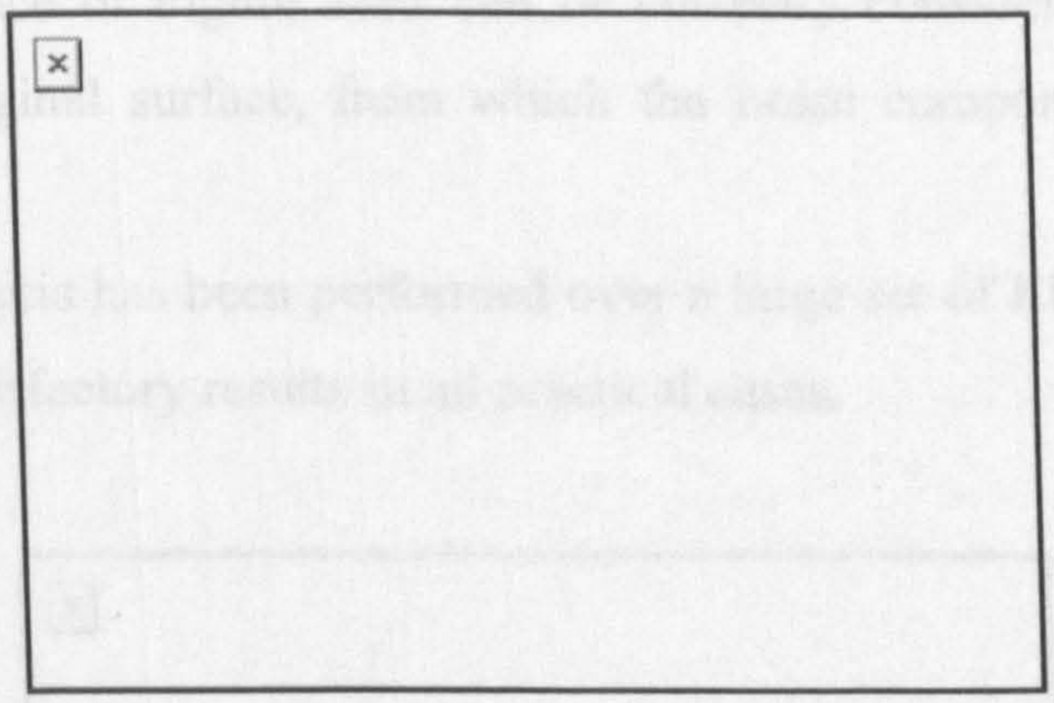

Figure 2-30 - Residual surface.

Figure 2-29 shows the appearance of the reconstructed surface, and it is possible to appreciate the cleanliness of the surface. This could be foreseen, since Figure 2-29 was obtained by replicating the same pattern C_0. What has to be determined is whether this reconstructed surface can be seen as a filtered version of the original one, or if it is simply a different surface. This can be done by analysing the residual surface, defined as the height-to-height difference of the original and filtered surface and plotted in Figure 2-30. Its autocorrelation function is given in Figure 2-31 and Figure 2-32, and it is apparent that no

periodic component is present (there is just one peak at *(0,0)*, while the rest of the autocorrelation is almost constant and very small). This kind of autocorrelation function is typical of noise processes; if the noise were perfectly white, then the autocorrelation function would not show the slightly higher values in the central vertical stripe, which can actually be observed in Figure 2-31 and Figure 2-32. However this characteristic can be explained as the result of a slight skewness of the original surface (see Figure 2-25), which could be eliminated with form removal [Dong et al. 1994 (a)] [Dong et al. 1994 (b)]. It was preferred not to modify the original surface in order to show the capabilities of removing the effect of surface form on the data.

The statistical analysis of the heights distribution shows that the residual surface can be reasonably considered Gaussian (see Figure 2-34), while the original was not (see Figure 2-33), due to the deterministic pattern. Thus the reconstructed surface of Figure 2-29 can be correctly considered as a filtered version of the original surface, from which the noise components have been eliminated.

The same analysis has been performed over a large set of EBT surfaces (see section 3) with satisfactory results in all practical cases.

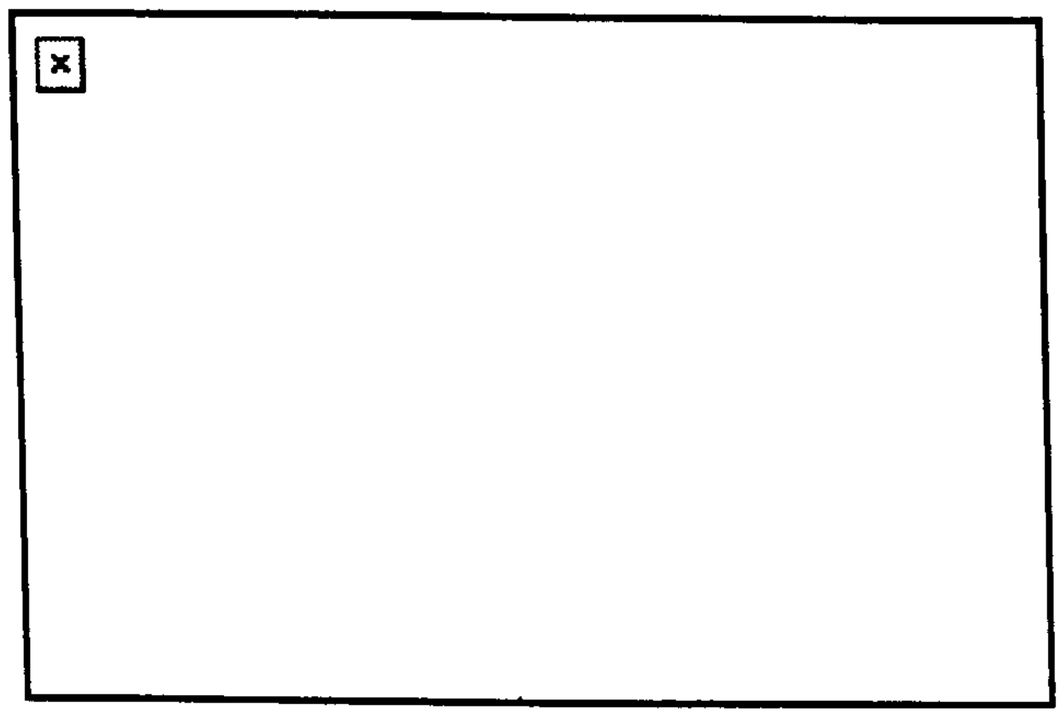

Figure 2-31 - Autocorrelation of the residual surface.

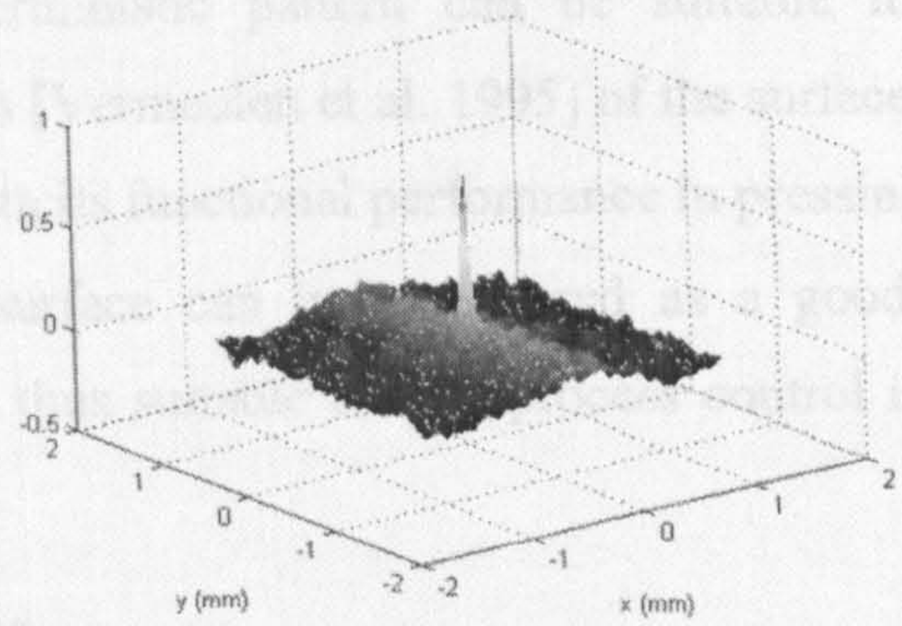

Figure 2-32 - Autocorrelation of the residual surface (Isometric view).

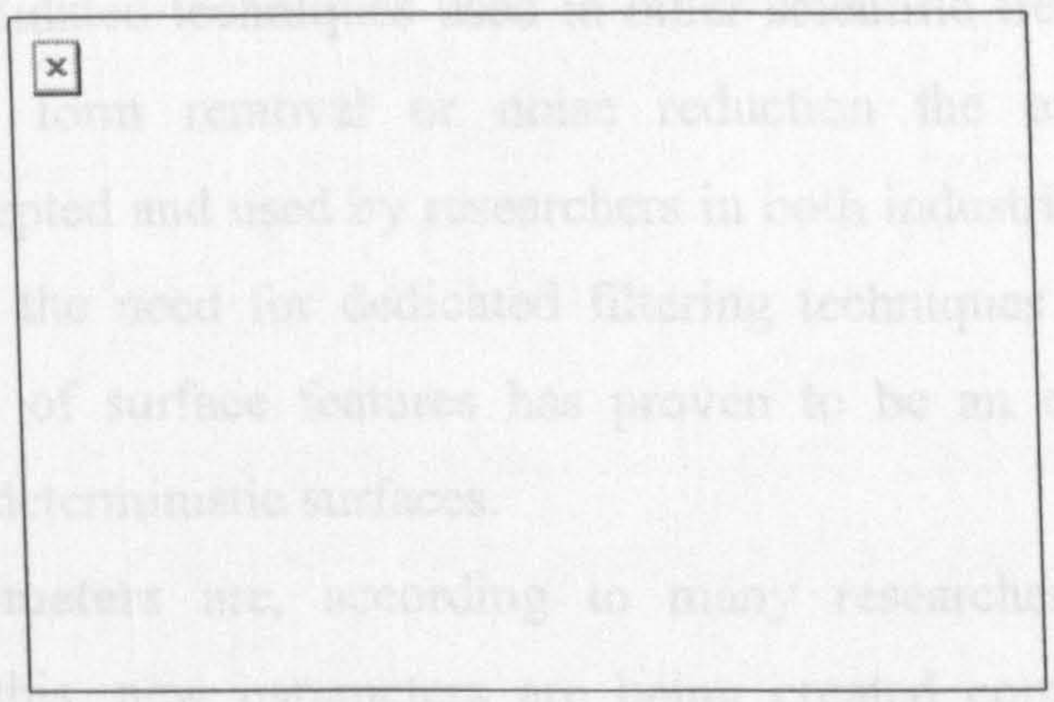

Figure 2-33 - Height distribution of the original surface (Non Gaussian).

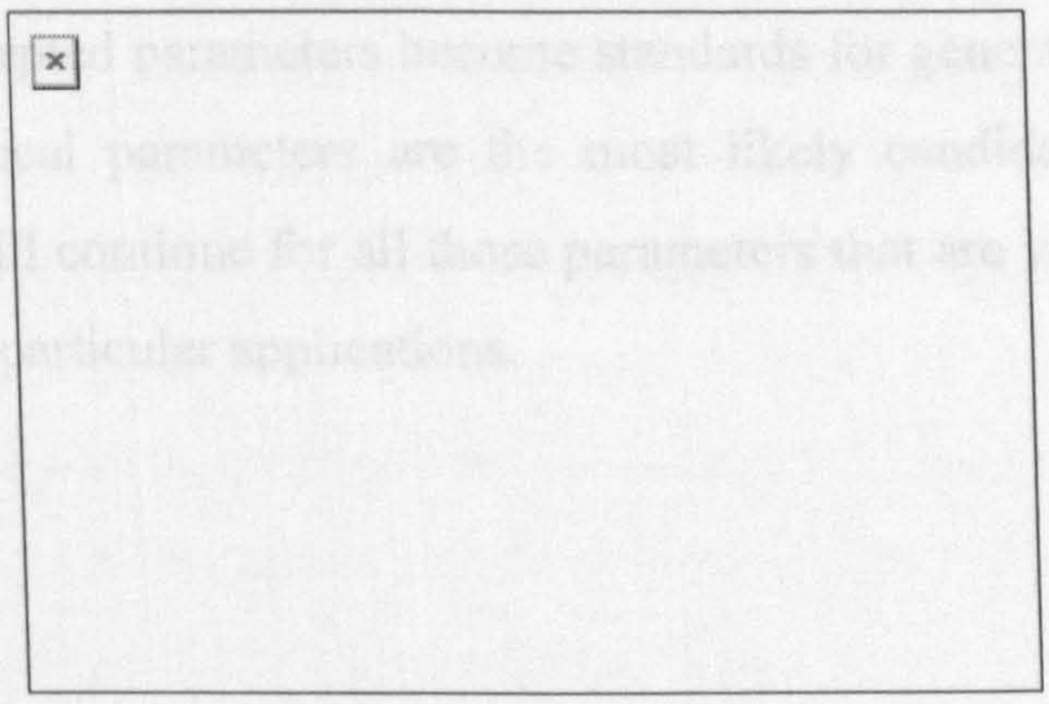

Figure 2-34- Height distribution of the residual surface (Gaussian).

In conclusion:

- The Gram-Schmidt decomposition has been proved as an effective way to filter EBT surfaces and separate the deterministic pattern.

- The pure deterministic pattern can be suitable for the geometrical characterisation [Vermeulen et al. 1995] of the surface and understanding correlations with its functional performance in pressing and painting.
- The residual surface can be considered as a good estimation of the "noise" and is thus suitable for the process control in the production of steel sheets.

2.6 Conclusions

Surface filtering is in the vast majority of cases a mere adaptation of existing and consolidated techniques used in other scientific fields. For general purposes such as form removal or noise reduction the existing filtering techniques are accepted and used by researchers in both industrial and academic environments, but the need for dedicated filtering techniques is evident. The statistical analysis of surface features has proven to be an effective way to characterise semi-deterministic surfaces.

Surface Parameters are, according to many researchers, excessive in number; despite this, new parameters are being created continuously, which strongly suggests the inadequateness of the existing ones. Considering the current trend, the probable evolution of this situation will see a few well-established and accepted parameters become standards for general description of the surface (statistical parameters are the most likely candidates), while the 'parameter rash' will continue for all those parameters that are very specific and needed to describe particular applications.

3. Research Methodology

The EBT Statistical Filter (initially named Gram-Schmidt Filter [Porrino et al. 2000]) has been the first feature-based statistical approach to industrial steel production control. It was proposed as an innovative filtering technique, although too specific because it can only be applied to EBT surfaces.

Further research led to the widening of the application range, at first to other semi-deterministic texturing methods, then to a statistically based control system.

This chapter illustrates the research methodology adopted for the project, as well as instruments, software and specifications used during this research.

3.1 The Knowledge Base: The Data Set

A large number of surfaces were analysed, partly from previous projects (essentially Autosurf) and partly from measurements taken by OCAS and Sidmar.

3.1.1 Data from previous projects

The extremely large amount of data extracted during the Autosurf Project was not all available for reasons of confidentiality and industrial secrecy, but this problem did not affect the samples that came from OCAS/Sidmar and both OCAS and Brunel University measured at the time, as part of the measurement framework of the project. Detailed information about the Autosurf Project measurement framework is contained in the Autosurf documentation [Autosurf website] and relative publications; in the following tables only the technical specifications regarding the instruments are reported.

Instrument	Type	Manufacturer	# Data Points	X/Y resolution (µm)	Surface Area (mm^2)	Measuring Time
1) Form Talysurf S2	Stylus	Taylor Hobson	256 / 256	10 / 10	2.56 x 2.56	±75 minutes
2) Talyscan	Optical	Taylor Hobson	500 / 500	2 / 2	1 x 1	± 2minutes
3) Form Talysurf S5	Stylus	Taylor Hobson	256 / 256	10 / 10	2.56 x 2.56	±75 minutes
4) RST Plus	Optical (Vertical Interferometry	Wyko Corp.	736 / 468	3.38 / 3.80	2.5 x 1.8	± 2 minutes
5) Surfascan 3D	Stylus	Somicronic	256 / 256	8 / 8	2 x 2	± 75 minutes
6) UBM	Stylus/ (Micro-focus)	UBM	300 / 300	10 / 10	3 x 3	±90 minutes
7) Form Talysurf S6 PGI	Stylus	Taylor Hobson	256 / 256	10 / 10	2.56 x 2.56	±75 minutes
8) RST Plus	Optical (Vertical Interferometry)	Wyko Corp.	736 / 468	3.38 / 3.80	2.5 x 1.8	± 2 minutes
9) UBM	Stylus (Micro-focus)	UBM	500/500	10/10	5 x 5	±20 minutes
10) RST Plus	Optical (Vertical Interferometry)	Wyko Corp.	736 / 479	3.38 / 3.80	2.5 x 1.8	± 2 minutes

Table 3-1

	Optical	Stylus
3D Roughness Parameters	S_a, S_z, S_k, S_{vk}, S_{pk}, S_{r1}, S_{r2}	S_a, S_z, S_k, S_{vk}, S_{pk}, S_{r1}, S_{r2}
Measurement Area	$\approx 2.5 \times 1.9\ mm^2$	$\approx 2.5 \times 2.5\ mm^2$
Resolution	$dx = 3.4\ \mu m$ $dy = 3.8\ \mu m$	$dx = dy \leq 10\ \mu m$
Other Settings:	Objective: 2.5 Field of View: 1	Stylus Radius :2 µm or 5 µm No Skid.
Traversing Speed	-	≈ 0.5 mm/s
Form removal	Tilt, Cylinder	Tilt, Linear
Filtering	No	No

Table 3-2

The Surface measurement specifications for the RRT on three-dimensional surfaces within Autosurf are shown in Table 3-2, while Table 3-1 illustrates the instruments used.

In addition to the measurements from Autosurf, OCAS could provide some measurements performed in previous projects, generally only accompanied by the name of the instrument used to obtain them.

All these data were used for the various stages of theoretical formulation and software development of the filter, not in the final stages of validation/tuning and statistical testing, therefore little attention has been devoted to the particular source of measurement.

3.1.2 Data extracted for the Statistical Filter Project

Ideally the experiments would have been performed in a structured way, using a Design Of Experiments (DOE) approach, in order to compare the influence of various factors (such as geometrical position on the sheet, state of wear of the roll, tandem or temper roll, etc.) and to correlate the various factors and the extracted parameters.

This would have required interrupting production at various stages, for a long period of time, performing the same experiments over different rolls and the sheets textured with them. Such work has not been possible for logistic and practical reasons, but during the Project OCAS provided numerous samples with various characteristics in order to test the capabilities of the filter.

Name	Sample	Type	Measured	X SIZE (mm)	Y SIZE (mm)	SIZE (mm2)	X SIZE (pix)	X SIZE (pix)	SIZE (pix2)	X SPAC (mm)	Y SPAC (mm)
C_W_01_1	1	Replica	Wyko	10,01	5,112	51,17112	1000	5000	5000000	0,01001	0,0010224
C_W_02_1	2	Replica	Wyko	5,13	5,149	26,41437	512	5120	2621440	0,01002	0,0010057
C_W_03_1	3	Replica	Wyko	5,13	5,233	26,84529	512	5120	2621440	0,01002	0,0010221
C_W_04_1	4	Replica	Wyko	5,13	5,212	26,73756	512	5120	2621440	0,01002	0,001018
C_W_05_1	5	Replica	Wyko	5,13	5,294	27,15822	512	5120	2621440	0,01002	0,001034
C_W_06_1	6	Replica	Wyko	5,13	5,113	26,22969	512	5120	2621440	0,01002	0,00099863
R_W_07_1	7	Roll	Wyko	2,56	40	102,4	256	4000	1024000	0,01	0,01
R_W_08_1	8	Roll	Wyko	2,56	40	102,4	256	4000	1024000	0,01	0,01
R_W_09_1	9	Roll	Wyko	2,56	40	102,4	256	4000	1024000	0,01	0,01
R_W_10_1	10	Roll	Wyko	2,56	40	102,4	256	4000	1024000	0,01	0,01
R_W_11_1	11	Roll	Wyko	2,56	40	102,4	256	4000	1024000	0,01	0,01
R_W_12_1	12	Roll	Wyko	2,56	40	102,4	256	4000	1024000	0,01	0,01
R_W_13_1	13	Roll	Wyko	2,56	40	102,4	256	4000	1024000	0,01	0,01
R_W_14_1	14	Roll	Wyko	2,56	40	102,4	256	4000	1024000	0,01	0,01
S_R_15_1	15	Sheet	RTH	1,8695	2,5184	4,7081488	471	736	346656	0,0039692	0,0034218
S_W_15_2	15	Sheet	Wyko	5,13	5,218	26,76834	512	5120	2621440	0,01002	0,0010191
S_R_16_1	16	Sheet	RTH	1,8695	2,5184	4,7081488	471	736	346656	0,0039692	0,0034218
S_W_16_2	16	Sheet	Wyko	5,13	5,251	26,93763	512	5120	2621440	0,01002	0,0010256
S_R_17_1	17	Sheet	RTH	1,8695	2,5184	4,7081488	471	736	346656	0,0039692	0,0034218
S_W_17_2	17	Sheet	Wyko	5,13	5,219	26,77347	512	5120	2621440	0,01002	0,0010193
S_W_18_1	18	Sheet	Wyko	3,005	2,095	6,295475	600	2000	1200000	0,0050083	0,0010475
S_W_18_2	18	Sheet	Wyko	3,005	2,0901	6,2807505	600	1000	600000	0,0050083	0,0020901
S_W_18_3	18	Sheet	Wyko	0,85946	0,64717	0,55621673	315	264	83160	0,0027285	0,0024514
S_W_18_4	18	Sheet	Wyko	0,84173	0,63377	0,53346322	621	626	388746	0,0013554	0,0010124
S_W_19_1	19	Sheet	Wyko	3,005	2,0921	6,2867605	600	1000	600000	0,0050083	0,0020921
S_W_19_2	19	Sheet	Wyko	3,005	2,0961	6,2987805	600	1000	600000	0,0050083	0,0020961
S_W_19_3	19	Sheet	Wyko	0,8459	0,66898	0,56589018	309	275	84975	0,0027375	0,0024326
S_W_19_4	19	Sheet	Wyko	0,86219	0,67628	0,58308185	315	278	87570	0,0027371	0,0024327
S_W_20_1	20	Sheet	Wyko	3,005	2,0861	6,2687305	600	1000	600000	0,0050083	0,0020861
S_W_20_2	20	Sheet	Wyko	3,005	2,0861	6,2687305	600	1000	600000	0,0050083	0,0020861
S_W_20_3	20	Sheet	Wyko	0,83229	0,65046	0,54137135	166	126	20916	0,0050138	0,0051623
S_W_20_4	20	Sheet	Wyko	0,84323	0,66226	0,5584375	308	272	83776	0,0027377	0,0024348
S_W_21_1	21	Sheet	Wyko	6,01	8,098	48,66898	600	8000	4800000	0,010017	0,0010123
SUM				106,2633	398,93862	1188,0668	14791	97009	44952631	0,2394544	0,12786673
MAX				10,01	40	102,4	1000	8000	5000000	0,01002	0,01
MIN				0,83229	0,63377	0,53346322	166	126	20916	0,0013554	0,00099863
AVG				3,2201	12,08904909	36,0020244	448,212121	2939,66667	1362200,94	0,007256194	0,003874749
STD				1,984949867	16,13811142	40,3591319	174,950843	2185,68143	1298443,4	0,003166616	0,003641859

Table 3-3 - Project Samples

The surface measurements considered for testing the various capabilities of statistical filter are listed in Table 3-3. This table contains the basic information about each measurement, plus a summary of the statistical distribution of the parameters along the columns (sum, maximum and minimum values, average and standard deviation). The table is here described more in detail, which will allow a few important observations about the data set.

- **Column 1: Name**. The files have been named in a way that would identify their characteristics: the first character in the name indicates a sheet sample ('S'), a roll sample ('R') or the replica of a roll ('C'). Replicas are copies of the roll obtained impressing a soft material on the roll's surface. The second character (separated by an underscore character '_') indicates a Wyko ('W') or RTH ('R') instrument. The two following numbers represent ordinal numbers associated with the sample and the repetition.

- **Column 2: Sample.** The sample's ordinal number. Only one measurement is available for most samples, while for some of them multiple measurements (in different positions) are available.
- **Column 3: Type.** Either sheet, roll or replica, as in column one. The samples are not evenly distributed between the three, in particular if considering the total areas.
- **Column 4: Instrument.** Either Wyko or RTH, as in column one. Unfortunately only three samples have been measured with both instruments, therefore no statistically meaningful comparison could be carried out.
- **Columns 5,6 and 7: Size in millimetres.** The lateral size in both dimensions is here listed in millimetres, and the area is calculated as their product. It is important to notice the distribution of the values, which all show high standard deviations. It is possible also to notice the high ratio between the larger and the smaller area.
- **Columns 8,9 and 10: Size in pixels.** The number of elements of the matrixes that represent the surfaces.
- **Columns 11 and 12: Spacing.** The spacing, as stored in the SDF files, is here reported, and corresponds to the ratios between the values in columns 5,6 and columns 8,9.

The set as a whole is composed of samples that cover a very large spectrum of conditions, which is ideal for testing the software on each single sample data set. However, it represents an impediment when trying to summarise the experiments into one comprehensive analysis. These samples have been 'dissected' one by one innumerable times using the GS filter, and the features have been isolated and analysed successfully on each one of them. The problem rises when trying to group the single experiments into one for validation of parameters and algorithms: due to the extreme diversity and casual distribution of the characteristics of the samples, a proper design results impossible, and only basic statistics can be performed. The analysis of the experiments will be discussed in section 6.

- **Samples from sheets :**

7 Samples were measured at Sidmar: 3 measured by both instruments, 3 that were also measured with CRM camera for cross-correlation, and a data set coming from a very large surface portion.

- **Samples from rolls :**

A set of seven very large samples have been measured with the Wyko equipment.

- **Samples from replicas :**

Seven samples of different areas were measured.

- **Samples with defects :**

In order to test the capability of the filter in recognising and cataloguing the possible defects of the sheets, a few samples were created with well-defined intentional defects. These files are not included in Table 3-3 because their artificial defects would perturb the statistical analysis of the data.

3.1.3 Homogeneous data set

The measurements have been rearranged into two homogeneous sets, i.e. sets of samples with the same area and the same number of points. Each surface has been divided into as many 1 x 1 mm whole squares as possible, so that small surfaces have been eliminated, and the larger surfaces have generated lists of smaller samples.

The same procedure has been repeated with 2x2 mm squares.

From the initial 1188 mm^2 available, a first set of 980 1x1mm surfaces has been extracted, and a second set of 220 2x2mm.

Each surface has been resampled on a regular grid of 256x256 points using a linear interpolation algorithm, giving final spacing of 1mm/256=0.0039mm and 2mm/256=0.0078mm in both directions.

3.1.4 Pre-Filtering

Each surface has been levelled (i.e.: a first order polynomial form removal), so that the mean of the heights for each sample is zero. It was chosen not to

apply any higher order form of pre-filtering in order to test the filter in a worst case scenario, in particular the limits of the autocorrelation in identifying the features in the presence of a skewed surface.

3.2 Measurement instruments

RTH (Taylor-Hobson)

- 2D & 3D - Measuring with mechanical stylus
- Based on Laser interferometry
- Large measuring surface possible (120 x 120 mm)
- Measuring time 2.5 x 2.5 mm ≈ 60 min

WYKO

- 3D - non contacting measuring method
- Based on Vertical Scanning Interferometry
- Max. possible surface 4.9 x 3.7 mm
- Measuring time 2.5 x 1.8 mm ≈ 2 min

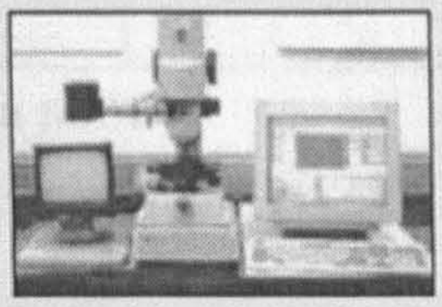

Figure 3-1 - Measurement Instruments

The data set used in the course of the project comes from two instruments available at Sidmar and OCAS (Figure 3-1): a contact-base Taylor-Hobson Form Talysurf and an optical Wyko Vertical Scanning Interferometer. The technical data of the equipment is here reported:

- **Contact:**

MANUFACTURER	TAYLOR HOBSON
CONFIGURATION	Taylor Hobson Form Talysurf Series S6 (PGI)
MEASURING METHOD	mechanical stylus (stylus force 0.7 - 1.0 mN) tip radius = 2 µm
LASER TRAVERSE UNIT	120 mm stroke
TRAVERSE TABLE	150 mm
VERTICAL RESOLUTION	10 nm over 10 mm range
STEPSIZE	1 µm * 10 µm (5120 * 512 data points)
SURFACE	5.12 mm * 5.12 mm

- **Optical:**

MANUFACTURER	WYKO
CONFIGURATION	WYKO RST+, RS105138
MEASURING METHOD	Vertical Scanning Interferometry (VSI)
INTERFEROM. TYPE	Michelson
VERTICAL RANGE	500µm
VERT. RESOLUTION	< 50nm
MAGNIF. OBJECTIVE	2.5*
FIELD OF VIEW	0.5
SPATIAL SAMPLING	X: 6.60µm Y: 7.65µm
MEAS. ARRAY SIZE	736*471
SURFACE	3.6*4.9 mm^2

3.2.1 On-line camera-microscope system

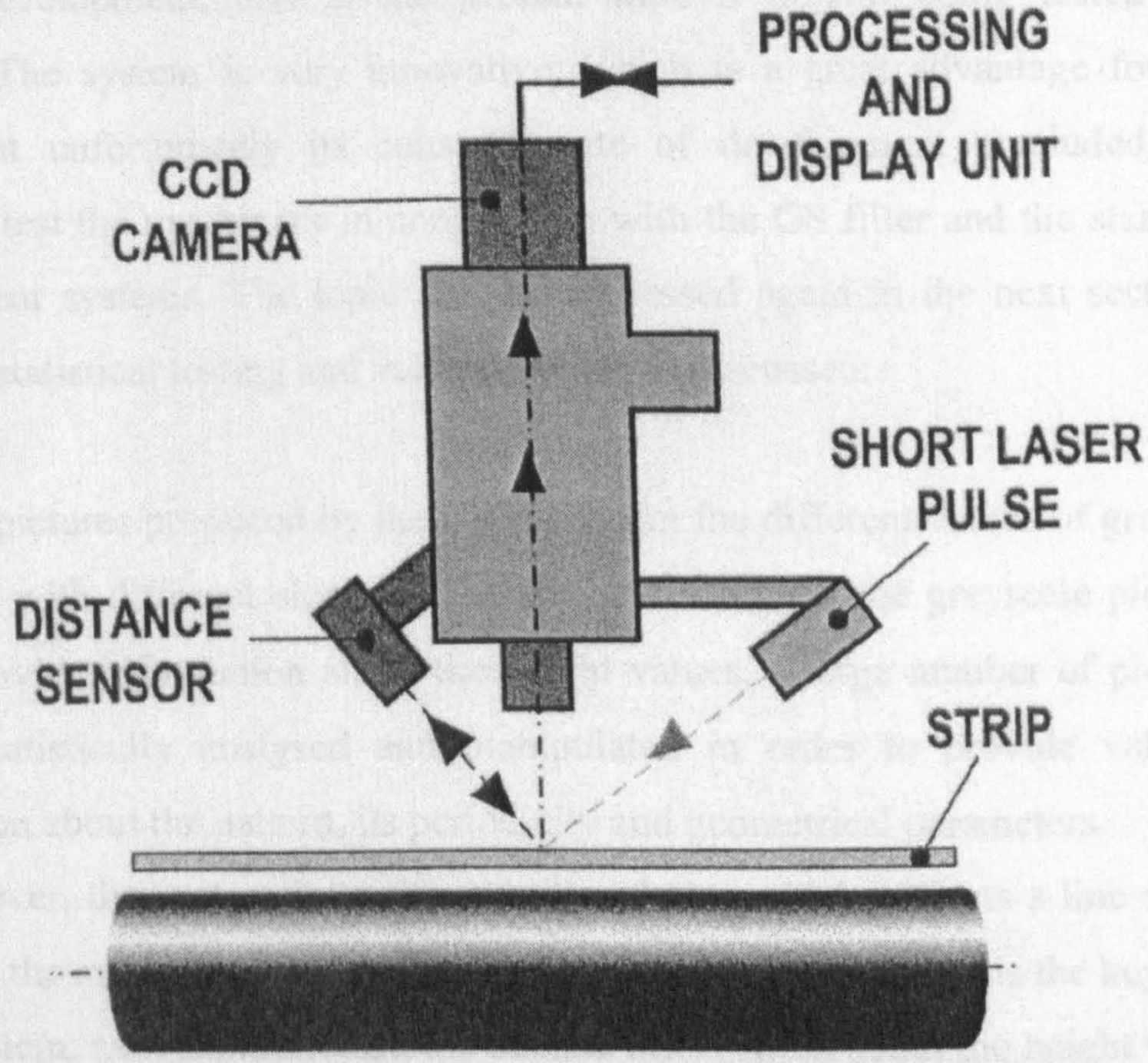

Figure 3-2 - CRM Camera-microscope System

Surface data can be acquired during the production process in order to achieve an innovative on-line control system of textured surfaces. Given the very harsh environmental conditions (up to 20m/s speed of the metal sheet and strong vibrations), a standard measuring procedure is impossible. Contact instruments cannot be applied for obvious reasons, and conventional optical systems prove to be highly inadequate.

A proper measurement is therefore not available for on-line applications, but a system of microscope and camera can produce a large number of greyscale pictures of the sheet being manufactured. The system has been implemented by CRM and it is schematically represented in Figure 3-2 [CRM internal documentation].

During the duration of the project the CRM System has been undergoing constant development, and at the present time it is still being tested and modified. The system is very innovative, which is a great advantage for the project, but unfortunately its constant state of development precluded any attempt to test the machinery in conjunction with the GS filter and the standard measurement systems. The topic will be addressed again in the next sections, where the statistical testing and validation will be discussed.

In the pictures produced by the CRM System the different values of grey are associated with different slopes of the surface. Although the greyscale pictures do not provide information about the height values, a large number of pictures can be statistically analysed and manipulated in order to provide valuable information about the pattern, its periodicity and geometrical parameters.

Moreover, the system is equipped with a Laser which projects a line on the surface at the moment the picture is taken; the analysis of the line is the keystone of the system, as it should return the needed information about the height values of the surface on that line.

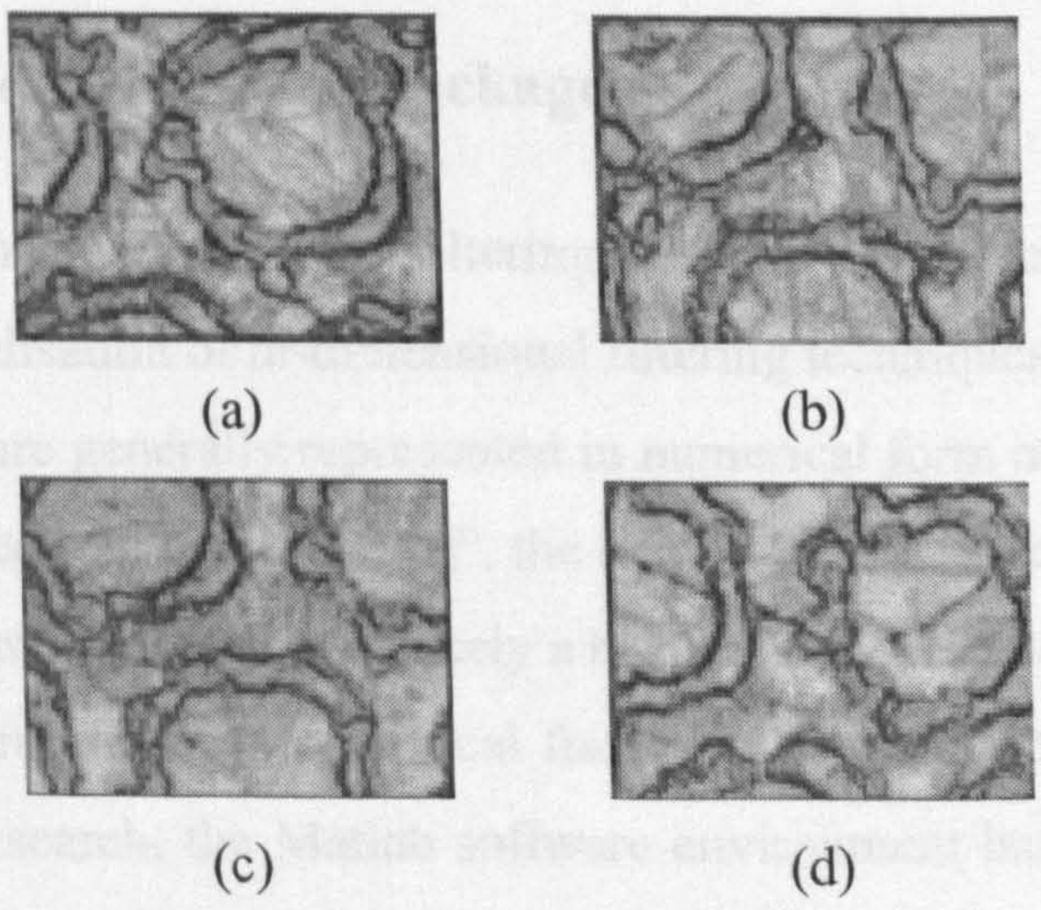

Figure 3-3 – Examples of Greyscale pictures

Figure 3-3 shows some examples of pictures taken from a steel sheet with the greyscale camera and microscope system.

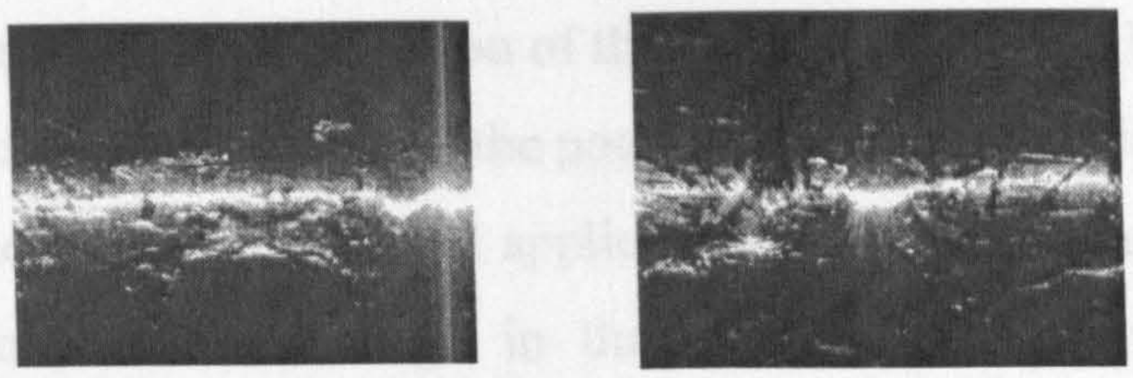

(a) (b)

(c) (d)

Figure 3-4 - Laser Lines

Figure 3-4 shows a few examples of pictures of the laser line projected on the sheet while been produced. The line is always drawn in the same position with respect to the picture. CRM has elaborated an algorithm for the evaluation of the heights of the profile corresponding to the laser line. The tests conducted so far have given positive results, and the technique has claimed to result in acceptable accuracy.

3.3 Software development package

As stated in chapter 2, surface filtering has been approached as a multi-dimensional generalisation of bi-dimensional filtering techniques.

Where signals are generally represented in numerical form as "sequences" of values, or more precisely "row vectors", the heights of a surface's points will be organised into a matrix, which is precisely a bi-dimensional vector.

For vectorial processing in numerical form, which represents the supporting structure of this research, the Matlab software environment has been chosen as preferred. The easy matrix manipulation and visual representation, together with the powerful mathematical tools available in the various toolboxes, helped the creation of a working prototype of the filter. Although slow and very

memory-consuming, the Matlab version of the software proved to be ideal for an immediate preliminary verification of the potentiality of the statistical approach.

To meet the needs of the industrial application, in terms of time and memory usage optimisation, a second stage in the software development has been planned: C++ was considered the most portable and reliable language for the software to be translated into, after the first mathematical testing stage.

This section will briefly analyse the aspects of the software development package as part of the Research Methodology; a more detailed and technical analysis is contained in section 7, where the software implemented during the project is described.

- Matlab Functions: a large set of general-purpose functions has been created in addiction to the SCOUT library [SCOUT website], in order to simplify the algorithmic work. Every major algorithm and operation has been created as a separate function, so that new programs would be easily written using the existing ones, and become available themselves for other programs. The software has subsequently been provided with a Graphical User Interface (GUI) for ease of use.
- Matlab Workspaces and data files: given the elevated processing time for some of the operations performed during the project, outputs were saved in Matlab compatible formats (as data files containing single variables, or as whole workspaces) for future quick reference.
- Matlab Figures: also figures need sometimes to be re-edited, so most of the interesting outputs were represented and saved as Matlab Figure Files.
- Minitab projects: for the statistical analysis of the parameters, a specific software package such as Minitab [Minitab website] was chosen. Matlab functions have been written for the exchange of data between the two software packages.

- Excel Worksheets: the tables automatically generated in Matlab were observed also using Microsoft Excel, due to its flexibility in the handling of tables.

3.4 Data representation format

Surface data can be acquired with various measuring instruments ([Stout et al. 2000]), obtaining data in different formats. All the different formats, or at least all the most used ones, have a common matrix representation structure, which allows a quick conversion from one format to the other. The function "surfconv", developed by Sacerdotti within the SCOUT project, is the conversion tool used for this research [SCOUT website]. The Autosurf consortium used SDF files as the standard format for surface representation, so other routines have been created in order to write and read SDF files within Matlab. The combined use of the SCOUT functions allows the analysis of different data types using the same Matlab software. Some more recently developed measurement instruments use 32-bit coding of data and are not compatible with the conversion tool, which might need constant updating to follow the evolution of measurement quality.

Matlab represents by default numbers as *double precision* (8 bytes), which allows a precision much greater than required by the surface analysis applications, causing thus a waste of memory and slower processing speed.

4. The "Statistical Filter"

The Statistical filter introduced in Chapter 2 "State-of-the-art" has been taken as the starting point for the development of a more complex statistical process control technique, of which the filter is the logical skeleton.

As discussed in chapter 2, the accuracy required of the measuring instruments and the great steel production speed, together with the prohibitive environmental working conditions, led the research to a non-conventional kind of approach.

Efforts have been directed not only towards the improvement of the single measurement precision, but also into increasing the number of measurements and into studying them statistically.

In this and the following chapters it will be shown that the statistical approach can lead to stable parameter definitions and meaningful surface characterisation if a sufficient number of measurements are available.

4.1 Application of the Statistical filter to multiple patterns

Recently developed textured surfaces such us Sibetex (Figure 4-1) can be created with the overlapping of two different EBT patterns [Vermeulen et al. 1996]. Having the benefit of a regular and strictly controlled production process, still the obtained surface looks "pseudo-stochastic" and the originally regular patterns are not clearly visible anymore [Sheers at al. 1998].

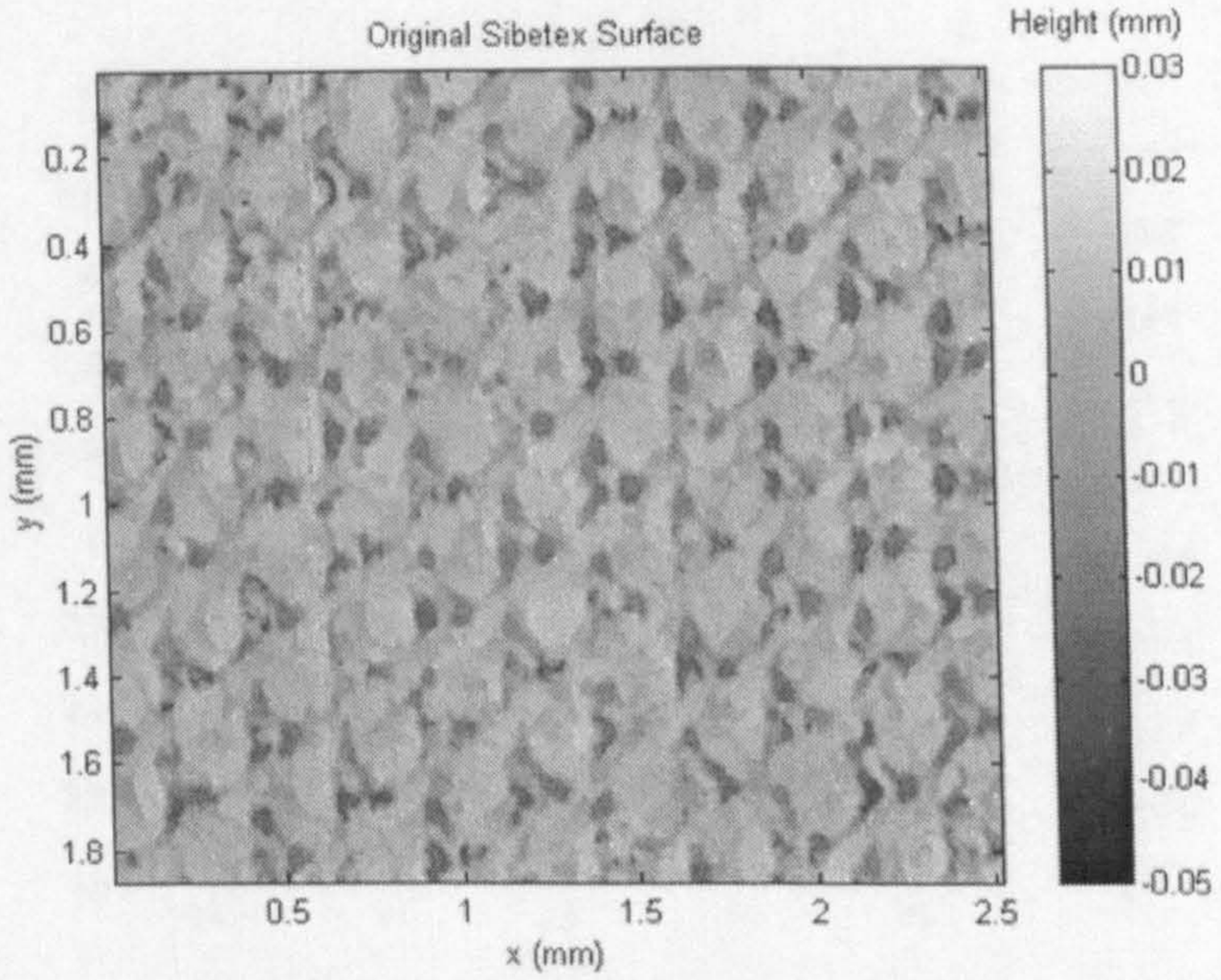

Figure 4-1 – Sibetex Surface

The main disadvantage is that when trying to correlate surface characterisation with functional performance it is generally impossible to separate the two different textures one from the other, and both from the noise.

This can effectively be done through dedicated filtering, where to a "double" EBT texture, the GS filter is applied twice. Although this could seem quite easy to implement, there are many steps to be taken into account in order to ensure success.

4.1.1 Filtering a double textured surface

The ACF of a double textured surface can be seen in Figure 4-2 (calculated from the measurement of Figure 4-1) and always presents a pattern of hexagonal symmetry.

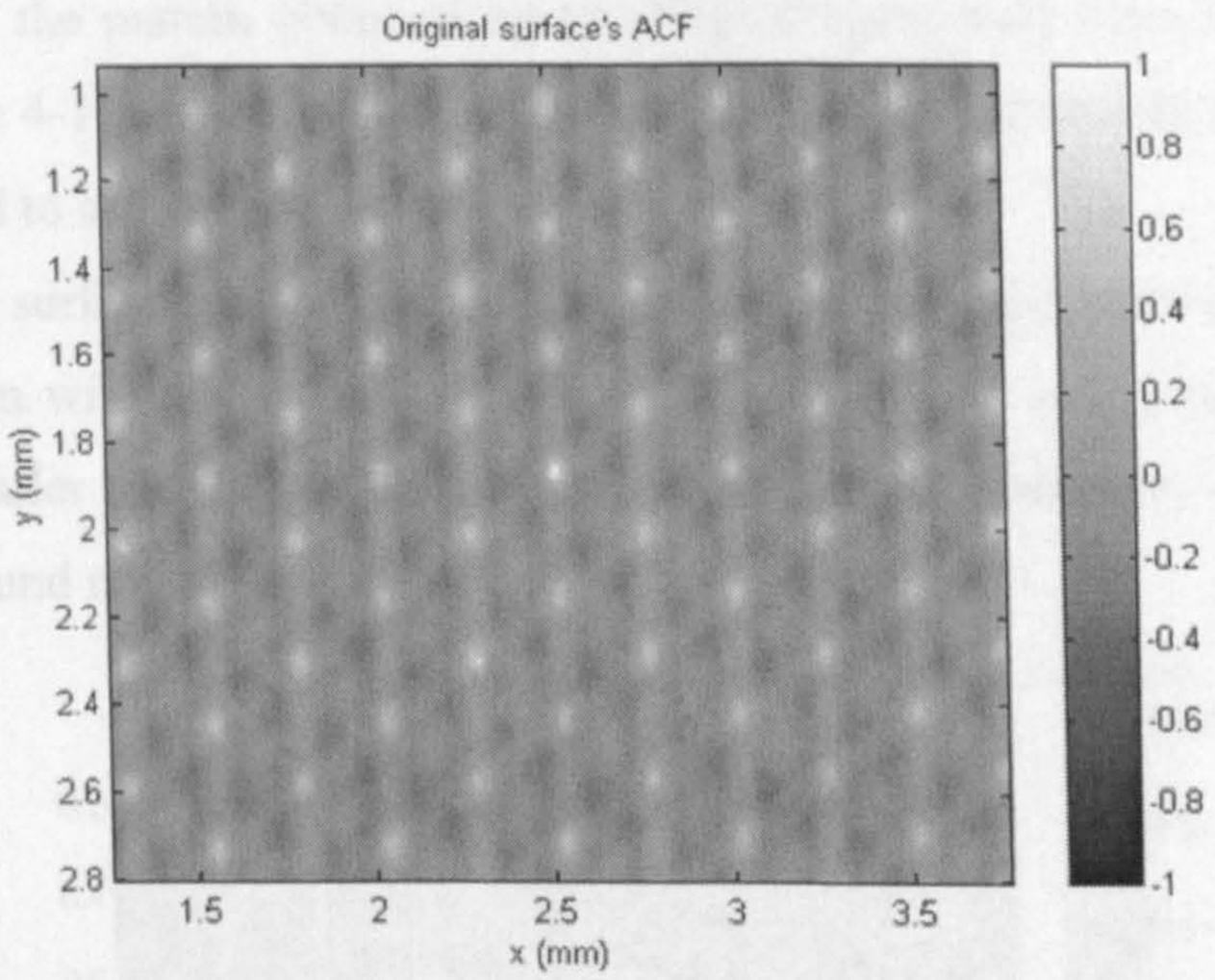

Figure 4-2 – ACF of Sibetex Surface

When running the GS filtering on the ACF, the filter will automatically isolate a main pattern such as the one represented in Figure 4-3. Any other patterns will be interpreted as noise and thus removed.

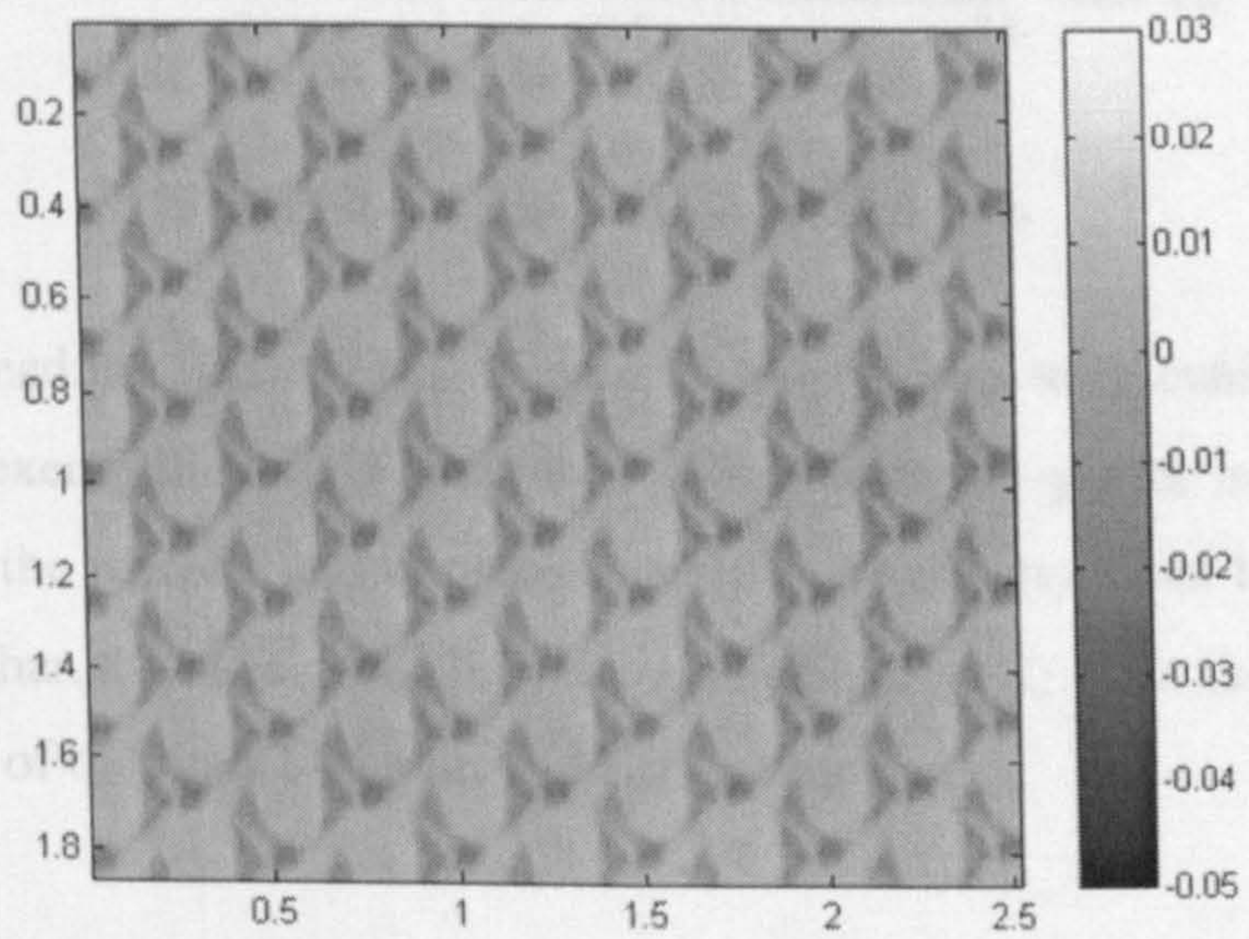

Figure 4-3 – First Pattern extracted

Subtracting the pattern obtained by the filter (Figure 4-3) from the original surface (Figure 4-1) the surface presented in Figure 4-4 is obtained; this surface will be referred to as first residual surface.

Even if this surface looks like a stochastic noise, a second pattern is hidden in it. The problem with the second pattern is that its depth is nearly one order of magnitude smaller than the depth of the first pattern, so it becomes comparable to the background noise.

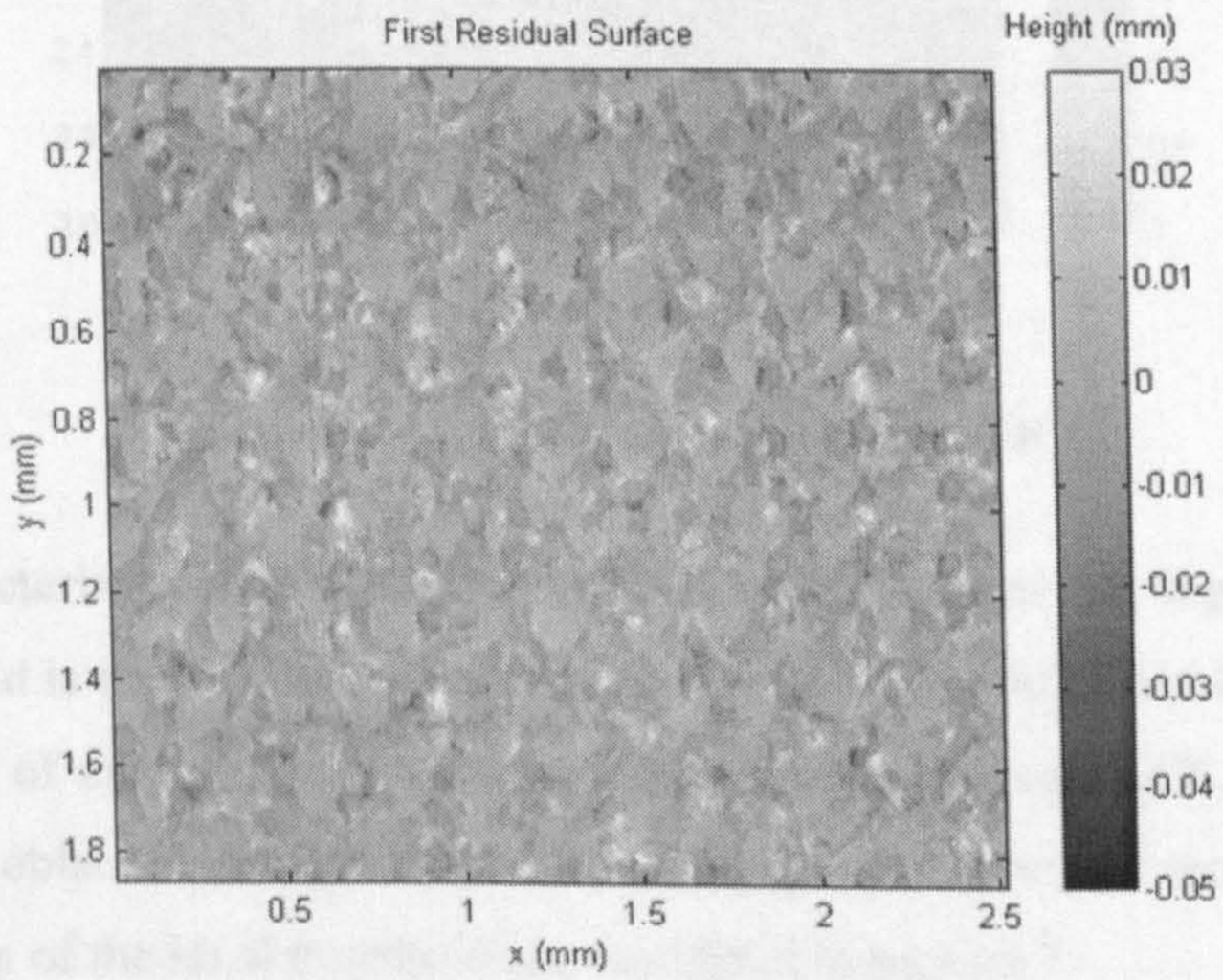

Figure 4-4 – First Residual Surface

Having defined the first residual surface the next step is to calculate its ACF (second run), exemplified in Figure 4-5. Identifying the peaks is the most delicate part of the whole filtering process as it can be observed that their height is much lower than the ones of the first run ACF (Figure 4-2). This fact is due to the small depth of the rings of the second EBT pattern.

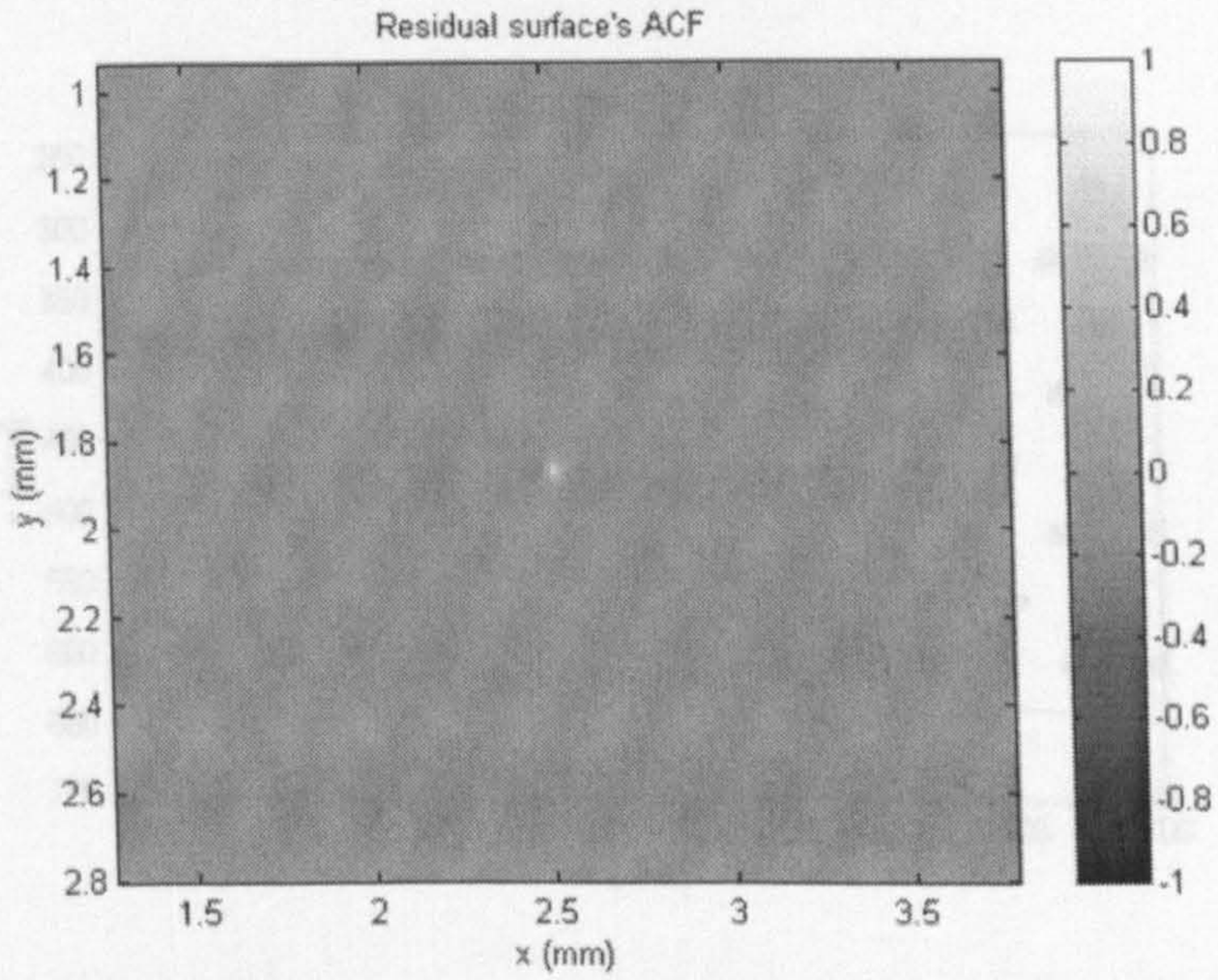

Figure 4-5 – Residual Surface's ACF

The characterisation of peaks as regions whose heights are higher than a given threshold is in this case more difficult. The arbitrary threshold has to be of a lower order of magnitude than the one used for the first run ACF, and it had initially to be obtained through a trial and error process; automatic techniques for the calculation of the ideal threshold are described in section 7.

Figure 4-6 shows the second run ACF intersected at an arbitrary threshold of 0.06 (0.2 was used for the first run ACF). Indicated by the arrows, some ACF peaks are due to stochastic noise (or a not enough sharp pre-filtering) and are not part of the pattern grid. In order to avoid reconstruction errors, those need to be removed.

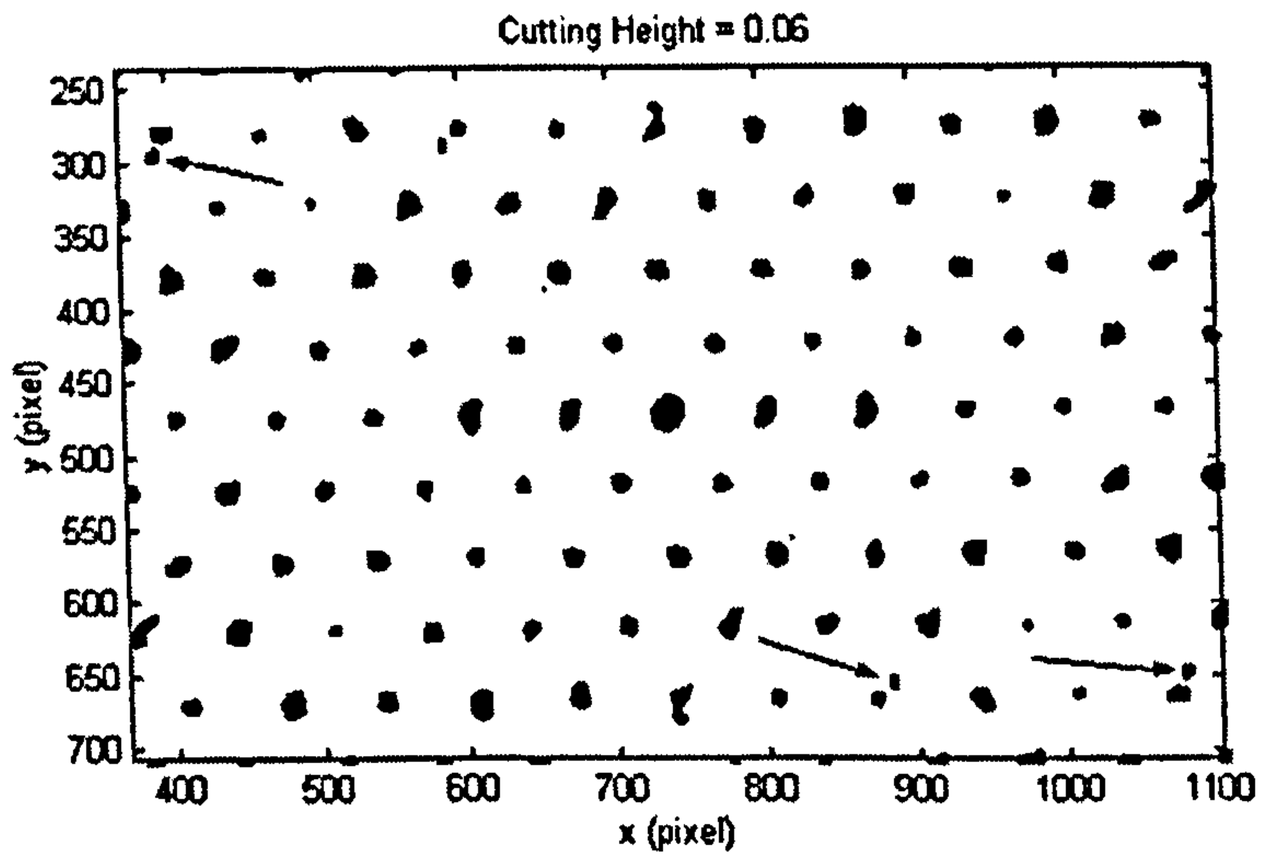

Figure 4-6 – ACF sectioned at 0.06

Figure 4-7 shows the map obtained with an intersecting height of 0.08. Now the opposite problem manifests: the circles in the figure show the positions in which a point is missing to complete the grid.

The above shows that in some cases it is impossible to isolate all and only the deterministic peaks of the 2nd ACF, as the stochastic noise is sometimes greater than the deterministic second pattern.

In general it is better to avoid extra points, preferring to have some missing. The reason is that in most cases, the clusters have a sufficient diameter to overlap any missing ones.

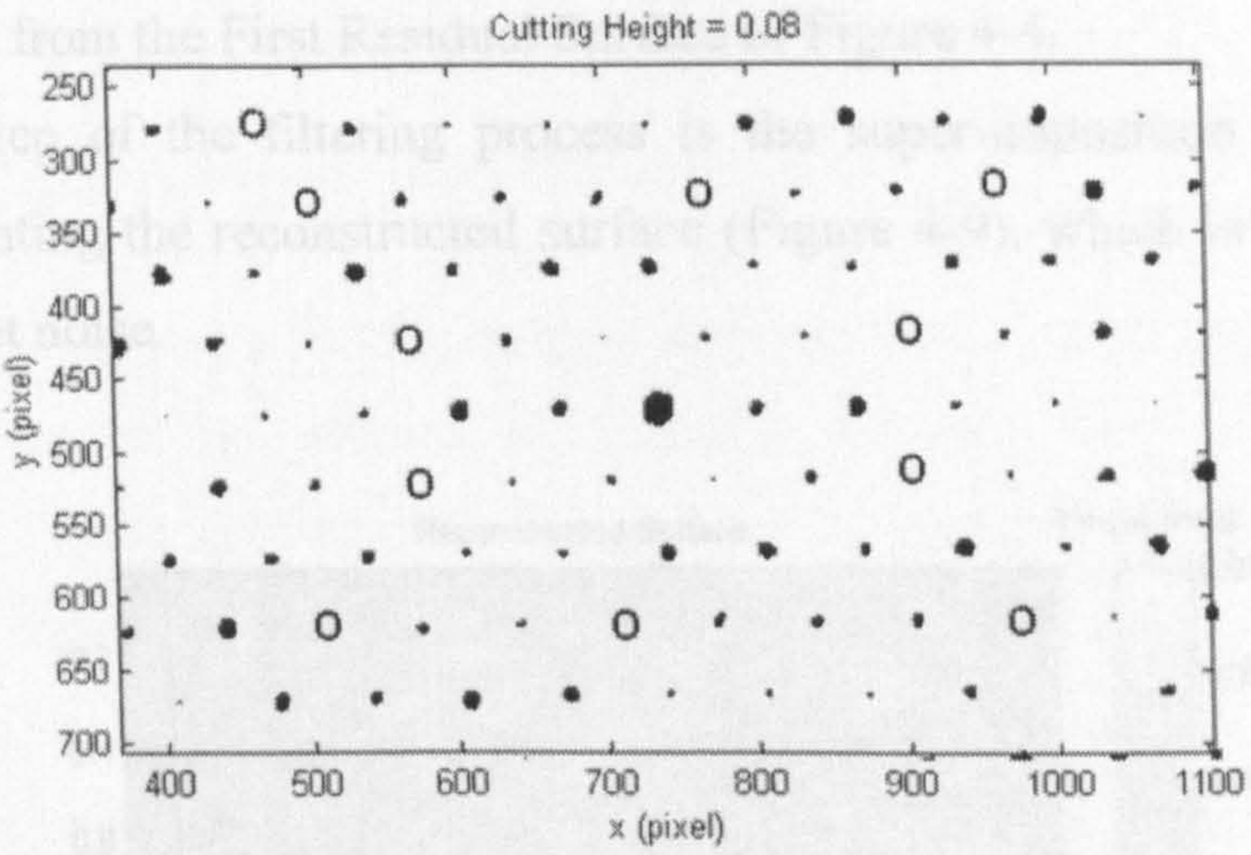

Figure 4-7 – ACF cut at 0.08

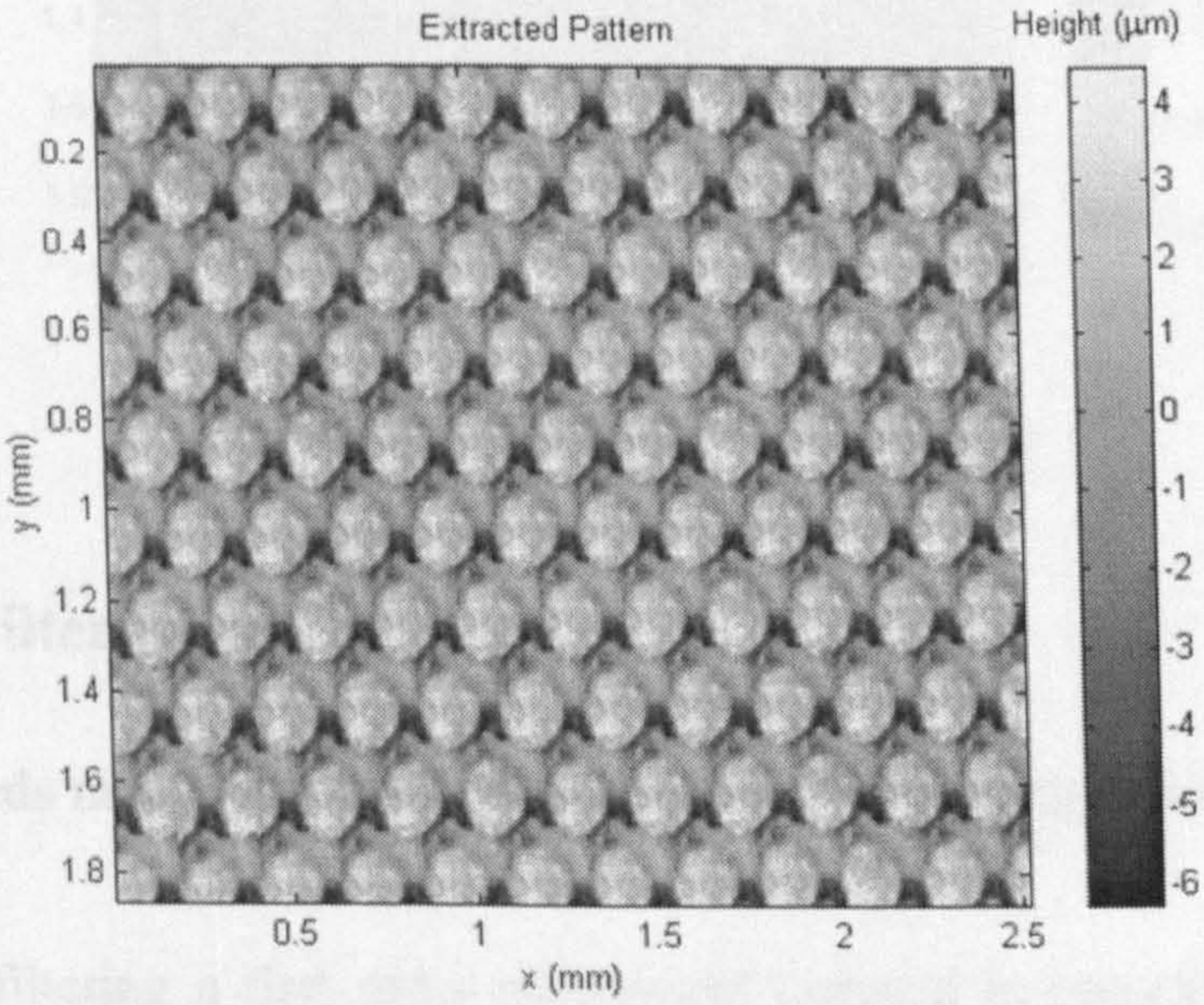

Figure 4-8 – Second Extracted Pattern

Having determined the best threshold, the GS filter is applied again. Figure 4-8 shows the aspect of the second pattern extracted from the original surface.

The Second Residual Surface is obtained subtracting both patterns from the original surface (or subtracting the second pattern from the First Residual

Surface). No figure of it is shown because for a human eye it is impossible to see the differences from the First Residual Surface of Figure 4-4.

The last step of the filtering process is the super-imposition of the two patterns generating the reconstructed surface (Figure 4-9), which is the original surface without noise.

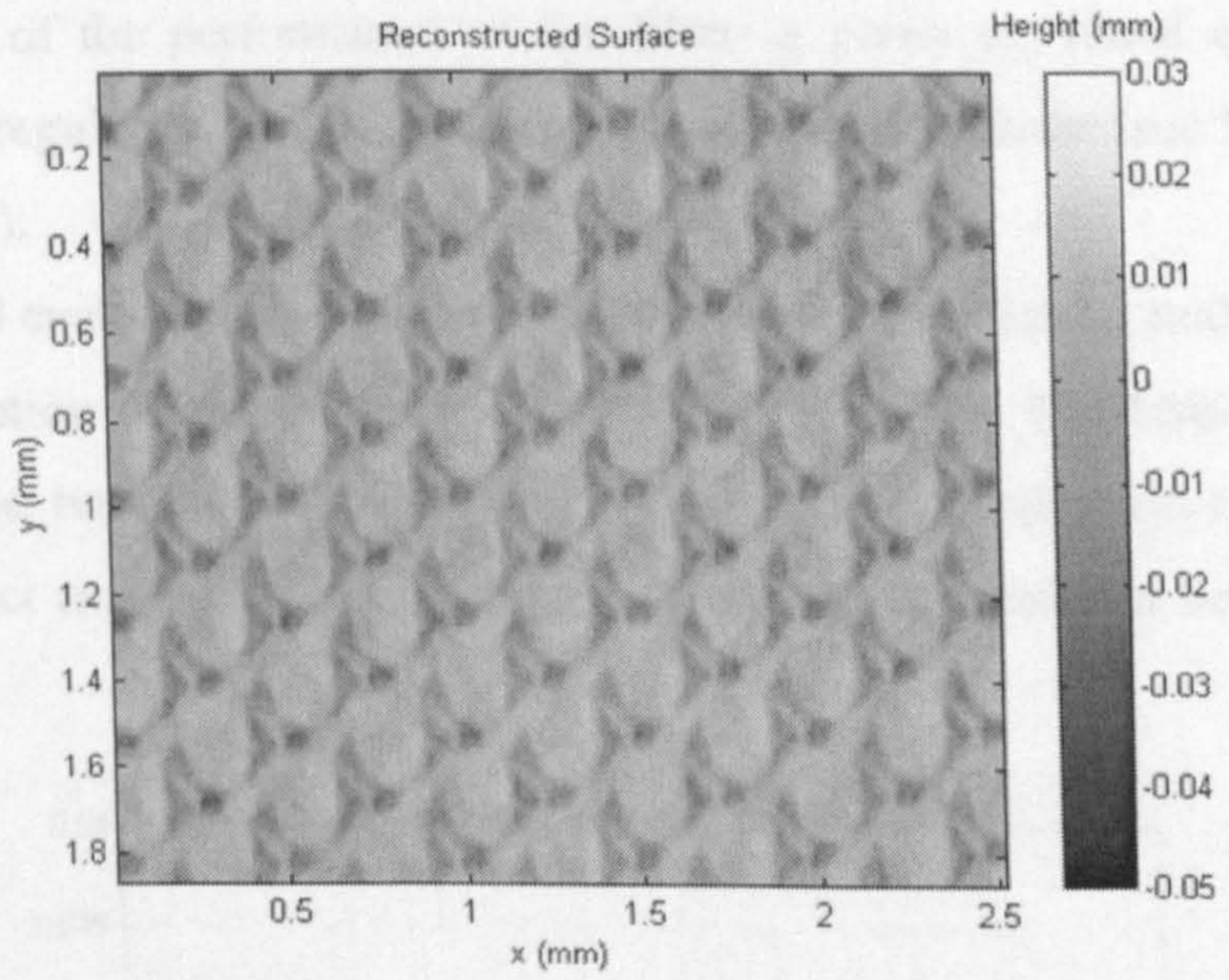

Figure 4-9 – Reconstructed Surface

4.2 Pre-Filtering issues

A few words must be devoted to the surface conditioning before calculating the ACFs.

For EBT filtering a first order polynomial removal is generally enough to have a conditioned ACF on which peaks are clearly showing. On double patterned texture this preliminary work becomes much more delicate and essential, and a 2^{nd} order polynomial is generally recommended for calculating the first run ACF.

The second run ACF presents problems in recognising peaks from stochastic noise. In the worse cases after the polynomial form removal a high-pass filter is

needed to avoid most of the imperfections on the ACF. That is done through Gaussian or (in the worst cases) Robust filtering [Sacerdotti et al 2000(a)].

4.3 Statistical Analysis and Discussion

At the end of the whole filtering process two surfaces were obtained, each one representing one of the patterns of a double textured steel sheet. A first demonstration of the performance of the filter is given by visual evaluation, observing the regularity and smoothness of the filtered surfaces (see Figure 4-3 and Figure 4-8).

A technical evaluation of the results can be given by statistical analysis of the height distribution of the surfaces. Figure 4-10 illustrates the density for the original surface: two features are shown representing the depth of the rings of the patterns. In fact rings cause an asymmetry in the density, being a deterministic feature.

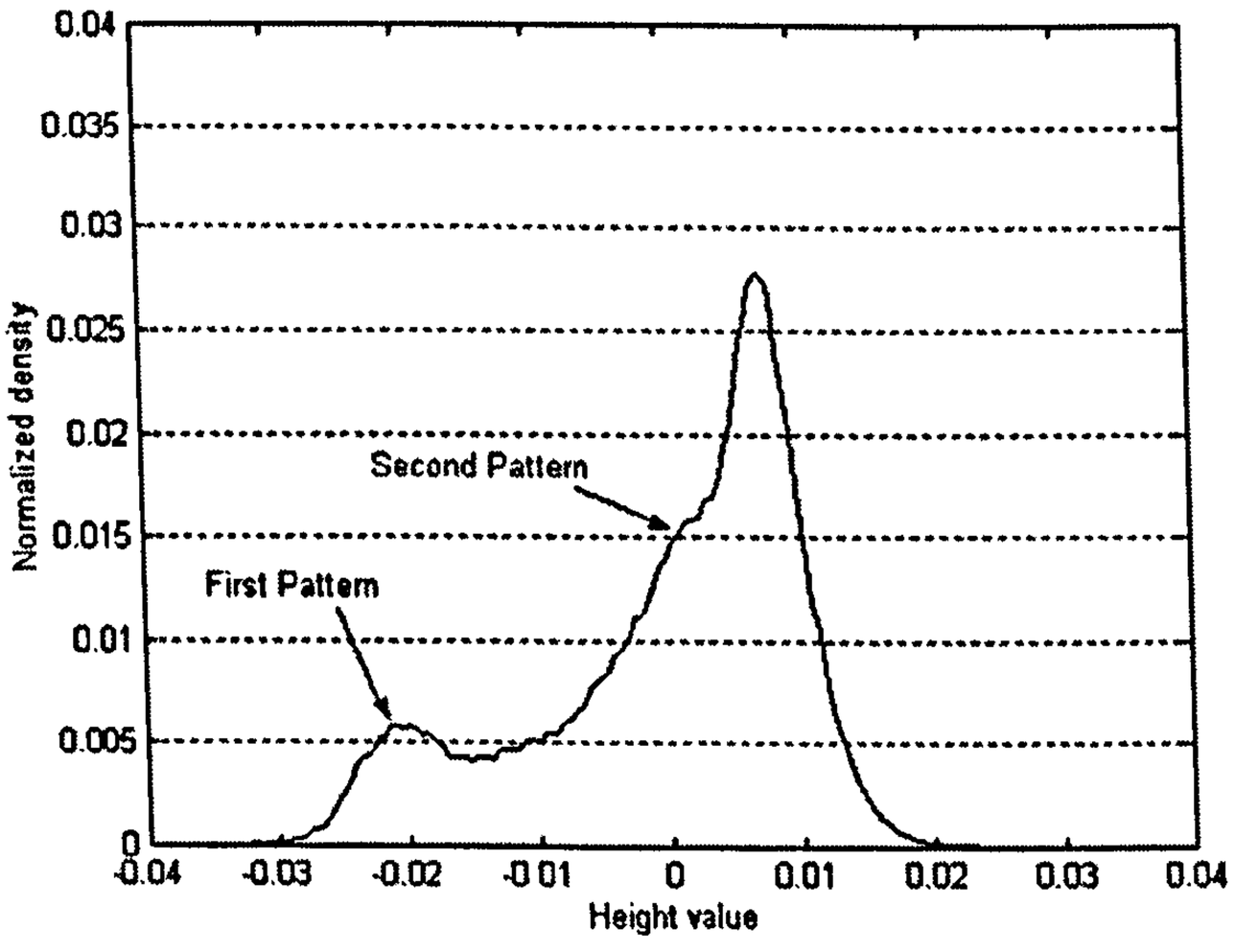

Figure 4-10 – Height distribution of Original Surface

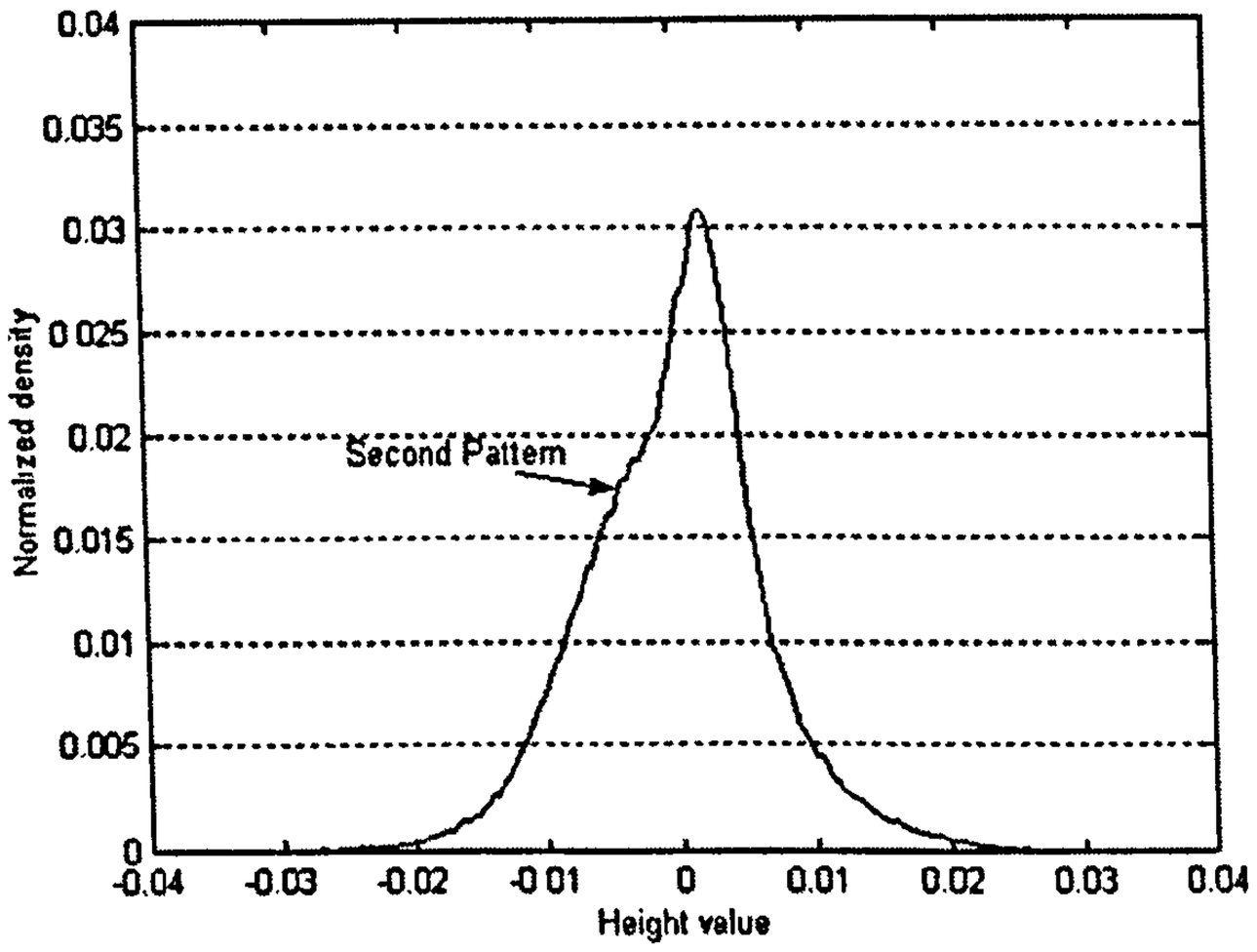

Figure 4-11 - Height distribution of First Residual Surface

Figure 4-11 shows the density of the residual surface obtained subtracting the first pattern from the original surface. The rings belonging to the first pattern have been removed and, as it was expected, their presence is no longer noticeable in the density graph.

Removing also the second pattern the final residual surface has a perfectly symmetric density, because all the deterministic features have been removed and only noise remains (see Figure 4-12).

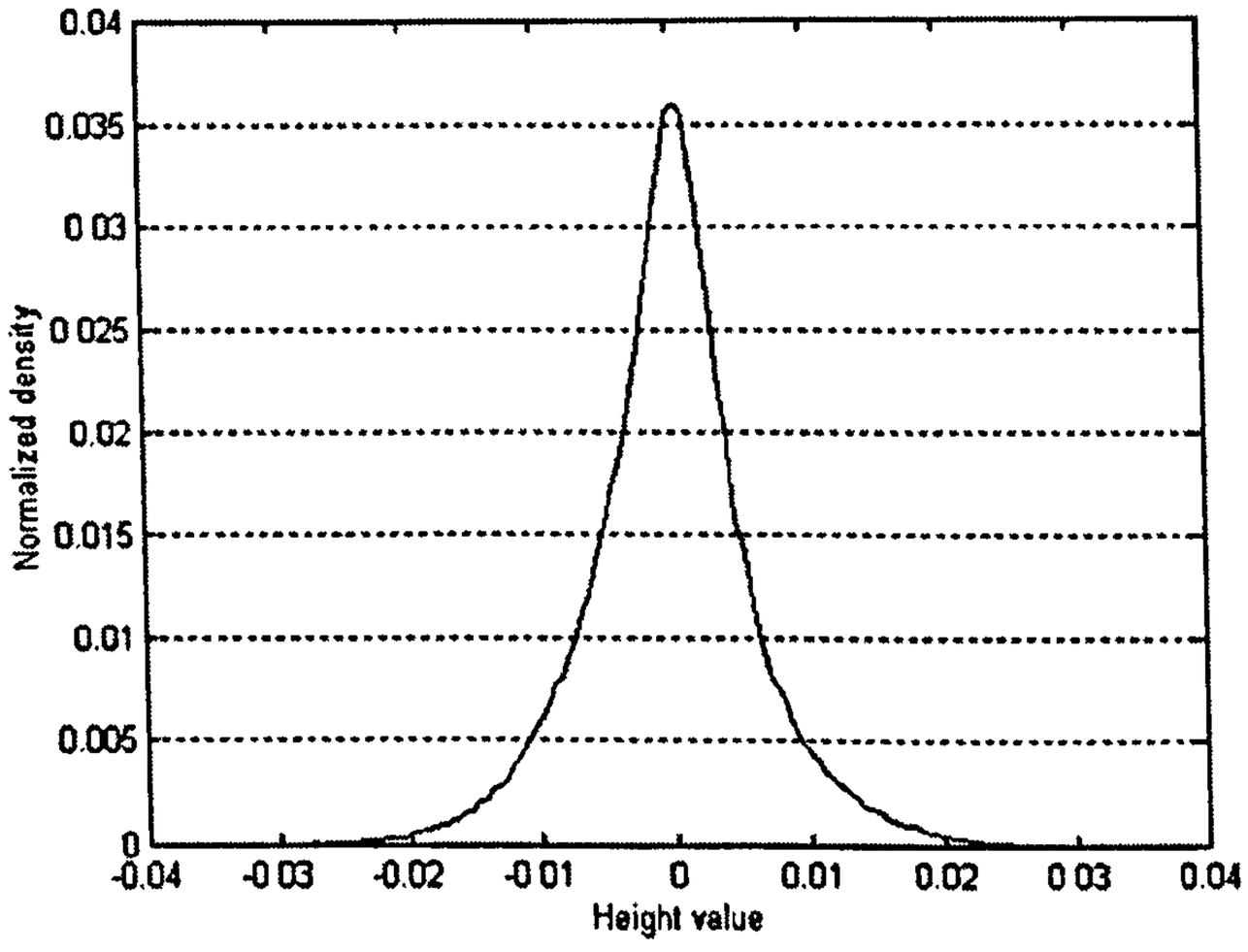

Figure 4-12 - Height distribution of Second Residual Surface

The filter effectively separates the patterns one from the other, and both from the background noise. The average depth of the rings can be quickly evaluated from the density of the original surface as shown in Figure 4-13.

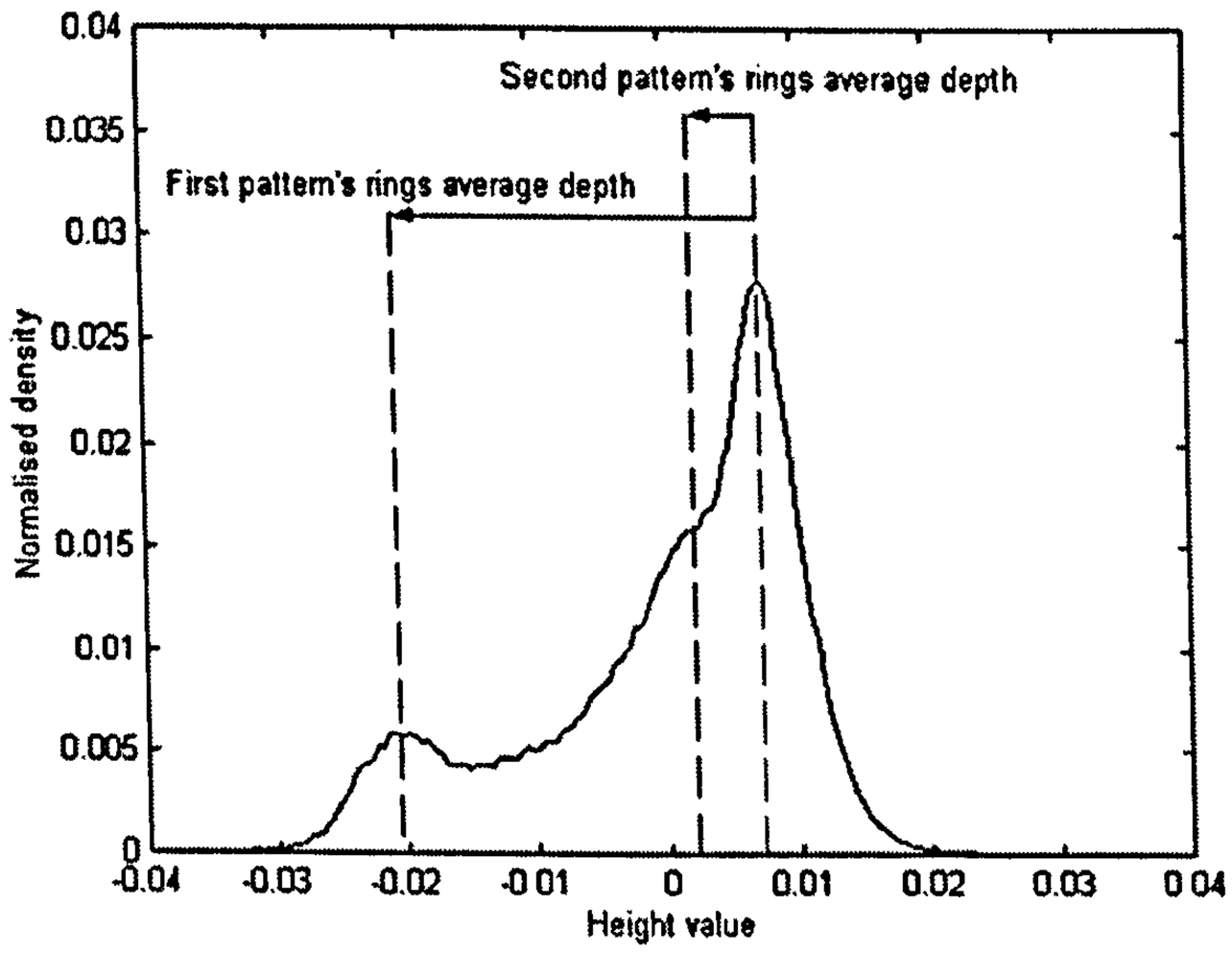

Figure 4-13 – Graphical Parameter Evaluation

The variance of the background noise density (Figure 4-12) gives an idea of the "roughness" of the panel ignoring the textures, and can be thus considered as a quality-related parameter.

4.4 Discussion

- The Statistical filter has been proven to be a good tool to filter double textured surfaces and separate the two periodic patterns one from the other.
- The outcomes of the filter are suitable for parameters calculation and qualitative/quantitative evaluation of the texturing process.
- The residual noise surface obtained at the end of the filtering procedure can give useful indications about the quality of the steel sheet productive process.
- Further research will be performed in order to create a self-tuning software system capable of identifying the ideal cutting height with the minimum need for human interaction.